International Atomic Energy Agency

INDC(CCP)-182
Distr.: G

INDC(CCP)-182

INDC INTERNATIONAL NUCLEAR DATA COMMITTEE

Institut Teplo- i Massoobmena AN BSSR

Heat and Mass Transfer Institute
Academy of Sciences of the Bylorussian SSR

LEVEL DENSITY OF TRANSACTINIUM ISOTOPES

G.V. Antsipov, V.A. Konshin, V.M. Maslov

This work is carried out within the framework of the IAEA-NDS Coordinated Research Programme on the Intercomparison of Actinide Neutron Cross Section Evaluations, Research Agreement No. 2328/R2/CF.

February 1982

IAEA NUCLEAR DATA SECTION, WAGRAMERSTRASSE 5, A-1400 VIENNA

INDC(CCP)-182
Distr.: G

Institut Teplo- i Massoobmena AN BSSR

Heat and Mass Transfer Institute
Academy of Sciences of the Bylorussian SSR

LEVEL DENSITY OF TRANSACTINIUM ISOTOPES

G.V. Antsipov, V.A. Konshin, V.M. Maslov

This work is carried out within the framework of the IAEA-NDS Coordinated Research Programme on the Intercomparison of Actinide Neutron Cross Section Evaluations, Research Agreement No. 2328/R2/CF.

February 1982

ABSTRACT

A review is made of the available data on the average neutron resonance spacings of transactinides. The known schemes of low-lying levels are used to consider, how the level density of these nuclei depend on the parity and angular momentum. The superfluid nuclear model involving the collective effects and the constant-temperature model are employed to parametrize the data on the neutron resonance and low-lying level density. The convenient systematics are deduced. Using these systematics, the parameters for calculating the nuclear level density from ^{225}Th to ^{254}Cf are obtained.

CONTENTS

		Page
1.	Introduction	4-6
2.	Level Density Formalism	6-10
3.	Low Energy Level Density	10-12
4.	Data on the Neutron Resonance Density	12-20
5.	Data on the Low-Lying Level Density	20
6.	Parity Dependence of the Level Density.	21-22
7.	Angular Momentum Dependence of the Level Density . . .	22-25
8.	Parametrization of the Data on the Low-Lying Level Spectra	25-26
9.	Parametrization of the Data on the Low-Lying Level Spectra	26-32
10.	References	33-37
11.	Tables 1 - 3	38-46
12.	Figures 1 - 26	47-81

1. INTRODUCTION

Solution of many problems of fast reactor fuel cycles is connected with obtaining the data on neutron cross sections for a variety of transactinide nuclei. Experimental data are rare or non-existent for them and, therefore, the nuclear data evaluation is based on nuclear model calculations. Calculation of the main body of the data is, to this or other extent, based on the knowledge of the low-lying level spectra of excited nuclei. The nuclear data evaluation makes especially high demands of the knowledge of the low-lying level spectra that follow from the required accuracy of the predicted cross sections. It is therefore natural to use the individual initial information for each nucleus, including the data deduced from systematics if the above information is not available.

The upper limit of the discrete level spectrum of transactinides known from various experiments is usually 0.5 - 1.5 MeV. At higher energies the nuclear model calculations of the level density are used. Since the calculated cross sections are very sensitive to the presently used level density models and their parameter values, in particular, the radiative capture cross section /1/, these can be employed only if the correct fitting of the available experimental data is obtained. Direct information is obtained from the discrete level spectra and neutron resonance density ρ_{exp} at the neutron binding energy.

During the past years the comprehensive spectroscopic information on low-lying states has been accumulated for the nuclei with the mass numbers $A \geqslant 225$. The available data are consistent with the concepts of the rotational nature of the bands which can be distinguished in the low-lying states. The band structure implies that all transactinides are axially symmetric. The concept of the level density enhancement due to the rotational-vibrational levels of the excited nuclei may be used to describe the density of neutron resonances as well as of the low-lying states. However, this procedure faces certain difficulties, which follows from Figs. 1 and 2 where the cumulative number of the levels of even-even (^{238}U) and even-odd ^{233}U) nuclei are presented using the superfluid level density model involving the enhancement factor due to the collective modes /2/. The main parameter of this model is found from the data on the neutron resonance spacing. These figures are typical, and only for odd-odd nuclei the model curve fits well the histogram, which is however caused by the level missing but not by the applicability of the model. The missing of the levels also explains a rapid decrease in the slope of the cumulative number of the levels (Figs. 1 and 2). Owing to this fact, at low energies, use should be made of the model, whose parameters are specified by fitting the cumulative numbers of the levels in the region where the number of the missed levels is negligible. This model must ensure the matching with the curve obtained by the model employed for the neutron resonance density description.

The experimental data on the neutron resonance spacing available for transactinides are reviewed in this work. The need for this work is due to the progress of the experimental techniques for resonance cross section measurements. The available reviews on $\langle D \rangle_{exp}$ /3,4/ cannot be considered sufficiently comprehensive.

The analysis of the data on the low-lying level spectra of transactinides has allowed some conclusions to be made, how the level density depends on the parity and angular momentum. The data on the neutron resonance spacing and low-lying level spectra were parametrized using the chosen level density formalism. The systematics obtained were employed to deduce the nuclear level density parameters from ^{225}Th to ^{254}Cf.

2. LEVEL DENSITY FORMALISM

The level density of the deformed axially symmetric nuclei such as transactinides at equilibrium deformations is given by the following expression /5/ which allows for a contribution of the rotational modes:

$$\rho_{in+rot}(U,J) = \frac{\omega(U)}{2\sqrt{\pi}\sigma_{\parallel}} \sum_{K=-J}^{J} \exp\left[-\frac{J(J+1)}{2\sigma_{\perp}^2} - K^2\left(\frac{1}{2\sigma_{\parallel}^2} - \frac{1}{2\sigma_{\perp}^2}\right)\right] \qquad (1)$$

where $\omega(U) = \exp S/\left[(2\pi)^{3/2}\,\mathrm{Det}^{1/2}\right]$ is the total density of the intrinsic excited states; S the entropy; $\sigma_{\perp}^2$ and $\sigma_{\parallel}^2$ the parameters of the angular momentum dependence related to the moments of the inertia $F_{\perp}$ and $F_{\parallel}$ about the axis perdendicular and parallel to that of the symmetry by the formulae $\sigma_{\perp}^2 = F_{\perp}\,t$ and $\sigma_{\parallel}^2 = F_{\parallel}\,t$; K the projection of the angular momentum on the nuclear symmetry axis; t the nuclear temperature.

For the values of the angular moments J and deformations $\varepsilon = 0.24$ typical of transactinides, expression (1) assumes the form:

$$\rho_{in+rot}(U,J) = \frac{(2J+1)\omega(U)}{2\sqrt{2\pi}\,\sigma_{\parallel}} \exp\left[-\frac{J(J+1)}{2\sigma_{\perp}^2}\right] \quad . \quad (2)$$

At the neutron binding energy, the vibrational enhancement may be allowed for by introducing, into expressions (1) and (2), the coefficient K_{vib} obtained in the adiabatic approximation /2/:

$$K_{vib} = \exp\left[1.7\left(\frac{3m_oA}{4\pi\,\sigma_{LDM}}\right. \frac{C_{LDM}}{C}\, t^{4/3}\right], \qquad (3)$$

then

$$\rho(U,J) = K_{vib}\,\rho_{in+rot}(U,J) \qquad (4)$$

Here σ_{LDM} is the surface tension coefficient in the liquid drop model ($4\pi r_0^2\sigma_{LDM}$= 18 MeV) and the ratio C_{LDM}/C characterizes, how the surface energy coefficient for an excited nucleus differs from that for the liquid drop model (In this case it is assumed to be unity).

Thermodynamic functions of a nucleus have been found in the framework of the modified superfluid model given in /2,6/. The condensation energy $E_{cond} = \pi^2 q\Delta f^2/48$ in the model /6/ differs from $E_{cond} = 1/4\ q\Delta_0^2$ used at temperatures above the critical /2/. The following procedure is adopted to achieve the coincidence between both models.

Let us assume that two condensation energies are equal, then

$$\begin{aligned} &\frac{\pi}{48}\, q\Delta f^2 = \frac{1}{4}\, q\Delta_0^2 \\ &\Delta_0 = 0.907\Delta f \\ &t_{crit} = \frac{1}{2}\,\Delta f = 0.551\,\Delta_0 \end{aligned} \qquad (5)$$

The obtained value of t_{crit} is close to $t_{crit} = 0.567\Delta_o$ which is found when Δ_o tends to zero at the critical point. Henceforth, the value of $t_{crit} = 0.567\Delta_o$ /2/ will be employed. Using the correlation functions Δ_{oZ} and Δ_{oN} determined in terms of the nuclear masses yields:

$$t_{crit} = 0.567\ \max(\Delta_{oZ}, \Delta_{oN}). \qquad (6)$$

At temperatures above the critical, the excitation energy U, temperature t, entropy S and other quantities are related as:

$$U = at^2 + E_{cond}$$

$$S = 2at = 2\sqrt{a(U - E_{cond})}, \qquad Det = \frac{18}{\pi^4} a^3 t^5$$

$$F_{\parallel} = \frac{6}{\pi^2} a\bar{m}^2(1 - \frac{2}{3}\varepsilon), \qquad F_{\perp} = \frac{2}{5} m_o r_o^2 A^{5/3}(1 + \frac{1}{3}\varepsilon) \qquad (7)$$

$$a = \tilde{a} \left\{1 + \left[1 - \exp\left[-\gamma(U - E_{cond})\right]\right] \frac{\delta W_{exp}}{U - E_{cond}}\right\}.$$

Here ε is the quadrupole deformation parameter; $\tilde{a}$ is the asymptotic value of the parameter a at $U \to \infty$ and is obtained from the neutron resonance density; $\bar{m}^2$ is the average taken ove single-particle angular momentum projections near the Fermi energy; δW_{exp} is the shell correction to the nuclear ground state mass binding energy and γ is the energy dependence parameter. The condensation energy, E_{cond}, is

$$E_{cond} = 3a_{crit}(\Delta_{oZ}^2 + \Delta_{oN}^2)/4\pi^2 \qquad (8)$$

where the value of the parameter a at t_{crit} is given by:

$$a = \tilde{a}\left\{1 + \left[1 - \exp(-\gamma\, a_{crit}\, t^2_{crit})\right] \frac{\delta W_{exp}}{a_{crit}\, t^2_{crit}}\right]. \tag{9}$$

Below the phase transition point, expressions (7) are replaced by:

$$U = U_{crit}(1 - \varphi^2) \quad S = S_{crit}\, \frac{t_{crit}}{t}\, (1 - \varphi^2)$$

$$Det = Det_{crit}(1 - \varphi^2)(1 + \varphi^2)^3, \qquad a = a_{crit} \tag{10}$$

$$F_{\parallel} = F_{\parallel\, crit}\, \frac{t_{crit}}{t}\, (1 - \varphi^2)$$

$$F_{\perp} = \frac{F_{\perp\, crit}}{3}\left[1 + \frac{2t_{crit}}{t}\, (1 - \varphi^2)\right]$$

where the function $\varphi = (1 - \frac{U}{U_{crit}})^{1/2}$ is related with a temperature by the equation:

$$\varphi = th(\varphi \frac{t_{crit}}{t}). \tag{11}$$

The parameter values at the critical point in equation (10) are determined by expressions (7) when $t = t_{crit}$ and $a = a_{crit}$. The evaluation /7/ is used to find F in (10). In this case, $F_{\perp}$ for the ground state is equal to $F_{\perp}$ /3.

The above expressions correspond to even-even nuclei. Even--odd differences may be allowed for by the appropriate excitation energy shift /2/:

$$U^* = U + \begin{cases} \Delta_{oN} & \text{- even-even nuclei} \\ \Delta_{oZ} & \text{- odd-even nuclei} \\ \Delta_{oZ} + \Delta_{oN} & \text{- odd-odd nuclei} \end{cases} \tag{12}$$

The parameters of Myers and Swiatecki /8/ were used to calculate shell corrections. The values of the correlation functions Δ_{o_Z} and Δ_{o_N} were determined from the pairing energies according to the data /9/. The remainder parameters were taken from /2/. Note that for nuclei, when at the neutron binding energy t was less than t_{crit}, it was assumed that $a = a(S_n)$ for $t < t(S_n)$, and relation (9) was employed for $t \geqslant t(S_n)$.

Figs. 1 and 2 show that the model employed fails when attempting to fit the cumulative numbers of the levels if the parameter is deduced from $\langle D \rangle_{exp}$. So, the constant-temperature model widely used up to now was adopted.

3. LOW ENERGY LEVEL DENSITY

Gilbert and Cameron 3/10/ have stated that the cumulative number of levels N(E) in the semi-logarithmic scale can be fitted by a straight line,i.e.

$$N(E)=\exp\left[(E-E_o)/T\right] \tag{13}$$

Then, the level density is

$$\rho(E)= \frac{dN(E)}{dE} \tag{14}$$

and

$$T=\left[\frac{d}{dE}\ln \rho(E)\right]^{-1} \tag{15}$$

where E_o and T are the model parameters. It is clearly seen in the case of even-even transactinides (Fgs. 3 and 4).The missing of levels is the prime reason of poor fitting with the calculated line the staircase plot. In the case of odd

-odd nuclei and nuclei with odd A, such a linear dependence is, generally speaking, inevident (Figs. 5 through 7). However, it should be borne in mind that the level density of these nuclei is much higher than that of even-even nuclei. As a result, the number of the missed levels is much greater, which is attributed to the fact that the superfluid nuclear model (Fig.7) can be adopted to describe satisfactorily the cumulative number of levels N(E).

The constant-temperature model is quite a simple parametrization of the level density. Calculations performed by the equations of the model described in /2/ give N(E) almost linear in the semi-log scale. Hence, the use of the constant-temperature model looks like the adjustment of the model parameters /2/.

The level density was described in /10,11/ using the same approach but the neutron resonance density was calculated within the Fermi-gas model. Note that the expression

$$\frac{1}{T} = \sqrt{\frac{a}{E_c}} - \frac{3}{2E_c} \qquad (16)$$

known for the Fermi-gas model with allowance for the rotational mode contribution in the adiabatic approximation assumes the form:

$$\frac{1}{T} = \sqrt{\frac{a}{E_c}} - \frac{1}{E_c} \qquad (17)$$

where a is the parameter of the level density and E_c is the point at which two models match. Moreover, in /11/ transactinides were not considered.

The parameters of the constant-temperature model were chosen with regard for the following criteria:

(1) acceptable description of the cumulative number of levels

(2) $$\rho_1(E_c) = \rho_2(E_c) \qquad (18)$$

then

$$E_o = E_c - T\ln(\rho_2(E_c)T) \qquad (19)$$

(3)

$$\frac{d}{dE}\ln \rho_1(E)\Big|_{E_c} = \frac{d}{dE}\ln \rho_2(E_c)\Big|_{E_c} \qquad (20)$$

or

$$T^{-1} = \frac{d\ln\rho_2(E)}{dE}\Big|_{E_c} \qquad (21)$$

where $\rho_1(E)$ and $\rho_2(E)$ are the level densities in the constant--temperature model and in the model involving the pair correlations and collective mode contribution.

4. DATA ON THE NEUTRON RESONANCE DENSITY

When using the data on the neutron resonance density, ρ_{exp}, deduced by the resolved resonance cross section analysis it should be kept in mind that the result may change drastically if (a) some resonances are lost because of their "weakness" or overlapping of resonances and poor spectrometer resolution and (b) wrong spin assignment of resonances and p-resonance excitation. The last statement is applied to even-even targets.

As a result of the available data on the resonance parameter analysis, mainly evaluated parameters, preference was given to the values $\langle D\rangle_{exp}$ presented in Table 1. At present there are data on $\langle D\rangle_{exp}$ for 32 transactinides. Note that in

/12/ for ^{234}Th (compound nucleus) the value 0.55 ± 0.04 eV is given with reference to the ENDF/B-V library. However, the study of ENDF/B-IV and ENDF/B-V versions /13/ has shown that there are no resonance parameters for this nucleus. Therefore, this value was not included into the current analysis.

Table 1 also comprises the spins and parities of the ground states of targets and neutron binding energies /9/.

Below, a brief review of the average resonance spacings $\langle D \rangle_{exp}$ will be made.

<u>^{229}Th.</u> The value $\langle D \rangle_{exp}$ = 0.40 eV obtained in /14/ may be considered most reliable. It is evaluated by the fission cross section parametrization in the region 1 - 7 eV (17 resonances). With increasing energy interval, $\langle D \rangle_{exp}$ grows too, which points to the level loss. The level missing is not taken into account to obtain this value. However, it may be expected that it will not be substantial due to low neutron energy.

<u>^{230}Th.</u> In /15/, the parameters of 28 resonances are obtained from the measurements of the total cross section of ^{230}Th up to 600 eV. The diagram of the cumulative number of levels shows that the level missing starts above 180 eV and $\langle D \rangle_{exp}$ = 9.8 ± 1.6 eV. The minimum value of $g\Gamma_n^0$ is 0.2 meV, which indicates that there are only s-wave resonances.

A similar value $\langle D \rangle_{exp}$ = 11 ± 3 eV is also obtained in /16/. However, we have used the value from /15/ as it includes some resonances omitted in /16/.

^{232}Th. According to the data of different authors, the value $\langle D \rangle_{exp}$ for this nucleus varies from 13 to 24 eV /17/. We have given preference to the evaluation /18/, $\langle D \rangle_{exp}$ = = 16.6 ± 0.9 eV obtained from the resonance parameters for the s-wave and well consistent with the data of /19/ (17.00 eV), /20/ (16.70 eV). This uncertainty is a statistical error.

^{231}Pa. In /21/, $\langle D \rangle_{exp}$ = 0.45 eV is obtained from the measurements of the total cross section where below 11 eV 24 resonances are identified. However, the comparison of the experimental and theoretical neutron width distributions points to approximately 5 levels, which is possible due to small values of the neutron widths or the observed doublets. With this in view, $\langle D \rangle_{exp}$ = 0.37 eV.

^{233}Pa. In /22/, $\langle D \rangle_{exp}$ = 0.69 eV is obtained from sample transmission measurements. The authors give the parameters of 27 resonances up to 18 eV. Six of these parameters are introduced to improve the fitting. This value is obtained allowing for that 4 resonances are lost in experiment.

^{232}U. In /23/, the fission cross section is measured in the region of 5 - 1900 eV. The authors do not give the value $\langle D \rangle_{exp}$. However, Lynn /3/ gives $\langle D \rangle_{exp}$ = 4.1 eV with reference to /23/. Here, the value $\langle D \rangle_{exp}$ = 4.1 eV is also taken but its reliability is unknown.

^{233}U. The value $\langle D \rangle_{exp}$ = 0.61 ± 0.07 eV /24/ is taken for this nucleus and obtained from the resonance parameters up to 30 eV where the level missing is insignificant.

^{234}U. In /25/, the parameters of 118 resonances are obtained from the measurements of the total cross section and fission cross section of ^{234}U up to 1.5 eV. The authors have introduced a correction for the level missing by comparison of the experimental neutron width distributions and that of Porter-Thomas and obtained $\langle D \rangle_{exp} = 10.6 \pm 0.5$ eV. The minimum Γ_n^o value, above which all resonances are observed, is in the range 0.1-0.2 meV. This indicates that the p-wave resonances are not observed in this experiment.

<u>^{235}U.</u> The value $\langle D \rangle_{exp} = 0.438 \pm 0.038$ eV proves to be most reliable /25/. It is obtained after treating the fission cross section measurements by means of a polarized neutron beam and allows for the level missing. This procedure enables a number of doublets to be resolved, which considerably decreases $\langle D \rangle_{exp}$.

<u>^{236}U.</u> In /27/, $\langle D \rangle_{exp} = 16.2 \pm 0.8$ eV is obtained from the total cross section measurements from 40 eV to 4.1 keV assuming that all resonances are related to the p-wave. The level missing is allowed for by the Porter-Thomas neutron width distribution fitting of the experimental histogram. The statistical analysis of the resonance parameter samples indicates that there is no need to take into account the p-resonances.

<u>^{237}U.</u> In /28/, the fission ^{237}U cross sections are measured from 43 eV to 220 eV, and the resonance parameters are deduced. The value $\langle D \rangle_{exp}$ is evaluated using the data for reliably identified resonances within 65-100 eV and equals 3.5 ± 0.8 eV.

<u>^{238}U.</u> The results of /29/ included into the ENDF/B-format seem to be most reliable. The authors have thoroughly analyzed the available measurements up to 4 keV and evaluated the para-

meters for 164 s- and 280 p-wave resonances as well as their missing . The obtained $\langle D \rangle_{exp}$ values for the s- and p-resonances are 24.8 ± 2 eV and 8.91 ± 0.1 eV, respectively. At the same time it should be noted that this value $\langle D \rangle_{exp}$ is much higher than the previously evaluated ones.

<u>^{239}Np.</u> To our opinion, the value $\langle D \rangle_{exp}$ ^{237}Np =0.740± 0.061 eV proves to be most reliable /30/. It is found from the self-consistent parametrization of the measured capture cross section , elastic scattering and total cross sections in the range from 8 to 204 eV. This value allows for the level missing.

<u>^{238}Pu.</u> Using the radiative capture and fission cross section measurements of ^{238}Pu /32,33/, the authors /31/ have obtained $\langle D \rangle_{exp}$ = 9.2 ± 0.7 eV (43 resonances below 400 eV). The cumulative number of resonances illustrates that the noticeable level missing is not observed. In /32/, the similar value $\langle D \rangle_{exp}$ = 9.5 ± 0.7 eV is also obtained. We have adopted the value from /31/, i.e. $\langle D \rangle_{exp}$ = 9.2 ± 0.7 eV.

<u>^{239}Pu.</u> Here, we have used the value $\langle D \rangle_{exp}$ = 2.38 ± 0.06 eV /34/ obtained by the self-consistent parametrization of the experimental data for fission, capture and total cross sections up to 500 eV. This value allows for the missing of 5 levels between 300 and 500 eV due to the overlapping.

<u>^{240}Pu.</u> The value $\langle D \rangle_{exp}$ = 13.5 ± 0.5 eV for our new version of ^{240}Pu file. It is based on the analysis of the known resonance parameters up to 1 keV with allowance for the missing of "weak" resonances, resonance overlapping and the presence of the p-wave resonances.

<u>^{241}Pu.</u> The value $\langle D \rangle_{exp}$ = 1.34 ± 0.10 eV is obtained for a complete ^{241}Pu file /35/. It allows for the level missing which proves to be significant up to 150 eV and is based on the self-consistent resonance analysis of all available experimental cross sections.

<u>^{242}Pu.</u> The value $\langle D \rangle_{exp}$ = 14.23 ± 0.54 eV is used for ^{242}Pu. In /36/, it is obtained from the analysis of all available resonance parameters, resonance missing and the presence of the p-resonances.

<u>^{244}Pu.</u> In /37/, 4 resonances are found in fission cross section measurements up to 60 eV. This gives $\langle D \rangle_{exp}$ = 11.4 ± 4 eV (statistical error). No other data are available.

<u>^{241}Am.</u> Numerous data on $\langle D \rangle_{exp}$ are available for ^{241}Am. Preference is given to $\langle D \rangle_{exp}$ = 0.58 ± 0.04 eV obtained from the evaluation /8/ which allows for the level missing and is consistent with the results reported after 1975.

<u>^{242m}Am.</u> In /39/, the fission cross section of ^{242}Am is measured for the metastable state (5^-) between 0.01 eV and 20 MeV. Resonance parameters are obtained up to 20 eV. The value $\langle D \rangle_{exp}$ is determined by the cumulative number of the resonance fitting and equals 0.45 eV. The authors of /39/ neither give the resonance parameters nor indicate the number of the missed resonances.

<u>^{243}Am.</u> The resonance region of ^{243}Am is more thoroughly measured and parametrized in /40/ where the parameters are given up to 250 eV. The cumulative number of resonances and the comparison of the experimental and theoretical neutron width dis-

tributions show that about 9 levels are missed up to 50 eV at $\langle D \rangle_{exp}$ = 0.68 ± 0.06 eV.

^{242}Cm. The present authors know only the experimental work /41/ on ^{242}Cm where 9 resonances are observed up to 154.6 eV, which yields $\langle D \rangle_{exp}$ = 17.6 ± 3.3 eV. The authors of /41/ do not mention the allowance for the level missing. In /42/, based on the same data, the value $\langle D \rangle_{exp}$ = 13.0 ± 3 eV with allowance for the level missing is obtained. On the other hand, using the maximum likelihood function, Coceva and Stefanon have obtained the value of 17.0 ± 5 eV /43/. Therefore, we have used the value $\langle D \rangle_{exp}$ = 17.6 ± 3.3 eV from /41/.

^{243}Cm. In /44/, the total cross section is measured, and 15 resonances of ^{243}Cm are observed up to 30 eV. The deviation of the average trend of the cumulative number of resonances from the straight line illustrates the missing of resonances. Moreover, their identification is hampered by a complex composition of a sample. In /12/, the level missing is evaluated with the maximum likelihood function. The value $\langle D \rangle_{exp}$= =0.50 ± 0.20 eV is obtained and employed henceforth.

^{244}Cm. For this Cm isotope the value $\langle D \rangle_{exp}$ = 11.8 ± 1.2 eV is used. This value is found in /12/ using the maximum likelihood function with allowance for the level missing from the resonance parameters /45/ up to 500 eV.

^{245}Cm. In /46/, the fission cross section is measured in the region up to 35 eV where 11 resonances are observed. The cumulative number of levels is consistent with the negligible level missing. The statistical analysis does not also point to the level missing. In this case, the value $\langle D \rangle_{exp}$ =

= 1.14 ± 0.14 eV is adopted.

<u>^{246}Cm.</u> At present 11 ^{246}Cm resonances are identified, the latter is at 381.1 eV /47/. The statistical analysis of the level missing in this region /47/ yields $\langle D \rangle_{exp}$ = 21.3 ± 5.3 eV. In our case, this value is adopted. It should be noted that it is much lower than the values reported by other authors.

<u>^{247}Cm.</u> There are 34 ^{247}Cm resonances up to 61 eV. The values $\langle D \rangle_{exp}$ presented by different authors fluctuate strongly. The value $\langle D \rangle_{exp}$ = 1.2 eV is adopted here. It is taken from /48/ where the level missing has been analyzed. However, it should be noted that this value is average for diffe-rent procedure results of the $\langle D \rangle_{exp}$ evaluation which give strongly diverging results.

<u>^{248}Cm.</u> Here, preference is given to the value $\langle D \rangle_{exp}$ = = 40 ± 5 eV /49/ obtained from the resonance part of the total cross section measured in the region 0.5-3000 eV. The level missing is allowed for by comparing experimental and theoretical neutron width distributions. The authors /49/ consider that there are only s-wave resonances.

<u>^{249}Bk.</u> In /50/, the total cross section is measured using a liquid nitrogen-cooled sample. Below 130 eV, 47 resonances are identified. In the region up to 20 eV, there is no level missing as the plot of the cumulative number of resonances vs energy shows that $\langle D \rangle_{exp}$ is equal to 1.1 eV.

<u>^{249}Cf.</u> In the resonance region of ^{249}Cf, the fission cross section is measured in /51/ and the total cross section, in /52/. In /51/, in the region 15-70 eV 43 resonances are pa-

rametrized and the value $\langle D \rangle_{exp}$ = 1.07 ± 0.14 eV with allowance for the missing of 5 levels. In /52/, in the region 0.01-90 eV 52 resonances are parametrized. Comparison with the results of /51/ shows that a considerable level missing occurs. the authors of /52/ have obtained $\langle D \rangle_{exp}$ ^{249}Cf. However, their results are not available and hence we have used the value from /51/.

<u>^{252}Cf.</u> In /53/, the fission ^{252}Cf cross section is measured with the nuclear explosion in the region 20 eV-5 MeV. The authors do not mention the value $\langle D \rangle_{exp}$. However, Lynn /3/ gives, with reference to this work, $\langle D \rangle_{exp}$ = 16 eV. We have adopted this value here but its reliability is unknown.

In conclusion, it should be noted that the most unreliable values $\langle D \rangle_{exp}$ are those for the following isotopes: ^{229}Th, ^{231}Pa, ^{233}Pa, ^{232}U, ^{244}Pu, ^{242m}Am, ^{247}Cm and ^{252}Cf.

5. DATA ON THE LOW-LYING LEVEL DENSITY

We do not intend to analyze the available spectroscopic information on low-lying levels since such an analysis is regularly reported in Nuclear Data Sheets Evaluations. We have used the results accumulated during 1976-1978. And only for the ^{250}Cf nucleus use has been made of the data /54/, giving a more comprehensive picture of a low-lying state spectrum. The total number of the isotopes considered is about 100 from ^{225}Th to ^{254}Cf. Note that if the level energy is as a rule specified for many levels, their spin and parity assignment is very poor.

6. PARITY DEPENDENCE OF THE LEVEL DENSITY

As a rule, the level density models are based on the parity independence assumption. The model cited in Sect. 2 is not an exception. However, the calculations performed by the combinatorial /55,56/ and statistical methods /57/ show that in a number of cases this assumption is not valid at low energies. In /57/, it is stated that for deformed nuclei the deviations from the equality $\rho_+ = \rho_-$ are probably negligible. It is therefore advisable to check the validity of the equiprobable parity distribution assumption for the nuclei being greatly deformed. This may be, in principle, performed by analyzing the average resonance radiation widths, $\langle \Gamma_\gamma \rangle$, of different parity /57/, the average spacings of different-parity resonances or the spectroscopic data on the discrete spectrum. Unfortunately, even for the most thoroughly studied nucleus ^{238}U there are no radiation widths for the p-wave resonances.

The existing evaluations of the average s- and p-wave resonance spacings indicate that at the neutron binding energy $\rho_+ = \rho_-$. So, according to the evaluation /29/ for ^{238}U $\langle D \rangle_0 = 24.8 \pm 2$ eV and $\langle D \rangle_1 = 8.91 \pm 0.1$ eV, which is consistent with the (2J+1) law within the experimental errors.

The analysis of the discrete spectrum of nuclei from Th to Cf shows that the relation $\rho_+ = \rho_-$ is valid within ±50% (Fig. 8) for 69% of 51 nuclei. Proceeding from the insufficiently reliable data on the level parity and poor statistics, this coincidence seems to be quite satisfactory to consider that the assumption $\rho_+ = \rho_-$ does not contradict the available data for heavy deformed nuclei at low excitation energies.

The main bulk of the studied nuclei (71 of 98) having positive parity of the ground state, this may account for the ratio $N_-/N_+ \sim 1$. Otherwise, this may point to the effect of the first band-head states.

7. ANGULAR MOMENTUM DEPENDENCE OF THE LEVEL DENSITY

Expression (4) for the energy and spin dependence of the level density is given in the form:

$$\rho(U,J) = \rho(U)f(U,J) \tag{22}$$

with the total level density

$$\rho(U) = \frac{K_{rot}K_{vib}\,\omega(U)}{\sqrt{2\pi}\,\sigma_{\parallel}} \;. \tag{23}$$

K_{rot} is the factor allowing for the level density increase due to the contribution of rotational modes

$$K_{rot} = \sigma_{\perp}^{2} \quad , \tag{24}$$

$$f(U,J) = \frac{(2J+1)\ \exp\left[-J(J+1)/2\sigma_{\perp}^{2}\right]}{2\sigma_{\perp}^{2}} \quad . \tag{25}$$

Expression (25) is the well-known angular momentum distribution law in the Fermi-gas model except for the parameter σ^2 consistent with $\sigma_{\perp}^2$. This means that under the conditions which allow (2) instead of (1) the use of the collective modes does not change the angular momentum distribution law essentially.

The applicability of law (25) for the range of spins of interest to evaluate neutron cross sections causes no doubts. It is natural to try to extend law (25) to the low energy region for which the total level density is expressed by the constant-

-temperature model. The similar problem is considered in /11/, which however excludes transactinides.

The analysis of a discrete spectrum for the nuclei of interest shows that as a rule the level spin assignment is insufficiently reliable except the low-lying bands.

The maximum likelihood method gives for (25) the following $\sigma_{\perp}^2$ evaluation:

$$\sigma_{\perp\,exp}^2 = \frac{1}{2N} \sum_i J_i(J_i + 1) \qquad (26)$$

where N is the number of the spin-identified levels. Despite evaluation (26) is weakly sensitive to the level missing, $\sigma_{\perp\,exp}^2$ was found using only the data for the energy region with the relatively insignificant level missing. The latter was found by the constant-temperature model fitting of the cumulative number of levels. The parameters $\sigma_{\perp\,exp}^2$ for 41 nuclei with a well explored discrete spectrum are given in Fig. 9. For odd-odd nuclei $\sigma_{\perp\,exp}^2$ is seen to be much higher. But there are only two such nuclei. No difference in $\sigma_{\perp\,exp}^2$ is observed for even-even and odd nuclei. That is, there are no data on the nuclear parity dependence of $\sigma_{\perp\,exp}^2$. In spite of the difference between the ground state spins and the upper range boundary, $\sigma_{\perp\,exp}^2$ values may be fairly described by the linear dependence of the mass number A. The least square method yields the following parametrization:

$$\sigma_{\perp\,exp}^2 = 0.15624A - 26.76. \qquad (27)$$

The data available on the spin distribution of discrete levels may be approximately fitted by law (25) provided $\sigma_{\perp}^2 = \sigma_{\perp\,exp}^2$. It is illustrated in Fig. 10 showing the distributions for all nuclei with a relatively large number of spin-identified levels. The values of $\sigma_{\perp\,exp}^2$ enable us to describe fairly well, within the constant-temperature model, the cumulative number of levels N(E,J) of ^{234}U, ^{235}U, ^{239}Pu, ^{240}Pu, ^{245}Cm and ^{246}Cm that have a comparatively large number of the spin-assigned levels (Fig. 11). This indicates the possibility to substitute, if necessary, the discrete spectrum by the continuous one using the constant-temperature model and law (25) with $\sigma_{\perp\,exp}^2$ as well as to employ law (25) for the energies above the discrete spectum upper boundary provided that the $\sigma_{\perp}^2$ parameter is chosen appropriately.

It might be not quite correct to use the $\sigma_{\perp}^2$ calculations by the superfluid as well as by any other statistical model for low energies as the basic parameter a deduced from the average neutron resonance spacing or systematics can hardly represent the structure of low-lying levels. It seems therefore more reasonable /11/ to use $\sigma_{\perp}^2 = \sigma_{\perp\,exp}^2$ up to the energies, for which the discrete spectrum may be regarded reliably identified (this boundary is designated through E_{bound}); from E_{bound} up to the matching energy E_c, $\sigma_{\perp}^2$ is determined by the linear interpolation between $\sigma_{\perp\,exp}^2$ and $\sigma_{\perp}^2(E_c)$ calculated using the superfluid model. For the nuclei whose discrete spectrum is identified insufficiently to evaluate $\sigma_{\perp\,exp}^2$, expression (17) may be used along with the following values of E_{bound}:

E_{bound} = 1.2 MeV for even-even nuclei

E_{bound} = 0.6 MeV for odd nuclei

E_{bound} = 0.3 MeV for odd-odd nuclei .

The comparison of the energy dependence of the suggested $\sigma_{\perp}^2$ and that calculated by the constant-temperature model is presented in Fig. 12 for ^{234}U.

Table 2 comprises $\sigma^2_{\perp exp}$ and E_{bound} values for different nuclei deduced both from the experimental discrete level data and by systematics. The matching energy E_c being the upper $\sigma^2_{\perp}$ interpolation point is given below.

8. PARAMETRIZATION OF THE DATA ON THE LOW-LYING LEVEL SPECTRA

Based on the above experimental data on neutron resonances, the parameter a and its asymptotic value $\tilde{a}$ are found for the level density model employed. The quasi-classical evaluation $\bar{m}^2 = 0.24\ A^{2/3}$ is applied to evaluate the inertia moment $F_{\parallel}$ of an excited nucleus with the quadrupole deformation parameter ε assumed to be 0.24 for all nuclei considered. We have used $\gamma = 0.064$ /58/ for nuclei with the mass numbers $150 \leqslant A \leqslant 245$ to determine the energy dependence of the parameter a. The level density parameter systematics was reported in /58/ but included the transactinide average neutron resonance spacings measured till 1970 being less accurate and numerous than those in the present work.

Two sets of the a and $\tilde{a}$ parameters are obtained. One of them corresponds to the ground state correlation functions Δ_{oZ} and Δ_{oN} deduced from the even-odd nuclear mass difference systematics: $\Delta_{oZ} = \Delta_{oN} = 12/\sqrt{A}$ /5/. The values of Δ_{oZ} and Δ_{oN} based on the nuclear ground state masses from /9/ or from Nuclear Data Sheets for 1976-1978 are given in Figs. 13 and 14. It is obvious (Fig. 13) that within the range of the mass numbers considered the relation $12/\sqrt{A}$ describes only roughly the average trend of pairing neutron energies which are identified here with the neutron correlation function Δ_{oN}. Pairing proton energies are described by the curve

$12/\sqrt{A}$ more accurately (Fig.14). Therefore, the second set of the parameters for the experimental values of pairing energies was obtained using the systematics of $12/\sqrt{A}$ for Δ_{oZ} when no experimental data are available. The value of Δ_{oN} was taken from the systematics for the isotopes of the nucleus under consideration.

Figures 15 and 16 present the a and $\tilde{a}$ parameters obtained from the experimental data for both types of Δ_o. When using experimental pairing energies, the $\tilde{a}$ and a parameters decrease. Here, the quasi-classical approximation $\tilde{a}=\alpha A$ gives α equal to 0.0893. If $\Delta_{oZ} = \Delta_{oN} = 12/\sqrt{A}$, then α=0.0951. The use of the experimental Δ_{oZ} and Δ_{oN} values show no reduction in the fluctuations against the straight line. Strong fluctuations of $\tilde{a}/A$ for some nuclei (^{231}Th, ^{233}Th, ^{245}Pu and ^{253}Cf) are due to uncertainties in $\langle D \rangle_{exp}$ values.

The parameters $a(S_n)$ and $\tilde{a}$ for experimental $\Delta_{oZ(N)}$ are given in Table 1, shell corrections δW_{exp} and average spacings $\langle D \rangle_{I-1/2}$ and $\langle D \rangle_{I+1/2}$ for the s-wave being included.

9. PARAMETRIZATION OF THE DATA ON THE LOW-LYING LEVEL SPECTRA

Using the value Δ_o = 12/ A, resulting from the description of neutron and proton pairing energies for the entire range of mass numbers, as the correlation functions Δ_{oZ} and Δ_{oN} gives a set of parameters such as T, E_o and E_c. The parameters T, E_o and E_c for even-even nuclei with the data both on the neutron resonance density and on the low-lying level spectra are presented in Figs.17a through 21a. The temperature T weakly fluctuates against the average value T = 0.3850.

MeV for even-even nuclei. Fluctuations of $\bar{T}$ are stronger for odd nuclei (Fig. 18a), the value of $\bar{T}$ being practically equal to that for even-even nuclei. This is attributed to the missing of levels in odd nuclei spectra rather than to the odd-even parity effect. This is indirectly justified by the sfact that for the odd nuclei with the well explored spectra the values of T are close to $\bar{T}$ for even-even nuclei (^{235}U, for instance). Extremely low T for ^{245}Pu is due to the small, compared to well studied nuclei, number of discrete levels in the same energy range. Also, the value $\langle D \rangle_{exp}$ for this nucleus is not reliable, there are only four resonances in fission cross section.

The values of E_o for even-even nuclei are closely grouped around zero (Fig. 19a). Foe odd nuclei, E_o is, on the average, 0.7 MeV beloW the one for odd-odd nuclei. Evidently, E_o may be considered as an odd-even shift in the excitation energy equal to the correlation function for the ground state Δ_o. It is seen from Fig. 20a that $E_o + \Delta_o$ values for the nuclei with the well studied spectra are also close to zero.
The observed fluctuations of T and E_o are due to missing of levels.

In the case of the poor studied spectra thr average parameters $\bar{T}$ = 0.585 MeV and E_o = 0 may be used for even-even and $E_o = -\Delta_o$ for odd nuclei. Note that these average parameters enable one to describe the cumulative number of levels for nuclei, particularly, odd-odd ones, whose spectrum is well studied, and the data on $\langle D \rangle_{exp}$ are not available. The parameters E_c (Fig. 21a) are also subdivided into two groups corresponding to even-even and odd nuclei.

As is shown above, the satisfactory description of the cumulative number of levels for odd-odd nuclei in terms of the superfluid model involving collective modes results from the appreciable missing of levels since N(E) behaves in the same way as in the case of odd nuclei while it must rise more steeply. Hence, it seems unjustified to evaluate T, E_o and E_c. It may be assumed, as in the case of odd nuclei, that T= 0.385 MeV and $E_o = -2\Delta_o$.

The calculation of the observed neutron resonance spacing may well support the systematics suggested for the T and E_o parameters of constant temperature model. The calculation results are given in Fig. 22 as $\langle D \rangle_{theor} / \langle D \rangle_{exp}$. These are obtained assuming $a_{crit} = a(E_c)$, which does not affect the accuracy of calculations since the critical energy is quite close to E_c. It is seen that the greater bulk of the obtained values including those for odd-even nuclei are withing the limits of ± 50%. The case is different with ^{238}Np, ^{245}Pu, ^{243}Cm, ^{253}Cf. The $\langle D \rangle_{exp}$ data for ^{245}Pu and ^{253}Cf are rather unreliable.

The parameters T, E_o, E_c and, hence, the $\langle D \rangle_{theor} / \langle D \rangle_{exp}$ values may fluctuate either due to the missing of discrete levels or due to the use of systematics $\Delta_o = 12/\sqrt{A}$ which does not take into account the specific properties of nuclei. It highly overestimates neutron pairing energies, while among odd nuclei with $\langle D \rangle_{exp}$ data, ^{243m}Am alone is odd-even. It may be assumed that the use of experimental pairing energies for Δ_{oZ} and Δ_{oN} evaluation will improve the parameter systematics. We have obtained ahother set of the constant-temperature model parameters which correspond to the correlation functions Δ_{oZ} and Δ_{oN}. The parameters T, E_o aand E_c are given in Figs. 17b through 21b. No substantial of these parameters fluctuations is observed. Neither $\langle D\rangle_{theor}/\langle D\rangle_{exp}$ fluctuations are decreased as a result. We have therefore chosen the first parameter set. Note that $\Delta_{oZ(N)}$ being used gives somewhat lower average $\bar{T}$ =0.370 MeV when E=0 for even-even nuclei.

The constant-temperature model description of the cumulative number of levels of even-even nuclei with the $\langle D\rangle_{exp}$ data is given in Fig 3. The analogous description for odd nuclei is shown in Fig. 5. The conclusion on the possible use of the average $\bar{T}$ and E_o parameters is supported by the description of the cumulative number of levels of even-even nuclei by the average parameters $\bar{T}$ =0.385 MeV and E_o=0 (Fig. 4) and of odd nuclei with no $\langle D\rangle_{exp}$ data by $\bar{T}$ = =0.385 MeV and $E_o = -\Delta_o$ (Fig. 6). Obviously, $\bar{T}$ and $E_o$parameters estimated for these nuclei by the matching will fit the systematics.

Thus, the following procedure of the level density parameter evaluation may be suggested both for low and neutron binding energies for nuclei having no complete set of the experimental data.

1. $\langle D\rangle_{exp}$ being known for the nuclei, whose spectrum is not studied, either T or E_o is estimated as:

$$T = \bar{T}$$

$$E_o = \begin{cases} 0 & \text{- even-even nuclei} \\ \Delta_o & \text{- odd nuclei} \\ 2\Delta_o & \text{- odd-odd nuclei} \end{cases}$$

the other parameter being found from the matching conditions.

2. With the spectrum of low-lying levels known and no data on $\langle D \rangle_{exp}$, the parameter $\bar{T}$ may be used, E_o is specified by discrete spectrum and then the parameters E_c and are derived.

As is seen, the obtained parameter systematics gives fair description of the cumulative number of discrete levels for low energies. The data on $\langle D \rangle_{exp}$ available ,it may be regarded that the level density is reliably estimated for the energies being of interest for neutron cross section evaluation. If no data on $\langle D \rangle_{exp}$ are available, the accuracy of $\rho(E)$ prediction is not so high for the energies above E_c energy which is 4; 3.2 and 2.4 Mev for even-even, odd and odd-odd nuclei, respectively. In this case, the neutron channelcompetition in the cross section evaluation up to E_c energies may be also reliably taken into account through the interpretation of the discrete spectrum analysis. Care must be taken when applying the constant-temperature model near the ground state. Better to say, the discrete spectrum data are more appropriate in this case. All level density parameters as well as the average spacings between s-resonances have been obtained for different nuclei by fittingthe experimental data and by calculating in terms of the parameters following from the systematics. These data are listed in Table 3.

Analyse the parameters E_c and a estimated by the T and E_o systematics. Figure 23 presents the comparison of the parameter E_c obtained from the systematics and the experimental values. Its linear dependence is of interest. The agreement being good for even-even nuclei, the appreciable overestimation is seen for odd nuclei which is most probably due to the missing of levels in the discrete spectrum. In Fig. 24 the ratios of the basic level density parameter for the neutron binding energy $a(S_n)$ and its asymptotic value $\tilde{a}$ to the mass number estimated from the systematics and experimental data on $\langle D \rangle_{exp}$ are compared. The linear dependence $a(S_n)/A$ is of the form:

$$a(S_n)/A = -\ 1.487 \cdot 10^{-3} A + 0.4529 \quad . \qquad (28)$$

Its parameters differ strongly from the systematics of other authors. The decrease in $a(S_n)/A$ with increasing A may be attributed to the shell closure as for double magic nuclei.

To conclude, consider the fluctuation of the constant--temperature model parameters due to $\langle D \rangle_{exp}$ fluctuations only. To do this, temperatures and matching energies E_c are calculated for E_o equal to 0, $-\Delta_o$ and $-2\Delta_o$ for even-even, odd and odd-odd nuclei, respectively. The T values obtained are shown in Fig. 25. It is easily seen that only the values for ^{245}Pu and ^{253}Cf nuclei essentially differ from the average $\bar{T}$ = 0.388 MeV. It might be expected since the $\langle D \rangle_{exp}$ data for these nuclei are unreliable. Dense temperature grouping around $\bar{T}$ for other nuclei points to the relative reliability of the $\langle D \rangle_{exp}$ data.

Calculated E_c values are given in Fig. 26. The dependence $E_c(A)$ is linear but for the nuclei ^{245}Pu and ^{253}Cf which makes doubtful the reliability of their $\langle D \rangle_{exp}$ data.

The same figure shows the E_c dependence calculated from the systematics $\bar{T}$ = 0.388 MeV and $E_o = 0, -\Delta_o$ and $-2\Delta_o$ for the appropriate nuclei. They are straight lines in good agreement with the data obtained using the $\langle D \rangle_{exp}$ data. This supports once again the reliability of the suggested systematics and the data in Table 3 are therefore derived for $\bar{T}$ = 0.388 MeV.

ACKNOWLEDGEMENT

We would like to thank E.A. Zharkova for preparing the manuscript of this paper.

REFERENCES

1. Antsipov G.V., Zenevich V.A., Klepatskij A.B., Konshin V.A., Sukhovitskij E.Sh., Proc. of the IXth Intern. Symposium on Fast Neutron Interactions with Nuclei, Dresden, GDR, 26-30 Nov., 1979, ZFK-410, p. 141.
2. Ignatyuk A.V., Istekov K.K., Smirenkin G.N., Nuclear Physics, vol. 29, 1979, p. 875.
3. Lynn J.E., Systematics for Neutron Reactions of the Actinide Nuclei, AERE-R7468, 1974.
4. Baba H., Nucl. Phys., v. A159, 1970, p. 625.
5. Bohr O., Mottelson B., Atomic Nucleus Structure, vol. 2, Moscow, Ird. Mir, 1977.
6. Ignatyuk A.V., Shubin Yu.N., Izv. AN SSSR, Ser. Fiz., vol. 37, 1973, 1947.
7. Ignatyuk A.V., Proc. of Meeting on the Use of Nuclear Theory in Neutron Data Evaluation, Triest, 1975, IAEA, v. 1, 1976, p. 211.
8. Myers W.D., Swiatecki W.S., Ark. Fysik, v. 36, 1967, p. 593.
9. Kravtsov V.A., Atom Masses and Binding Energies of Nuclei, Moscow, Atomizdat, 1974.
10. Cameron A.G.W., Gilbert G., Can. J. Phys., v. 43, 1965, p. 1446.
11. Reffo G., Parameter Systematics for Statistical Theory Calculations of Neutron Reaction Cross Sections, RT/FI (78) 11, 1978.
12. Fröhner F.H., Fisher U., Jahn H., NEANDC(E)-202U, v. 5, INDC(Ger)-21L, 1979, p. 31.
13. ENDF-102 Data Formats and Procedures for the Evaluated Nuclear Data File, ENDF, revised by Garber D., Dunford C., Pearlstein S., BNL-NCS-50496, 1975.

14. Luers B.R., Felvinci J.P., Melkonian E., Havens W.W., ^{229}Th Fission Cross Sections and Resonance Parameters, BNL-NCS-24273, DOE/NDC-12/U, NEANDC(US)-203/U, INDC(USA)--79/U, 1978, p. 43.

15. Kalebin S.M., Palei P.N., Ivanov R.N., Karalova Z.K., Kukabadze G.M., Pyzhova Z.I., Rykolaine G.V., Atomic Energy, v. 26, 1969, p. 507.

16. Cote R.E., Diamond H., Gindler J.E., Hla Shwe, Phys. Rev. C, v. 176, 1968, p. 1421.

17. Ganeman S., Evaluation of Statistical Resonance Parameters for ^{232}Th in 4 to 41 keV Energy Region, INDC(IND)-26/GJ, RRC-42, 1980.

18. Vasiliu G., Mateescu S., Gheorghe D. et al., Nuclear Data Evaluation for ^{232}Th, INPR, Pitesti-Romania, 1979.

19. De Saussure G., Macklin R.L., Evaluation of the ^{232}Th Neutron Capture Cross Section above 3 keV, ORNL/TM-6161, ENDF--255, 1977.

20. Rahn F., Camarda H.S., Hacken G., Havens W.W., Liou H.I., Rainwater J., Slagowitz M., Wynchank S., Phys. Rev. C, v. 6, 1972, p. 1854.

21. Simpson F.B., Burgus W.H., Evans J.E., Kirby H.W., Nucl. Sci. Eng., v. 12, 1962, p. 243.

22. Simpson F.B., Codding J.W., Nucl. Sci. Eng., v. 28, 1967, p. 133.

23. Aughampaugh G.F., Bowman C.D., Evans J.E., Nucl. Phys., v. A112, 1968, p. 329.

24. Kolar W., Carraro G., Nastri G., Proc. IAEA Conf. on Nuclear Data for Reactors, Helsinki, v. 1, 1970, p. 387.

25. James G.D., Dabbs J.W.T., Harvey J.A., Hill N.W., Schindler R.H., Phys. Rev. C, v. 15, 1977, p. 2083.

26. Moore M.S., Moses J.D., Keyworth G.A., Dabbs J.W.T., Hill N.W., Phys. Rev. C, v. 18, 1978, p. 1328.

27. Carraro G., Brusegan A., Nucl. Phys., v. A257, 1976, p. 333.

28. McNally J.H., Barnes J.W., Dropesky B.J., Seeger P.A., Wolfsberg K., Phys. Rev. C, v. 9, 1974, p. 717.

29. De Saussure G., Olsen D.K., Perez R.B., Difilippo F.C., Progress in Nucl. Energy, v. 3, 1979, p. 87.

30. Mewissen L., Poortmans F., Cornelis E., Vanpraet G., Angeletti A., Rohr G., Weigman H., Nucl. Sci. Eng., v. 70, 1979, p. 155.

31. Caner M., Yiftah S., Neutron Cross Sections for Plunonium-238, IA-1301, INDC(ISL)-2/L, 1974.

32. Silbert M.G., Berreth J.R., Nucl. Sci. Eng., v. 52, 1973, p. 187.

33. Silbert M.G., Moat A., Young T.E., Nucl. Sci. Eng., v. 52, 1973, p. 176.

34. Konshin V.A., Morogovsky G.B., Sukhovitskij E.Sh., Izv. AN BSSR, Ser. Fir.-Energ. Nauk, No. 2, 1974, p. 21.

35. Konshin V.A., Antsipov G.V., Sukhovitskij E.Sh., Bakhanovich L.A., Klepatskij A.B., Morogovskij G.B., Porodzinskij Yu.V., Evaluation of Nuclear Data for Pu-241 in Neutron Energy Range from 10^{-3} eV to 15 MeV, INDC(CCP)-142/GJ, 1980.

36. Antsipov G.V., Bakhanovich L.A., Konshin V.A., Maslov V.M., Morogovskij G.B., Sukhovitskij E.Sh., Porodzinskij Yu.V. Collected Papers of HMTI of BSSR Academy of Sciences,

Nuclear Data Evaluation for ^{242}Pu in Neutron Energy Range from 10^{-5} eV to 15 MeV, Minsk, 1979, p. 3.

37. Aughampaugh G.F., Farrel J.A., Bergen D.W., Nucl. Phys., v. A171, 1971, p. 31.

38. Maino G., Menapace E., Motta M., Ventura A., ^{241}Am Neutron Cross Sections in the Resonance Region, 1979.

39. Browne J.C., Howe R.E., Dougan R.J., Dupsyk R.J., Landrum J.H., Proc. Intern. Conf. on Neutron Physics and Nuclear Data for Reactors and other Applied Purposes, Harwell, 1978, p. 887.

40. Simpson O.D., Simpson F.B., Harvey J.A., Slaughter G.G., Benjamin R.W., Ahlfred C.E., Nucl. Sci. Eng., v. 55, 1974, p. 273.

41. Artamonov V.S., Ivanov R.N., Kalebin S.M. et al., Proc. 4th All-Union Conference of Neutron Physics, Kiev, v. 2, 1977, p. 257.

42. Keyworth G.A., NEANDC(US)-199L, 1976, p. 353.

43. Menapace E., Motta M., Ventura A., Montaguti A., Evaluation of Cm-242 in the Resonance Region, Bologna, 1979.

44. Berreth J.R., Simpson F.B., Rusche B.C., Nucl. Sci. Eng., v. 49, 1972, p. 145.

45. Mughabghab S.F., Garber D.I., Neutron Cross Sections, v. 1, Resonance Parameters, BNL-325, 3rd ed., 1973.

46. Browne J.C., Benjamin R.W., Karraker D.G., Nucl. Sci. Eng., v. 65, 1979, p. 166.

47. Martinelli T., Menapace E., Motta M., Vaccari M., Ventura A., Evaluation of ^{246}Cm Neutron Cross Sections in the Resonance Region, RT/FI(80), 1980.

48. Martinelli T., Menapace E., Motta M., Vaccari M., Evaluation of Cm-247 Neutron Cross Sections in the Resonance Region, RT/FI(80), 1980.

49. Benjamin R.W., Ahlfred C.E., Harkey J.A., Hill N.W., Nucl. Sci.Eng., v. 55, 1974, p. 440.

50. Harvey J.A., Benjamin R.W., Hill N.W., Raman S., The Neutron Total Cross Section and Resonance Parameters of ^{249}Bk, BNL-NCS-21501, ERDA/NDC-3/U, 1976, p. 198.

51. Silbert M.G., Nucl. Sci. Eng., v. 51, 1973, p. 376.

52. Carlton R.F., Harvey J.A., Pandey M.S., Hill N.W., Benjamin R.W., Program of the Intern. Conf. on Nuclear Cross Sections for Technology, Knoxville, 1979, Report FC9.

53. Moore M.S., McNally J.H., Phys. Rev. C, v. 4, 1971, p. 273.

54. Reich C.W., Helmer R.G., Gehrke R.J., BNL-NCS-24273, 1978, p. 66.

55. Hillman M., Grover J., Phys. Rev., v. 185, 1969, p. 1303.

56. Soloviev V.G., Stoyanov Ch., Vdovin A.I., Nucl. Phys., v. A224, 1974, p. 411.

57. Blokhin A.I., Ignatyuk A.V., Proc. of 3rd All-Union Conference on Neutron Physics, Kiev, 1975, pt. 3, p. 3.

Table 1

Data on the Neutron Resonance Density and Parametrization Results

Compound nucleus	Iπ	S_n, MeV	$\langle D \rangle_{obs}$, eV	δW_{exp}, MeV	$\tilde{a}$, MeV^{-1}	$a(S_n)$, MeV^{-1}	$\langle D \rangle_{I-1/2}$, eV	$\langle D \rangle_{I+1/2}$, eV
1	2	3	4	5	6	7	8	9
^{230}Th	5/2+	6,790	0,40	-1,008	24,070	22,725	0,931	0,701
^{231}Th	0+	5,128	9,8 ± 1,6	-1,024	25,128	23,708		9,800
^{233}Th	0+	4,787	16,6 ± 0,9	-0,917	26,873	25,526		16,600
^{232}Pa	(3/2-)	5,560	0,37	-1,315	21,337	19,823	0,968	0,599
^{234}Pa	3/2-	5,197	0,69	-1,272	21,298	19,821	1,804	1,117
^{233}U	0+	5,744	4,1	-1,733	22,719	20,586		4,100
^{234}U	5/2+	6,841	0,61 ± 0,07	-1,704	22,649	20,559	1,422	1,068
^{235}U	0+	5,305	10,6 ± 0,5	-1,700	21,771	19,708		10,600
^{236}U	7/2-	6,546	0,438±0,038	-1,624	22,197	20,220	0,966	0,801
^{237}U	0+	5,125	16,2 ±0,8	-1,680	21,211	19,217		16,200
^{238}U	1/2+	6,143	3,5±0,8	-1,447	20,926	19,255	13,831	4,685
^{239}U	0+	4,804	24,8 ± 2	-1,418	21,717	19,975		24,800
^{238}Np	5/2+	5,480	0,740±0,061	-2,041	19,231	17,122	1,732	1,292
^{239}Pu	0+	5,655	9,2 ± 0,7	-2,365	19,566	17,044		9,200
^{240}Pu	1/2+	6,534	2,38± 0,06	-2,116	20,666	18,287	9,414	3,186
^{241}Pu	0+	5,241	13,5± 0,5	-2,118	20,044	17,702		13,500
^{242}Pu	5/2+	6,301	1,34± 0,10	-1,883	20,041	17,976	3,133	2,342

Table1(continued)

1	2	3	4	5	6	7	8	9
^{243}Pu	0+	5,037	14,23 ± 0,54	-1,917	22,268	19,874		14,230
^{245}Pu	0+	4,720	11,4 ± 4	-1,591	28,319	25,842		11,400
^{242}Am	5/2-	5,529	0,58 ± 0,04	-2,487	19,606	17,001	1,359	1,012
^{243}Am	5-	6,425	0,45	-2,128	17,592	15,612	0,952	0,853
^{244}Am	5/2	5,364	0,68 ± 0,06	-2,287	20,101	17,623	1,592	1,187
^{243}Cm	0+	5,701	17,6 ± 3,3	-2,692	18,403	15,703		17,600
^{244}Cm	5/2+	6,799	0,50 ± 0,20	-2,559	21,981	18,931	1,170	0,873
^{245}Cm	0+	5,519	11,8 ± 1,20	-2,676	19,964	17,039		11,800
^{246}Cm	7/2+	6,451	1,14 ± 0,14	-2,439	20,812	18,029	2,520	2,081
^{247}Cm	0+	5,157	21,3 ± 5,3	-2,430	21,378	18,473		21,300
^{248}Cm	9/2-	6,210	1,2	-2,193	20,418	17,955	2,561	2,258
^{249}Cm	0+	4,713	40 ± 5	-1,971	21,050	18,703		40,000
^{250}Bk	7/2+	4,969	1,1	-2,335	20,071	17,513	2,436	2,006
^{250}Cf	9/2-	6,618	1,07 ± 0,14	-2,955	19,498	16,377	2,290	2,008
^{253}Cf	0+	4,792	16	-2,013	24,057	21,312		16,000

Table 2

The Parameters of the Spin Dependence of the Level Density of Transactinides at Low Excitation Energy

Nucleus	$\sigma_{\perp}^2$ exp	E_{bound}, MeV	Nucleus	$\sigma_{\perp}^2$ exp	E_{bound}, MeV
1	2	3	4	5	6
225 Th	8,39	0,6	237 U	9,46	0,946
226 Th	8,55	1,2	238 U	13,25	1,290
227 Th	8,71	0,6	239 U	10,75	0,373
228 Th	6,13	1,169	240 U	10,74	1,2
229 Th	9,39	0,327			
230 Th	8,93	1,130	233 Np	9,64	0,6
231 Th	9,92	0,615	234 Np	9,80	0,3
232 Th	9,72	1,125	235 Np	12,57	0,201
233 Th	8,63	0,682	236 Np	10,11	0,3
234 Th	9,80	1,2	237 Np	14,02	0,515
			238 Np	10,74	0,343
229 Pa	9,02	0,6	239 Np	8,67	0,449
230 Pa	9,18	0,3	240 Np	10,74	0,3
231 Pa	8,38	0,352	241 Np	10,89	0,6
232 Pa	9,49	0,3			
233 Pa	8,21	0,367	233 Pu	9,64	0,6
234 Pa	9,80	0,3	234 Pu	9,80	1,2
235 Pa	9,96	0,6	235 Pu	9,96	0,6
236 Pa	10,11	0,3	236 Pu	10,11	1,2
237 Pa	7,93	0,393	237 Pu	8,98	0,591
238 Pa	10,43	0,3	238 Pu	6,71	1,229
			239 Pu	11,32	0,659
229 U	9,02	0,6	240 Pu	10,41	1,309
230 U	9,18	1,2	241 Pu	9,92	0,335
231 U	9,33	0,6	242 Pu	10,13	1,153
232 U	10,28	1,212	243 Pu	10,06	0,704
233 U	11,80	0,914	244 Pu	12,63	1,194
234 U	11,35	1,497	245 Pu	8,92	0,723
235 U	12,22	0,492	246 Pu	11,68	1,2
236 U	9,21	1,343			

Table 2 (continued)

I	2	3	4	5	6
^{238}Am	I0,43	0,3	^{244}Bk	II,36	0,3
^{239}Am	I0,60	0,386	^{245}Bk	II,52	0,6
^{240}Am	I0,74	0,3	^{246}Bk	II,68	0,3
^{24I}Am	I0,89	0,6	^{247}Bk	II,83	0,6
^{242}Am	I5,85	0,38I	^{248}Bk	II,99	0,3
^{243}Am	I0,25	0,344	^{249}Bk	II,00	0,829
^{244}Am	II,36	0,3	^{250}Bk	I5,8I	0,3I6
^{245}Am	II,52	0,6	^{25I}Bk	I2,46	0,6
^{246}Am	II,68	0,3			
^{247}Am	II,83	0,6	^{245}Cf	II,52	0,6
^{239}Cm	I0,58	0,6	^{246}Cf	II,68	I,2
^{240}Cm	I0,74	I,2	^{247}Cf	II,83	0,6
^{24I}Cm	I0,89	0,6	^{248}Cf	II,99	I,2
^{242}Cm	II,05	I,2	^{249}Cf	I3,I4	0,466
^{243}Cm	II,2I	0,6	^{250}Cf	I2,30	I,2
^{244}Cm	II,36	I,2	^{25I}Cf	I3,92	0,442
^{245}Cm	I3,24	0,9I3	^{252}Cf	I2,6I	I,2
^{246}Cm	I0,22	I,367	^{253}Cf	I2,77	0,6
^{247}Cm	I0,50	0,550	^{254}Cf	I2,92	I,2
^{248}Cm	II,99	I,2			
^{249}Cm	8,2I	0,498			
^{250}Cm	I2,30	I,2			

Table 3

Data on the Parameters of the Transactinide Level Density in the ^{225}Th – ^{254}Cf Region

Compound nucleus	Iπ	S_n, MeV	δW_{exp}, MeV	T, MeV	E_0, MeV	E_c, MeV	$a(S_n)$, MeV^{-1}	$\tilde{a}$, MeV^{-1}	$\langle D \rangle_{I+1/2}$, eV	$\langle D \rangle_{I-1/2}$, eV
1	2	3	4	5	6	7	8	9	10	11
^{225}Th	0+	5,760	-0,297	0,3879	0	3,610	24,550	24,955	2,725	-
^{226}Th	(3/2+)	7,181	-0,710	0,3879	0	4,380	24,250	25,232	0,309	0,498
^{227}Th	0+	5,456	-0,719	0,3879	0	3,560	23,950	24,935	5,640	-
^{228}Th	(3/2+)	7,128	-0,980	0,3879	0	4,326	23,702	25,052	0,365	0,589
^{229}Th	0+	5,239	-0,893	0,3879	0	3,502	23,400	24,614	9,598	-
^{230}Th*	5/2+	6,790	-1,008	0,4013	-0,1077	4,6	22,349	23,669	0,701	0,932
^{231}Th*	0+	5,128	-1,024	0,3849	-0,0250	3,6	24,614	26,080	9,8	-
^{232}Th	5/2(+)	6,434	-1,014	0,3879	0	4,212	22,550	23,897	1,346	1,794
^{233}Th*	0+	4,787	-0,917	0,3735	0,0500	3,4	26,039	27,408	16,6	-
^{234}Th	(1/2+)	6,179	-0,889	0,3879	0	4,160	21,950	23,097	5,326	15,720
^{229}Pa	(3+)	7,045	-0,955	0,3879	0	3,502	23,434	24,703	0,064	0,081
^{230}Pa	(5/2)	5,786	-1,171	0,3879	0	2,684	23,125	24,701	0,186	0,248
^{231}Pa	(2-)	6,818	-1,089	0,3879	0	3,454	22,838	24,266	0,142	0,206
^{232}Pa*	(3/2-)	5,560	-1,315	0,3917	0	2,576	21,259	22,902	0,593	0,967
^{233}Pa	(2-)	6,520	-1,173	0,3879	0	3,396	22,287	23,807	0,277	0,400
^{234}Pa*	3/2-	5,197	-1,272	0,3895	0	2,560	21,432	23,049	1,118	1,802
^{235}Pa	4(+)	6,122	-0,976	0,3879	0	3,348	21,673	22,902	0,456	0,534
^{236}Pa	(3/2-)	4,840	-0,954	0,3879	0	2,540	21,358	22,558	2,243	3,627
^{237}Pa	(1-)	5,930	-0,708	0,3879	0	3,292	21,117	21,975	1,563	3,059

Table 3 (continued)

I	2	3	4	5	6	7	8	9	I0	II
^{238}Pa	(I/2+)	4,480	-0,559	0,3879	0	2,494	20,80I	2I,477	8,220	24,284
^{229}U	0+	6,09I	-0,984	0,3879	0	3,502	23,400	24,744	I,509	-
^{230}U	(3/2+)	7,662	-I,286	0,3879	0	4,266	23,I43	24,870	0,I4I	0,227
^{23I}U	0+	5,898	-I,393	0,3879	0	3,454	22,800	24,7I0	2,438	-
^{232}U	(5/2)	7,264	-I,542	0,3879	0	4,2I2	22,590	24,665	0,248	0,332
^{233}U*	0+	5,744	-I,733	0,379I	0,II74	3,0	2I,655	23,9I6	4,I	-
^{234}U*	5/2+	6,84I	-I,704	0,3922	0,0I86	4,0	I9,933	2I,986	I,067	I,423
^{235}U*	0+	5,305	-I,700	0,40I3	-0,I5I3	3,8	2I,25I	23,500	I0,6	-
^{236}U*	7/2-	6,546	-I,624	0,383I	-0,0I56	4,I	22,6I4	24,863	0,80I	0,967
^{237}U*	0+	5,I25	-I,680	0,3864	0,025I	3,2	20,837	23,023	I6,2	-
^{238}U*	I/2+	6,I43	-I,447	0,3826	-0,0I00	4,I	22,707	24,700	4,686	I3,83I
^{239}U*	0+	4,804	-I,4I8	0,3793	0,0394	3,2	22,479	24,4I3	24,8	-
^{240}U	5/2+	5,933	-I,2I4	0,3879	0	3,992	20,209	2I,692	5,II5	6,847
^{233}Np	(4+)	7,350[I)]	-I,6I6	0,3879	0	3,396	22,356	24,453	0,039	0,046
^{234}Np	(5/2+)	6,I30[I)]	-I,967	0,3879	0	2,592	22,054	24,660	0,I22	0,I64
^{235}Np	(0+)	6,99I	-I,879	0,3879	0	3,348	2I,762	24,I96	0,369	-
^{236}Np	5/2+	5,690	-2,049	0,3879	0	2,540	2I,439	24,I25	0,3I8	0,427
^{237}Np	(6-)	6,62I	-I,839	0,3879	0	3,292	2I,I96	23,535	0,I62	0,I73
^{238}Np*	5/2+	5,480	-2,04I	0,3960	0	2,352	I7,935	20,I63	I,293	I,730
^{239}Np	2+	6,226	-I,688	0,3879	0	3,240	20,575	22,662	0,690	I,00I
^{240}Np	5/2+	5,I64	-I,822	0,3879	0	2,444	20,268	22,525	I,II4	I,496
^{24I}Np	(5+)	5,970	-I,454	0,3879	0	3,I92	I9,959	2I,690	0,773	0,86I
^{233}Pu	0+	6,370	-I,532	0,3879	0	3,396	22,290	24,327	I,039	-

1	2	3	4	5	6	7	8	9	10	11
^{234}Pu		7,768	-1,754	0,3879	0					
^{235}Pu	0+	6,252	-2,024	0,3879	0	3,348	21,712	24,418	1,496	-
^{236}Pu	(5/2+)	7,354	-2,094	0,3879	0	4,100	21,500	24,250	0,257	0,345
^{237}Pu	0+	5,860	-2,225	0,3879	0	3,292	21,152	24,119	3,446	-
^{238}Pu	7/2-	6,998	-2,190	0,3879	0	4,050	20,891	23,730	0,470	0,572
^{239}Pu*	0+	5,655	-2,365	0,3884	0,0473	3,0	18,743	21,560	9,2	-
^{240}Pu*	1/2+	6,534	-2,116	0,3874	-0,0010	4,0	20,496	23,214	3,188	9,390
^{241}Pu*	0+	5,241	-2,118	0,3870	0,0003	3,2	20,269	23,006	13,5	-
^{242}Pu*	5/2+	6,301	-1,883	0,3816	0,0502	3,8	20,325	22,705	2,345	3,125
^{243}Pu	0+	5,037	-1,917	0,3604	0,2095	2,6	22,255	24,934	14,23	-
^{244}Pu	7/2+	6,018	-1,640	0,3879	0	3,876	19,042	20,965	4,326	5,264
^{245}Pu*	0+	4,720	-1,591	0,3060	0,5567	1,6	28,393	31,071	11,4	-
^{246}Pu	(9/2-)	5,942	-1,472	0,3879	0	3,820	18,394	20,044	4,989	5,704
^{239}Am	1+	7,100	-2,477	0,3879	0	3,240	20,699	23,837	0,201	0,395
^{240}Am	(5/2)-	5,900	-2,724	0,3879	0	2,444	20,386	23,885	0,279	0,376
^{241}Am	(3-)	6,582	-2,402	0,3879	0	3,192	20,060	23,042	0,323	0,412
^{242}Am	5/2-	5,529	-2,487	0,3917	0	2,321	18,310	21,156	1,013	1,357
^{243}Am	1-	6,376	-2,128	0,3879	0	3,134	19,437	21,966	1,012	1,987
^{243}Am*	5-	6,425[2)]	-2,128	0,3935	0,0073	3,0	16,982	19,173	0,849	0,957
^{244}Am*	5/2-	5,364	-2,287	0,3891	0	2,317	18,661	21,313	1,188	1,591
^{245}Am	(6-)	6,046	-1,841	0,3879	0	3,084	18,806	20,904	0,813	0,875
^{246}Am	(5/2)+	5,055	-1,925	0,3879	0	2,296	18,452	20,630	2,134	2,878
^{239}Cm	0+	6,400	-2,653	0,3879	0	3,240	20,643	24,116	1,387	-

Table 3 (continued)

I	2	3	4	5	6	7	8	9	I0	II
^{240}Cm	(7/2)	7,400	-2,690	0,3879	0	3,992	20,377	23,799	0,25I	0,306
^{24I}Cm	0+	6,07I	-2,849	0,3879	0	3,I92	20,039	23,740	2,943	-
^{242}Cm	I/2+	6,969	-2,634	0,3879	0	3,938	I9,749	23,055	I,69I	5,008
^{243}Cm*	0+	5,70I	-2,692	0,4004	-0,05I6	3,2	I6,2I3	I9,0I6	I7,6	-
^{244}Cm*	5/2+	6,799	-2,559	0,3866	-0,02I9	4,0	20,339	23,657	0,874	I,I69
^{245}Cm*	0+	5,5I9	-2,676	0,3552	0,3I3I	2,0	I8,488	2I,705	II,8	-
^{246}Cm*	7/2+	6,45I	-2,439	0,3808	0,0688	3,6	I8,726	2I,635	2,083	2,5I9
^{247}Cm*	0+	5,I57	-2,430	0,3789	0,077I	2,8	I8,7I6	2I,665	2I,3	-
^{248}Cm*	9/2-	6,2I0	-2,I93	0,3824	0,0I23	3,8	I9,536	22,25I	2,262	2,554
^{249}Cm*	0+	4,7I3	-I,97I	0,3800	0,0232	3,0	I9,687	22,I74	40	-
^{250}Cm	(I/2+)	5,833	-I,54I	0,3879	0	3,7I0	I7,060	I8,667	25,222	74,729
^{244}Bk	(3/2-)	6,II0	-2,89I	0,3879	0	2,340	I9,258	22,76I	0,360	0,586
^{245}Bk	(4-)	6,990 I)	-2,734	0,3879	0	3,084	I8,959	22,I72	0,I83	0,2I7
^{246}Bk	3/2-	5,900	-2,796	0,3879	0	2,296	I8,59I	2I,859	0,638	I,039
^{247}Bk	(2-)	6,600 I)	-2,728	0,3879	0	3,032	I8,235	2I,353	0,675	0,983
^{248}Bk	(3/2-)	5,280	-2,926	0,3879	0	2,242	I7,907	2I,294	2,229	3,628
^{249}Bk	(6+)	6,500	-2,497	0,3879	0	2,976	I7,565	20,278	0,526	0,57I
^{250}Bk*	7/2+	4,969	-2,335	0,3848	0	2,244	I8,434	2I,I50	2,008	2,433
^{25I}Bk	(2-)	5,800	-I,686	0,3879	0	2,922	I6,7I0	I8,403	4,I48	6,048
^{245}Cf	0+	6,I45	-2,992	0,3879	0	3,084	I8,896	22,568	3,407	-
^{246}Cf		7,354	-3,0I8	0,3879	0					
^{247}Cf	0+	6,020 I)	-3,I84	0,3879	0	3,032	I8,2I7	22,039	5,I52	-
^{248}Cf	(7/2+)	7,000	-3,I36	0,3879	0	3,766	I7,946	2I,609	0,948	I,I63

Table 3 (continued)

I	2	3	4	5	6	7	8	9	I0	II
249	Cf 0+	5,594	-3,I72	0,3879	0	2,976	I7,537	2I,247	I2,976	*
250	Cf* 9/2-	6,6I8	-2,955	0,390I	-0,025I	3,8	I7,252	20,57I	2,0I0	2,288
25I	Cf 0+	5,II4	-2,744	0,3879	0	2,922	I6,729	I9,750	37,762	-
252	Cf I/2+	6,I65	-2,3I4	0,3879	0	3,652	I6,334	I8,725	I7,I20	50,733
253	Cf 0+	4,792	-2,0I3	0,3678	0	3,2I7	24,082	27,I27	I6	-
254	Cf (7/2+)	6,029	-I,633	0,3879	0	3,600	I5,342	I6,865	I0,774	I3,245

* The parameters for these nuclei are obtained using $\langle D \rangle_{exp}$.

** Column 6 includes E_o for even-even, $E_o + \Delta_{oN}$ for even-odd, $E_o + \Delta_{oZ}$ for odd-even and $E_o + \Delta_{oN} + \Delta_{oZ}$ for odd-odd nuclei, $\Delta_{oZ} = \Delta_{oN} = \Delta_o$.

1) Systematics is taken from Nuclear Data Sheets.

2) The data correspond to the isomeric 5^--(48.63 keV)^{242}Am state.

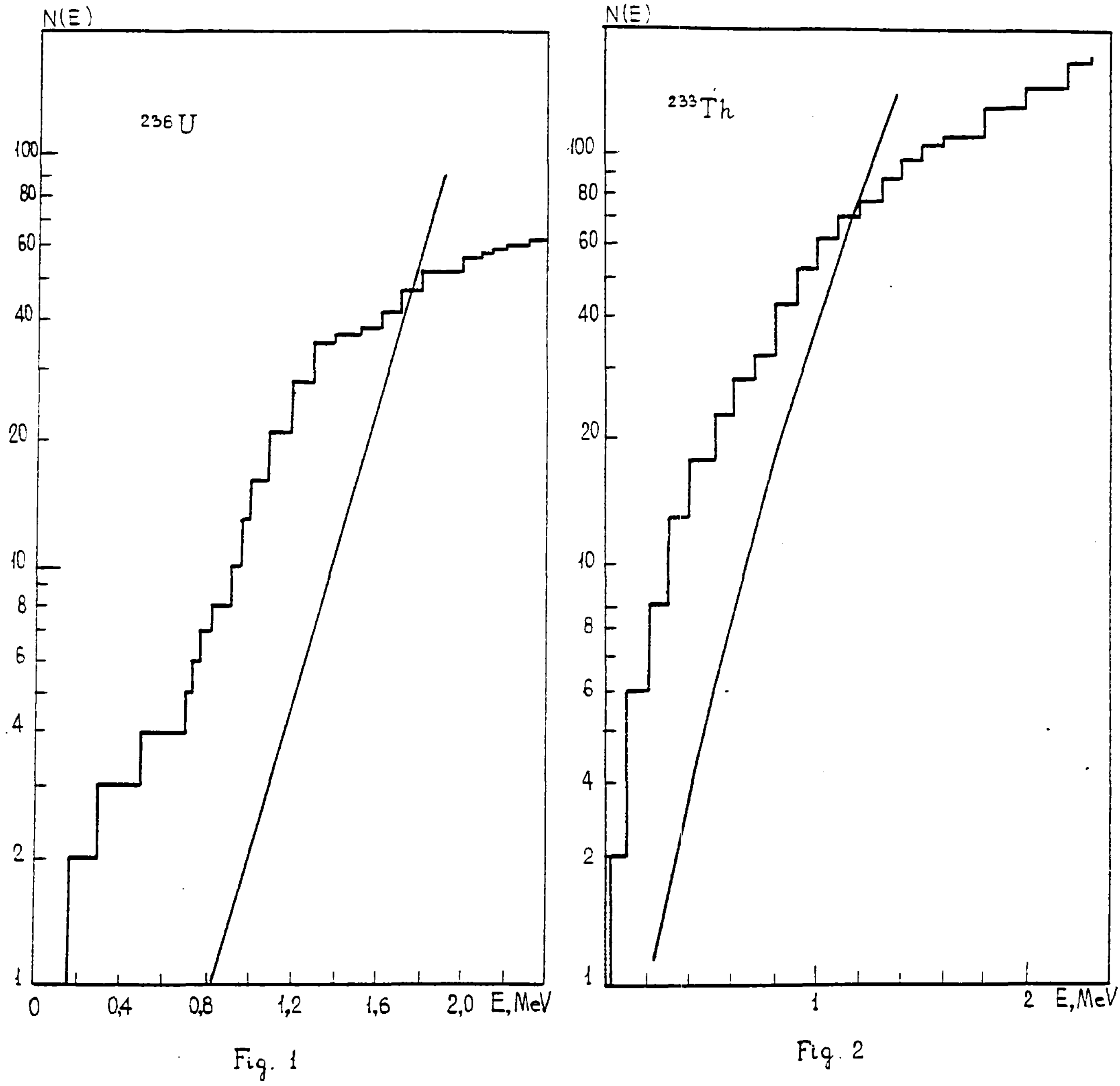

Fig. 1. Comparison of the cumulative number of levels of the even-even nucleus (^{238}U) with superfluid model calculations.

Fig. 2. Comparison of the cumulative number of levels of the odd nucleus (^{233}Th) with superfluid nuclear model calculations.

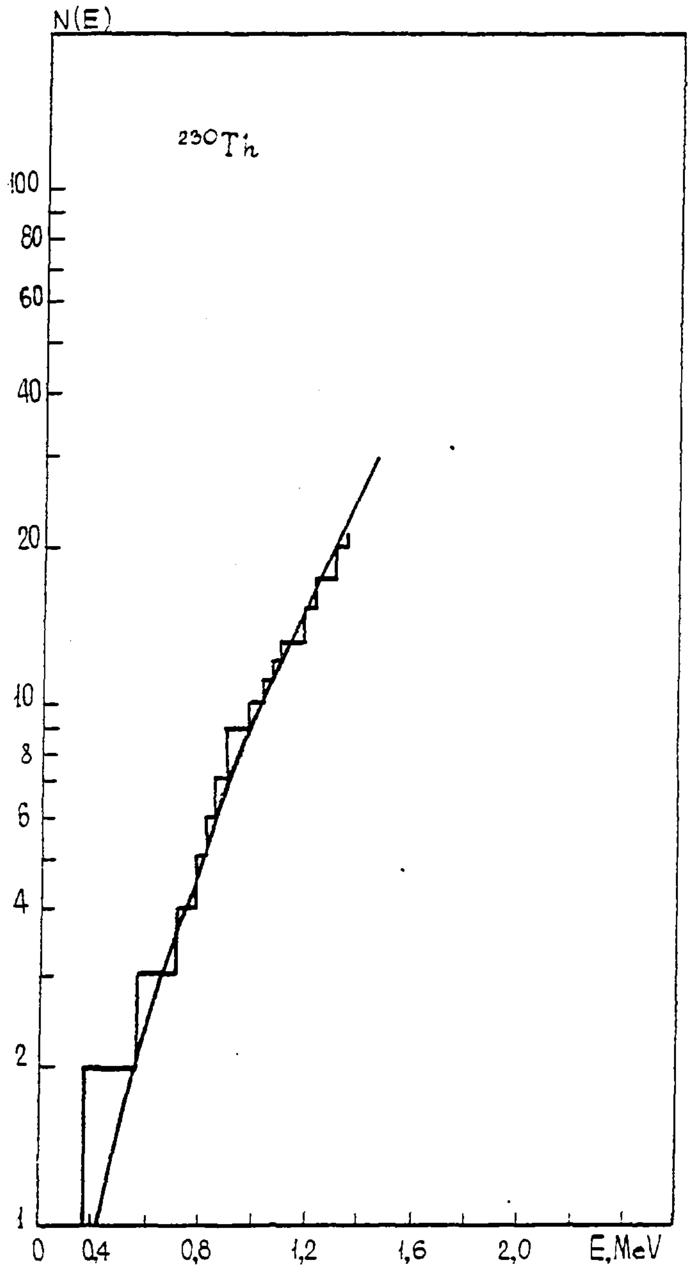

Fig. 3a

Fig. 3. The cumulative number of levels of the even-even nuclei, for which the data on $\langle D \rangle_{exp}$ are available. The constant-temperature model is used. The parameters T and E_0 are derived from the experimental data: a, ^{240}Th; b, ^{234}U; c, ^{236}U; d, ^{238}U; e, ^{240}Pu; f, ^{242}Pu; g, ^{244}Cm; h, ^{246}Cm; i, ^{248}Cm; j, ^{250}Cf.

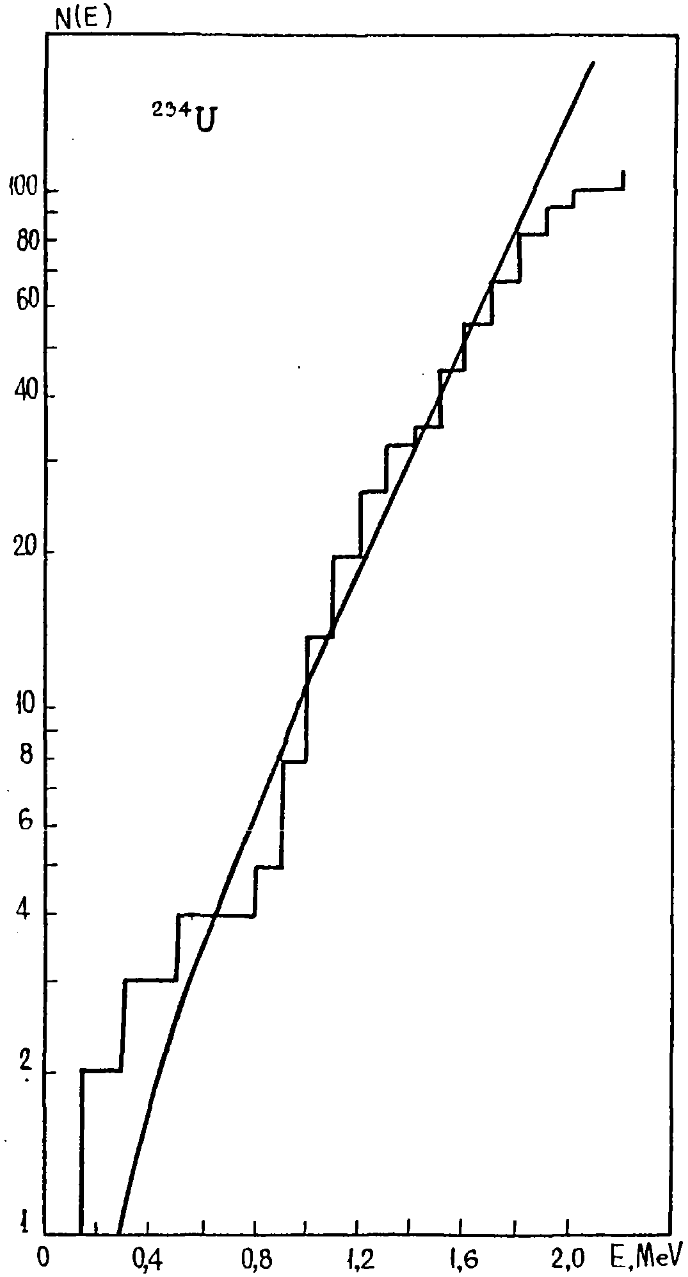

Fig. 3b

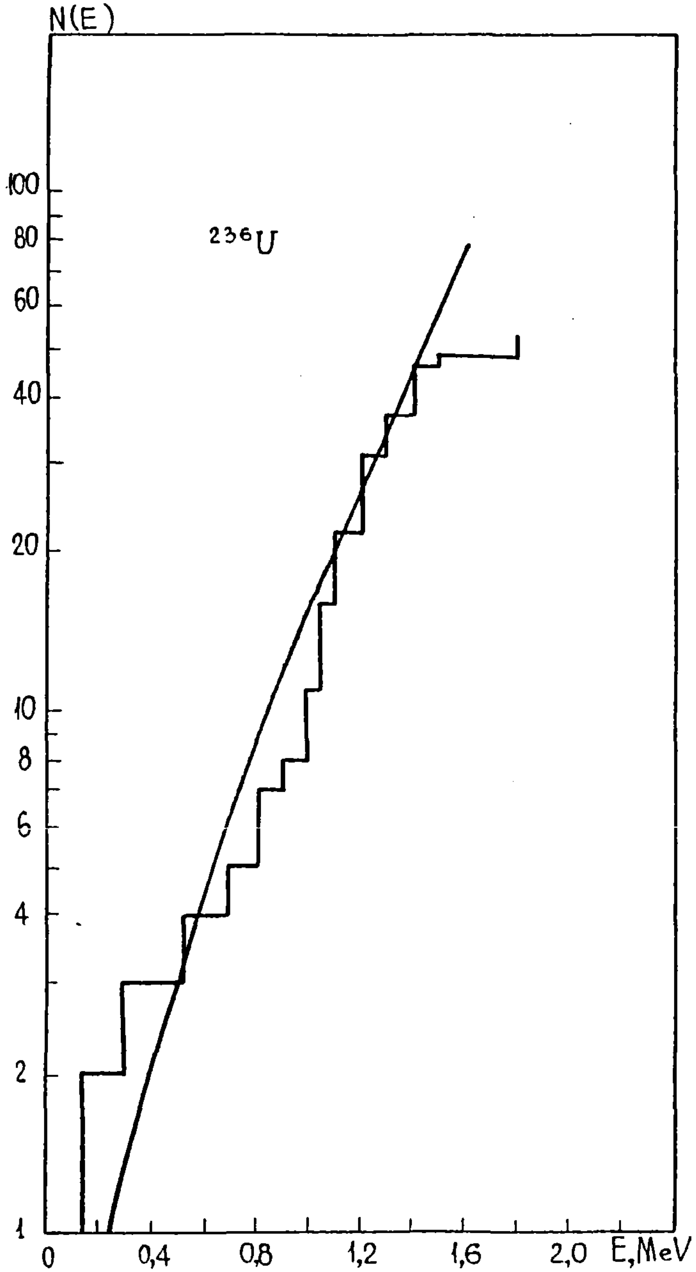

Fig. 3c

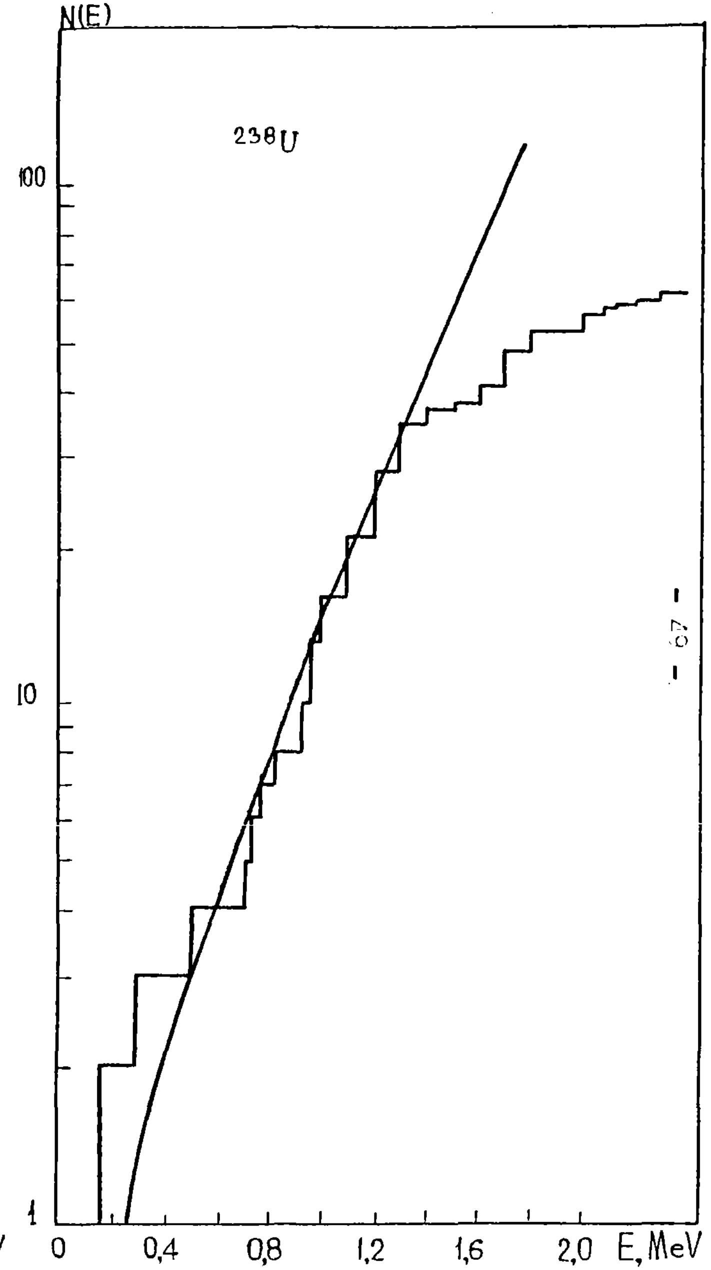

Fig. 3d

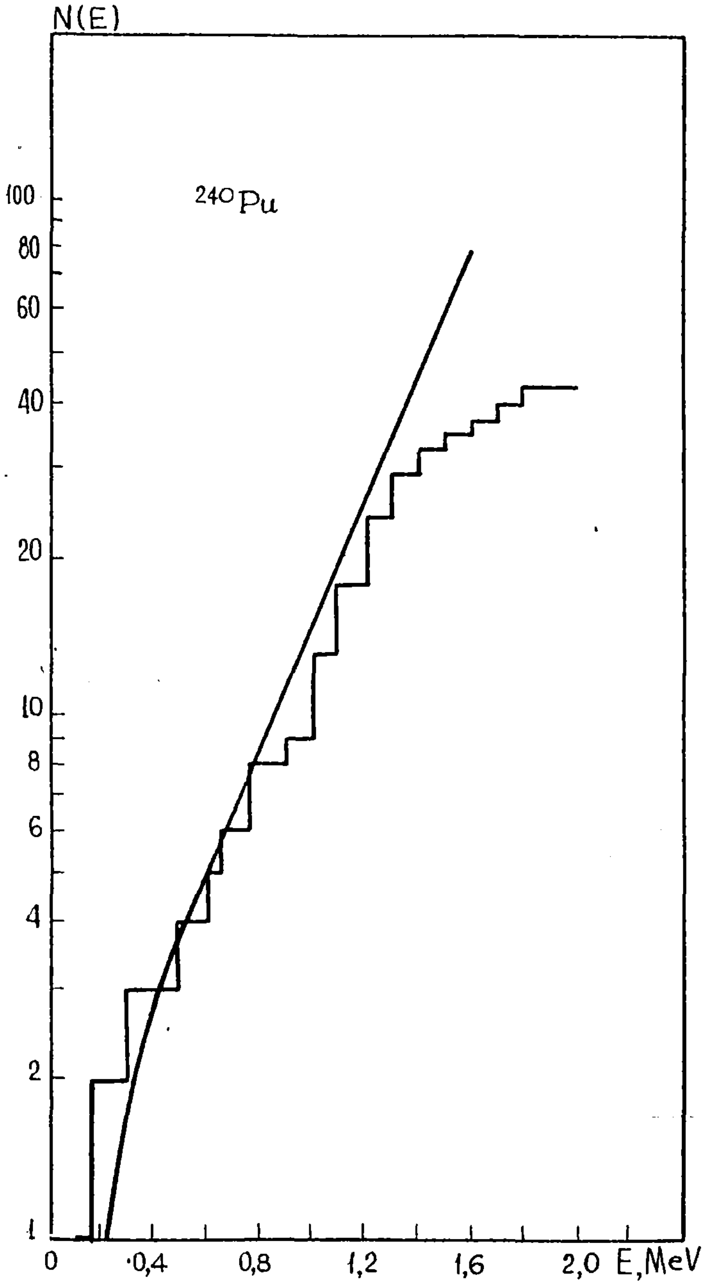

Fig. 3e

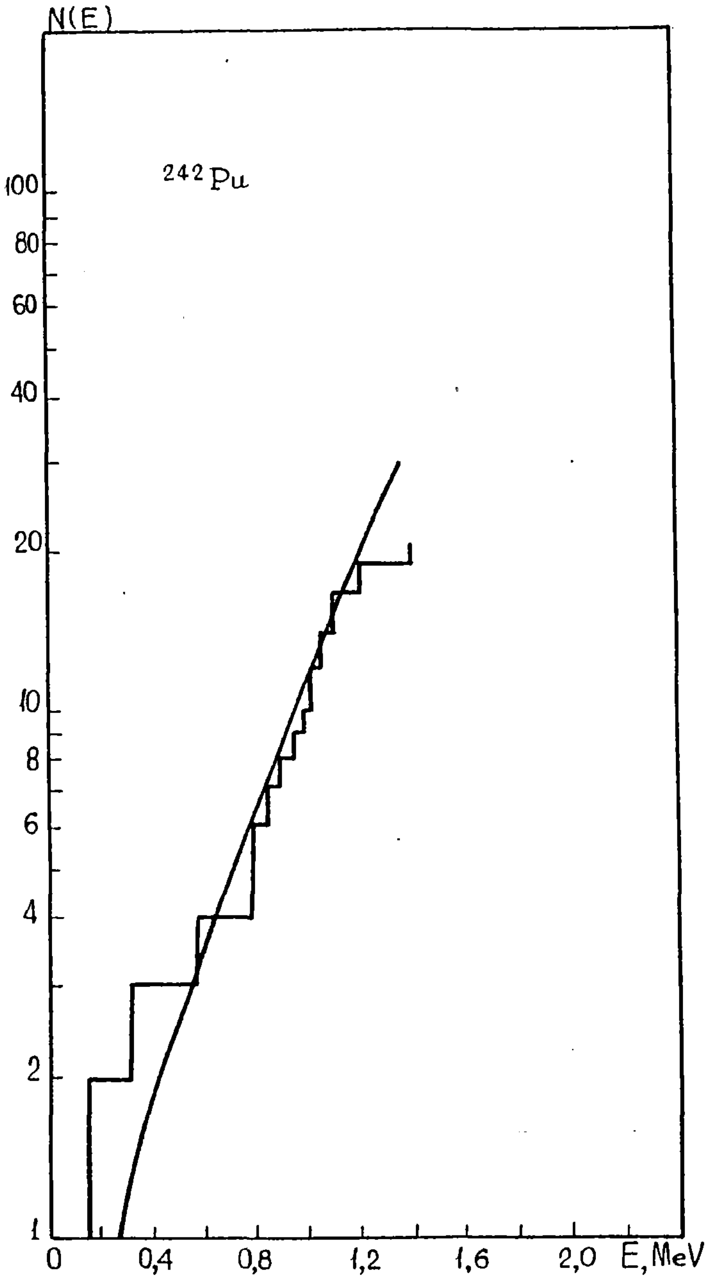

Fig. 3f

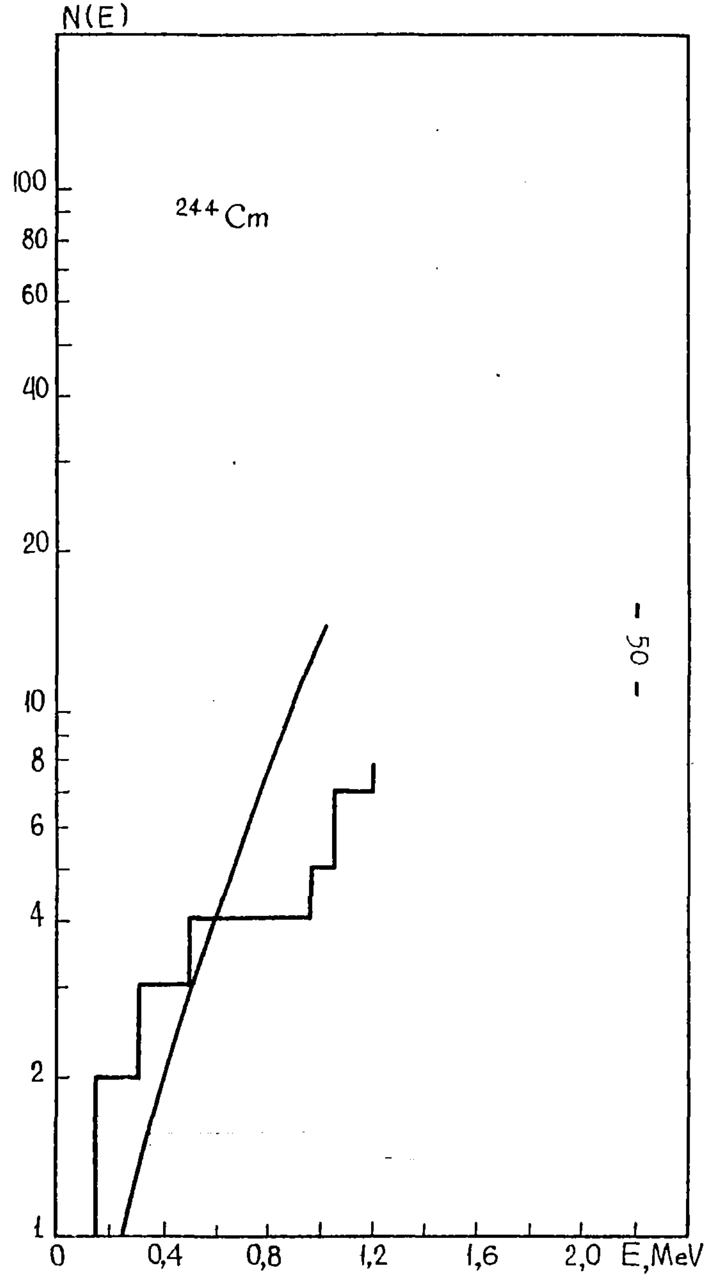

Fig. 3g

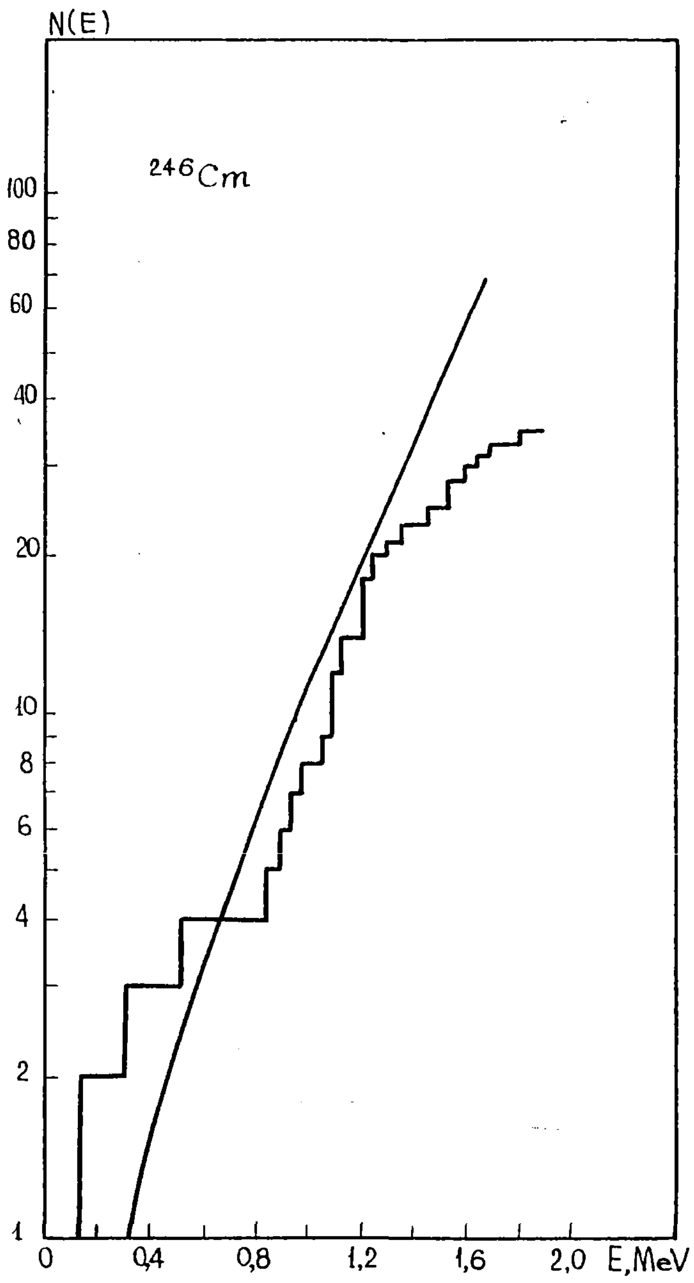

Fig. 3h

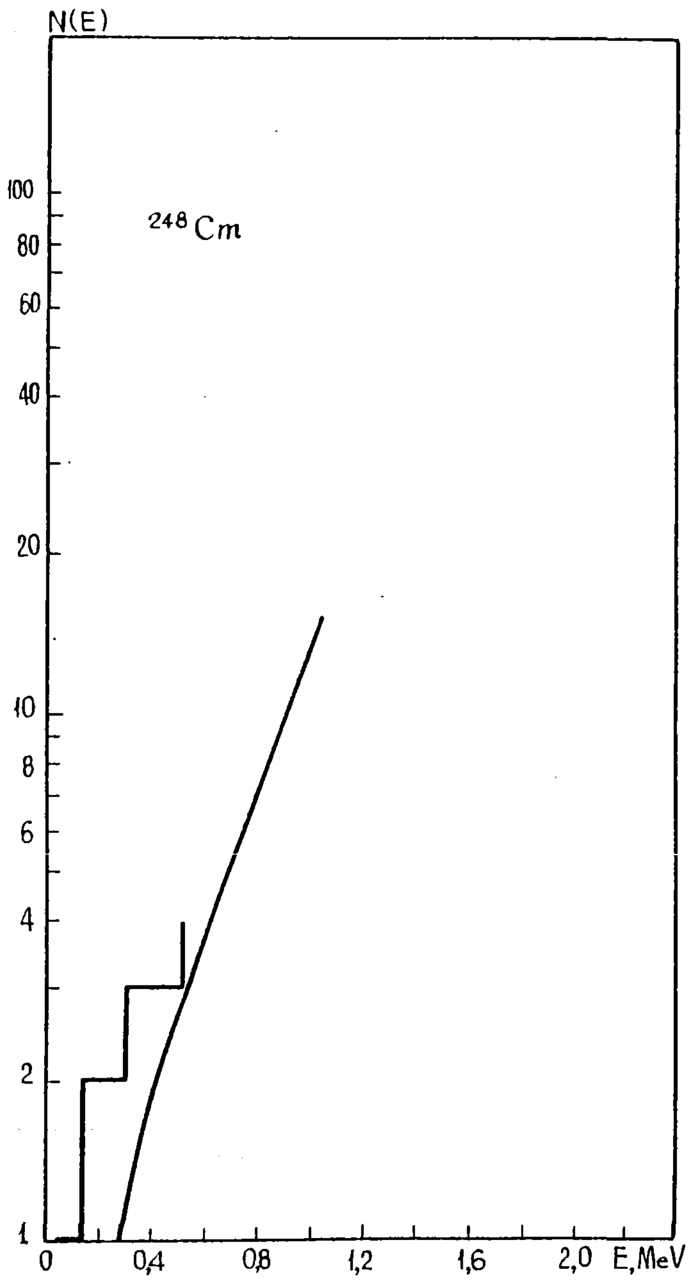

Fig. 3i

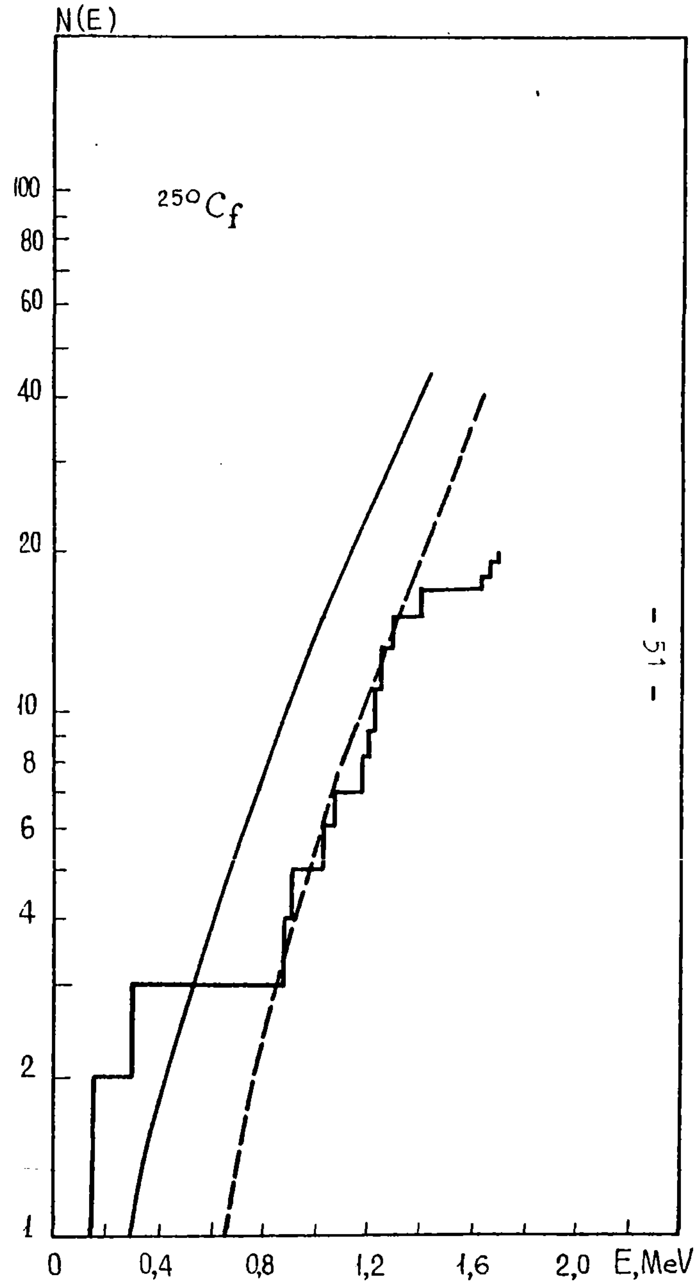

Fig. 3j

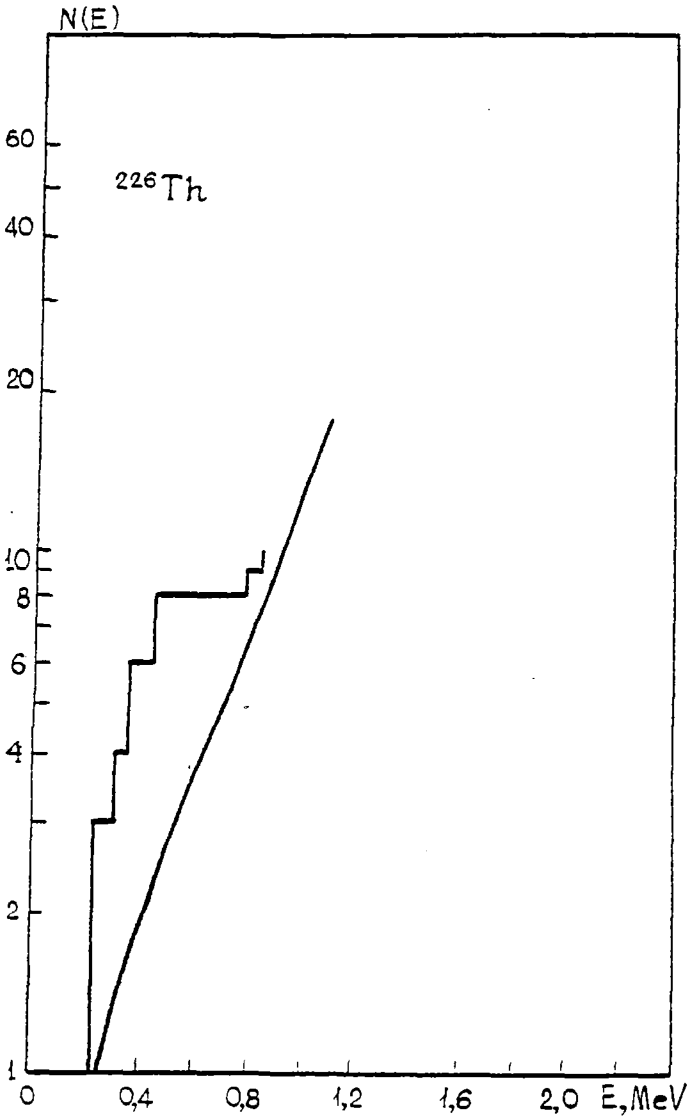

Fig. 4a

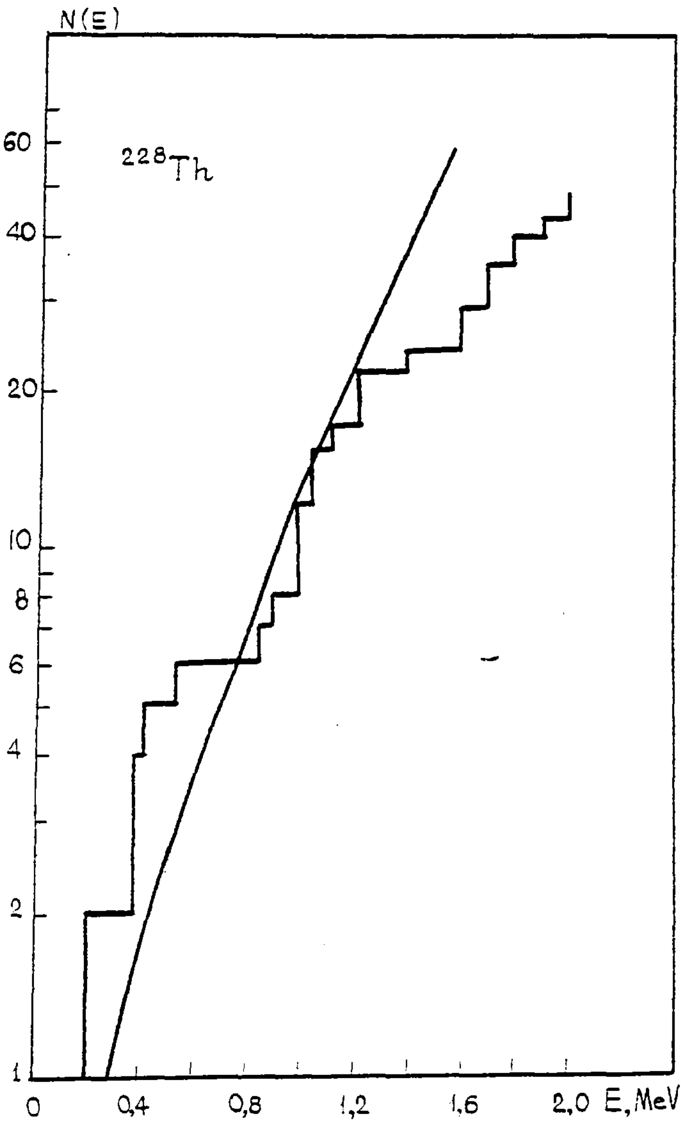

Fig. 4b

Fig. 4. The cumulative number of levels of the even-even nuclei, for which no data on $\langle D \rangle_{exp}$ are available, the constant-temperature model fit: $\bar{T} = 0.385$ MeV; $E_o = 0$. a, ^{226}Th; b, ^{232}Th; c, ^{232}U; d, ^{238}Pu; e, ^{244}Pu, f, ^{228}Th.

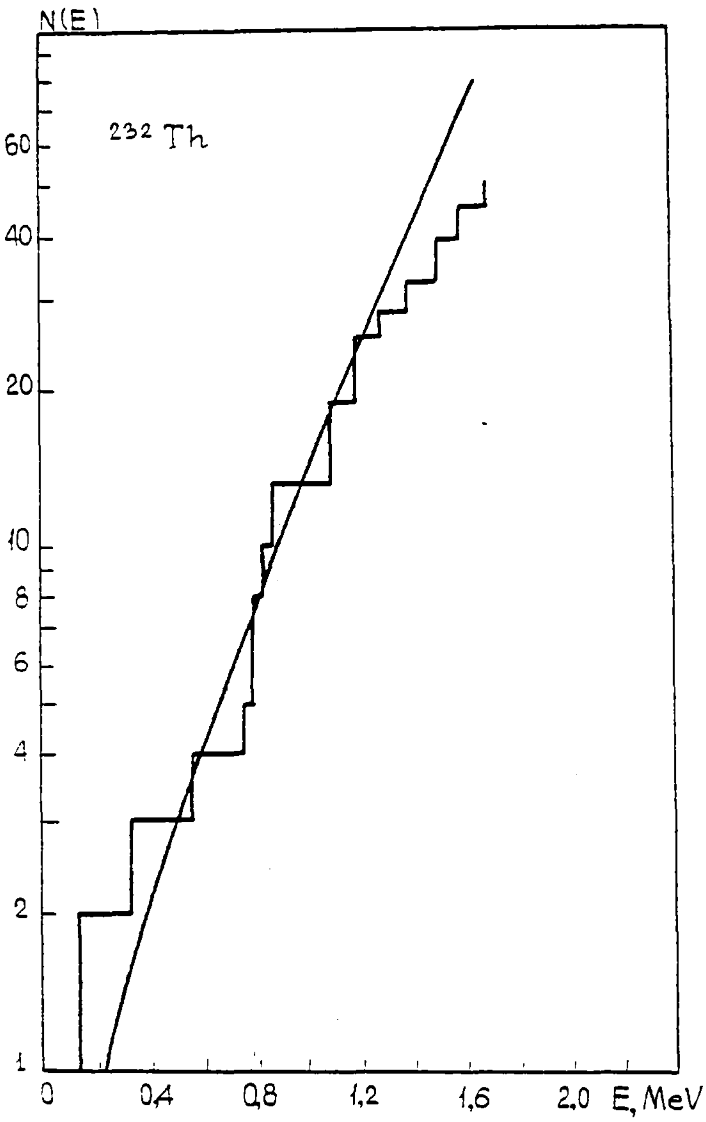
N(E)
232 Th
60
40
20
10
8
6
4
2
1
0
0,4
0,8
1,2
1,6
2,0
E, MeV

Fig. 4c

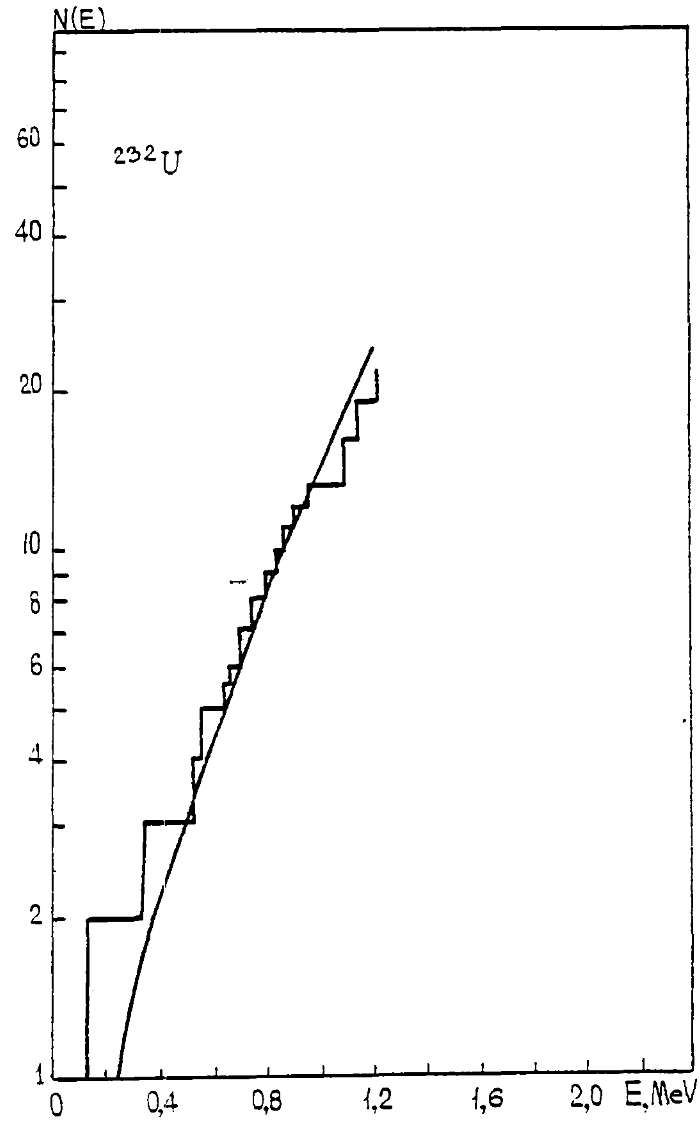
N(E)
232 U
60
40
20
10
8
6
4
2
1
0
0,4
0,8
1,2
1,6
2,0
E, MeV

Fig. 4d

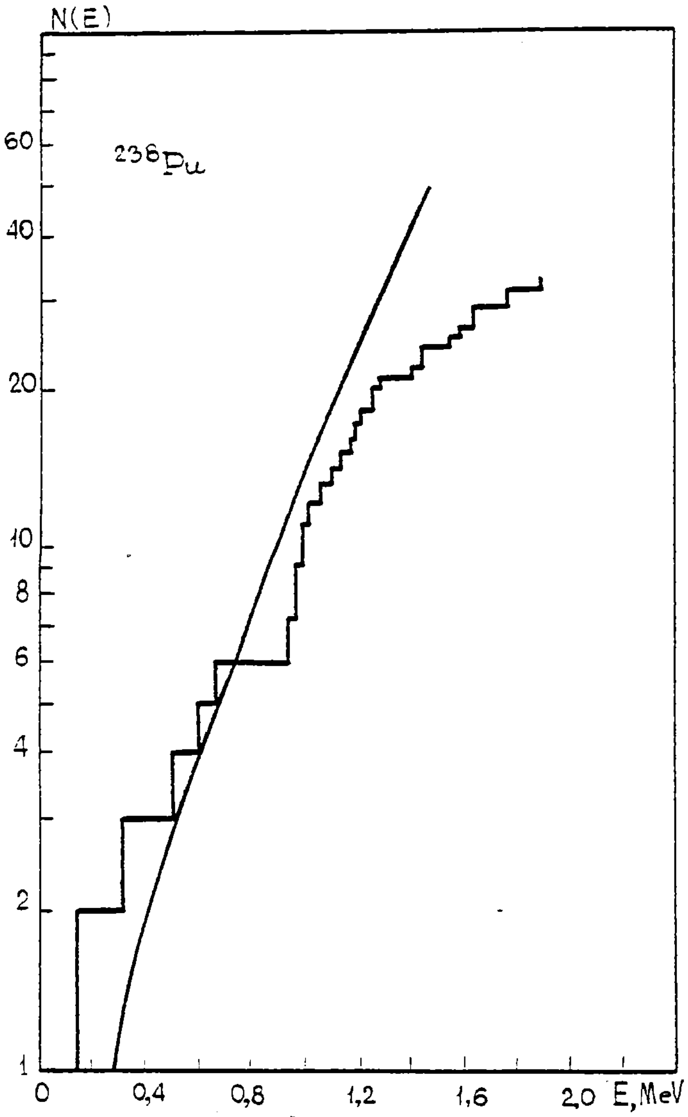
N(E)
^{238}Pu
60
40
20
10
8
6
4
2
1
0
0,4
0,8
1,2
1,6
2,0
E, MeV

Fig. 4e

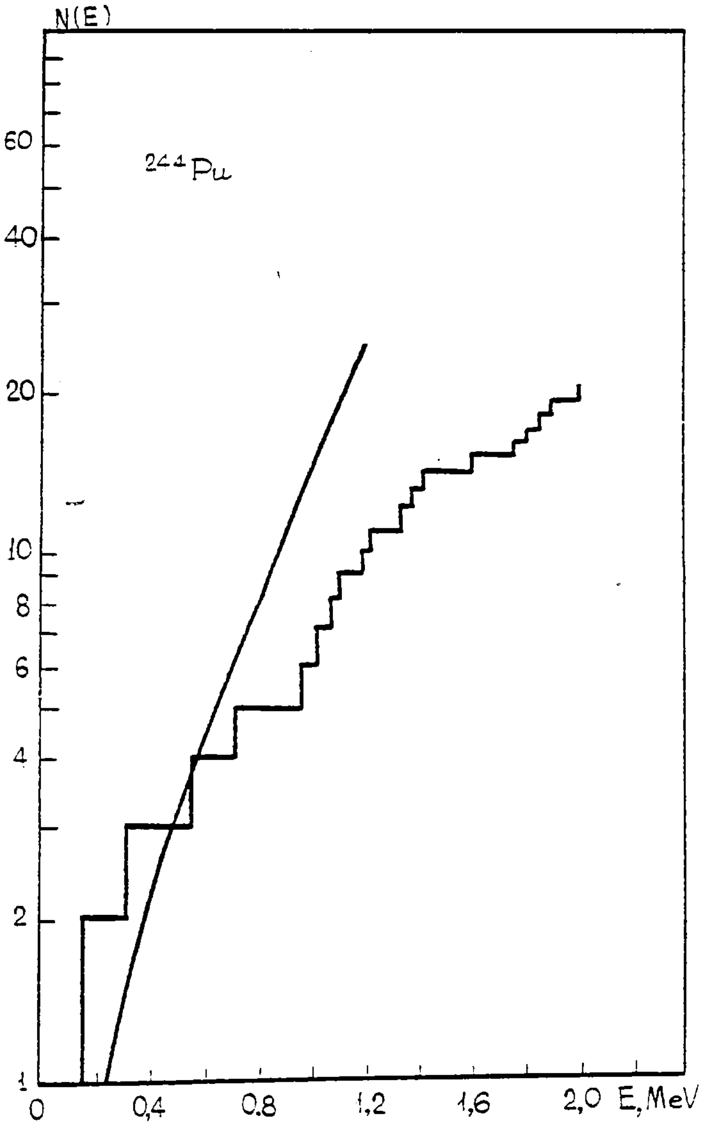
N(E)
^{244}Pu
60
40
20
10
8
6
4
2
1
0
0,4
0.8
1,2
1,6
2,0
E, MeV

Fig. 4f

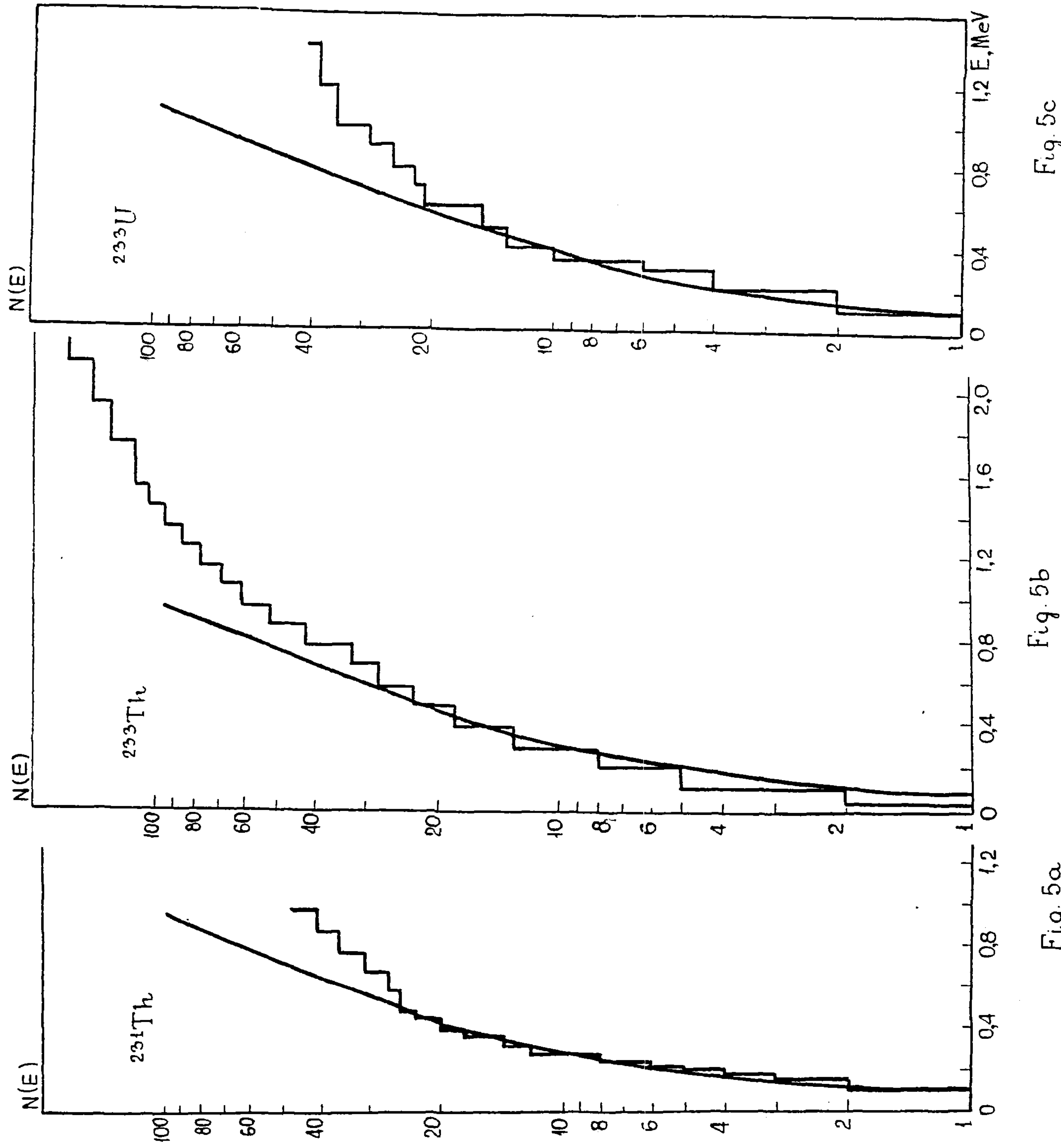

Fig. 5. The cumulative number of levels of the odd nuclei, for which data on $\langle D \rangle_{exp}$ are available, the constant-temperature model fit. The parameters T and E_o are derived from the experimental data: a, ^{231}Th; b, ^{233}Th; c, ^{233}U; d, ^{235}U; e, ^{237}U; f, ^{239}U; g, ^{239}Pu; h, ^{241}Pu; i, ^{243}Pu; j ^{245}Pu; k, ^{243}Am; l, ^{243}Cm; m, ^{245}Cm; n, ^{247}Cm; o, ^{249}Cm.

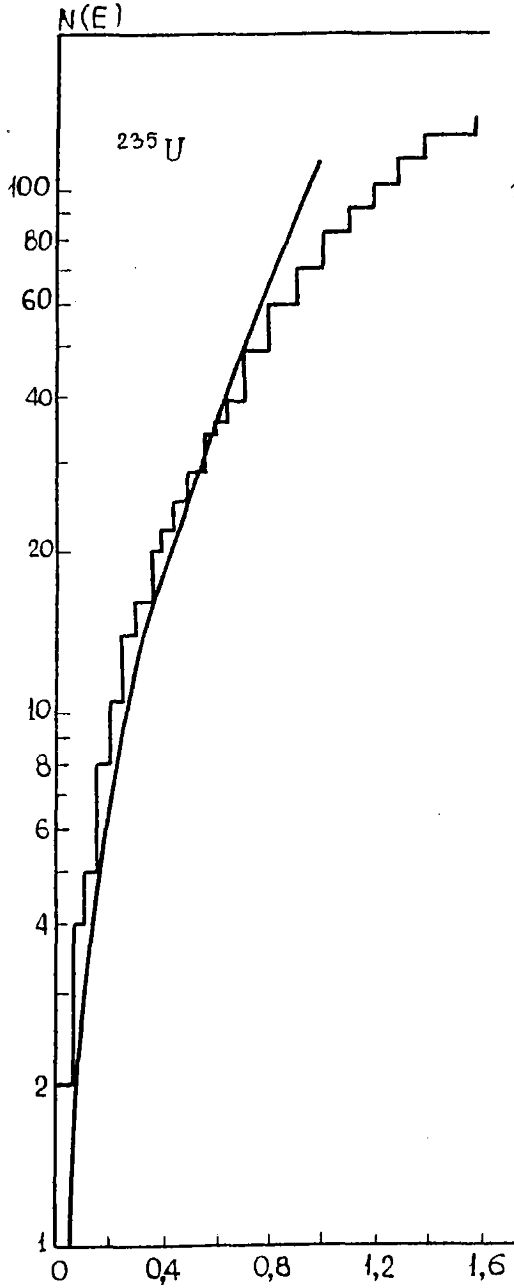

Fig. 5d

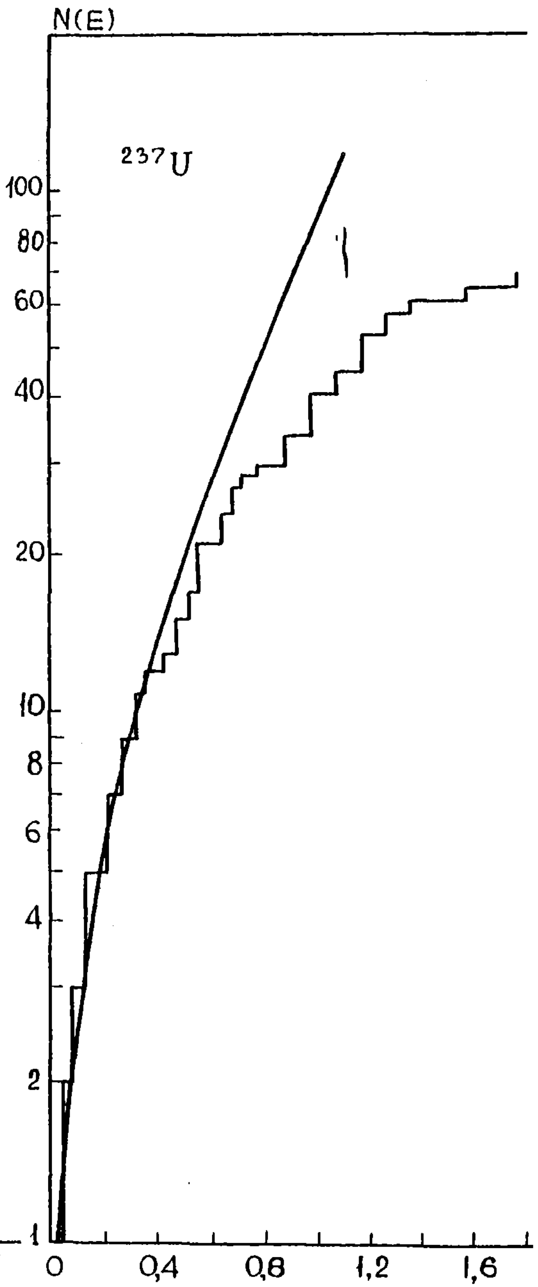

Fig. 5e

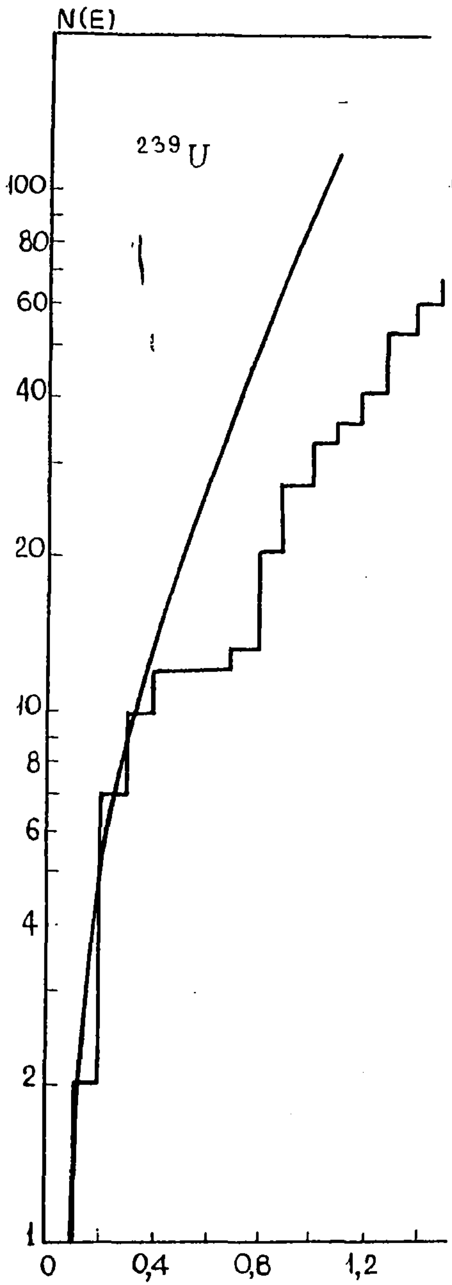

Fig. 5f

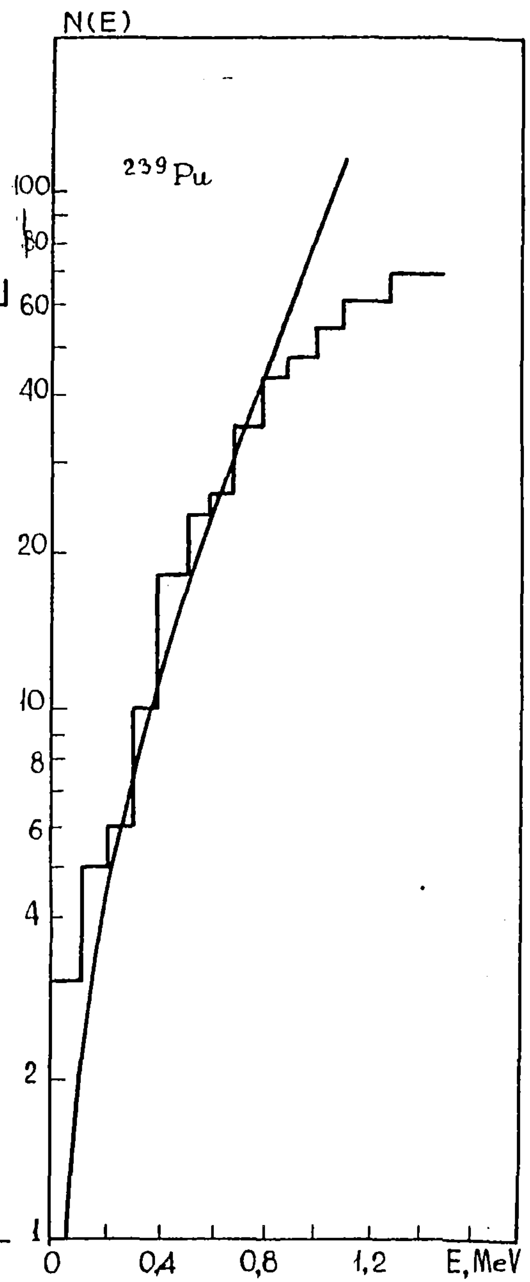

Fig. 5g

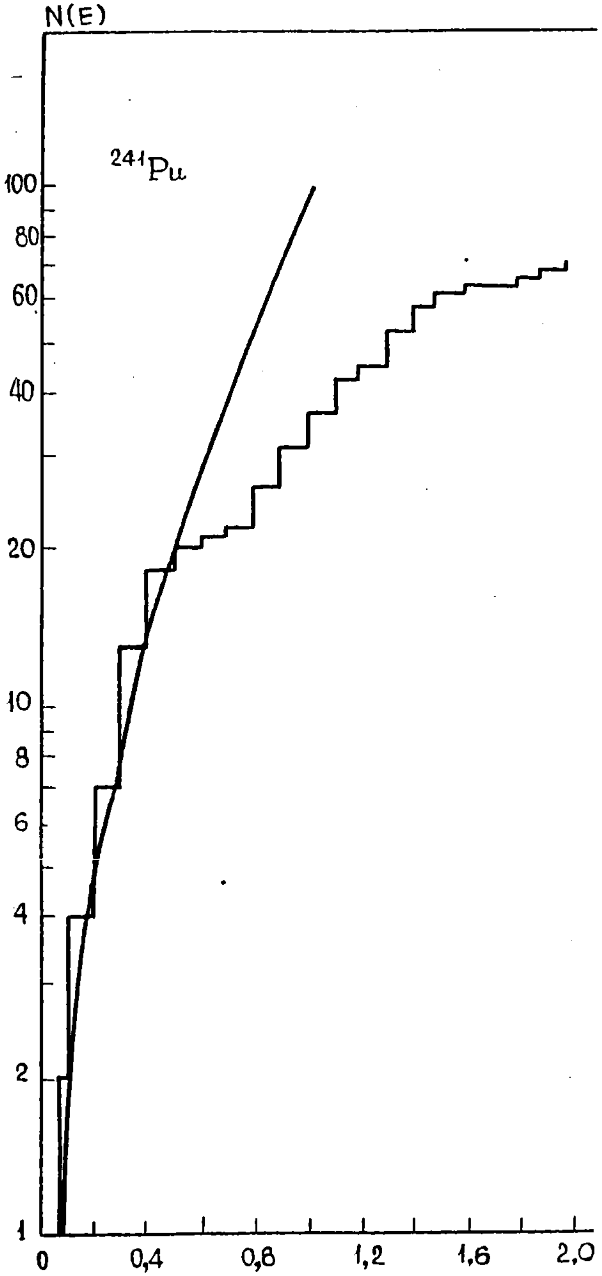

Fig. 5h

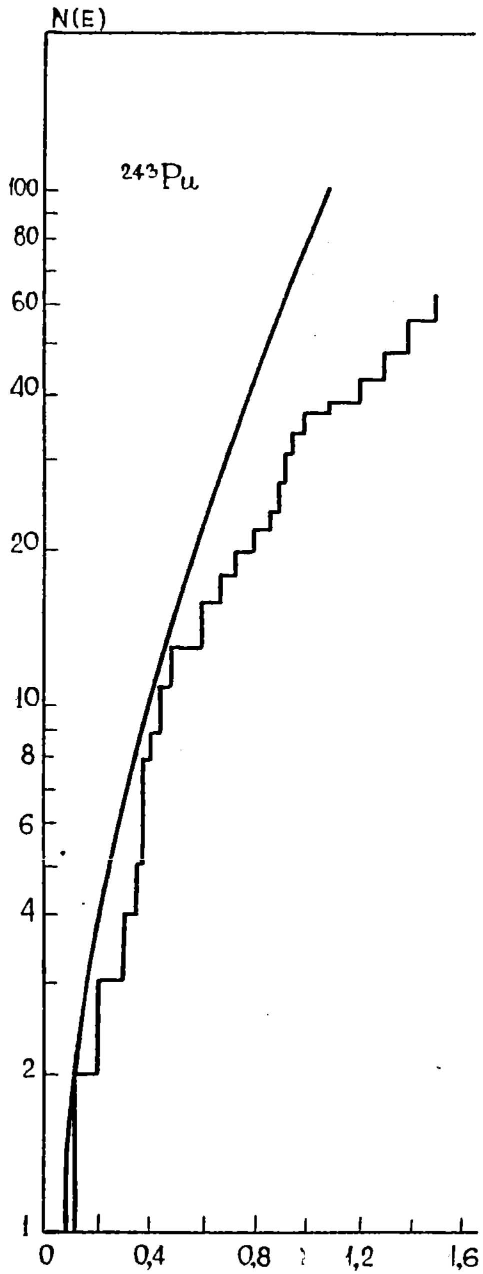

Fig. 5i

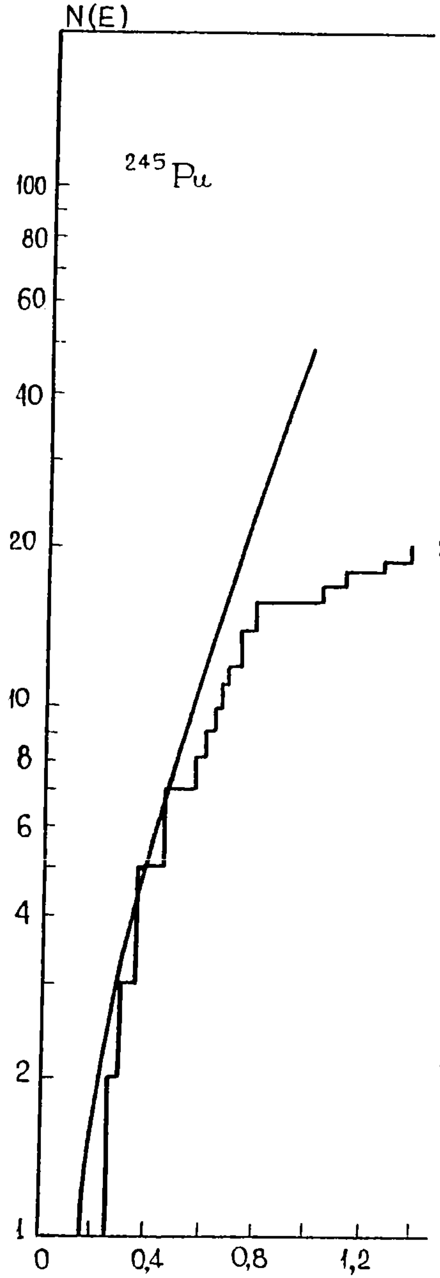

Fig. 5j

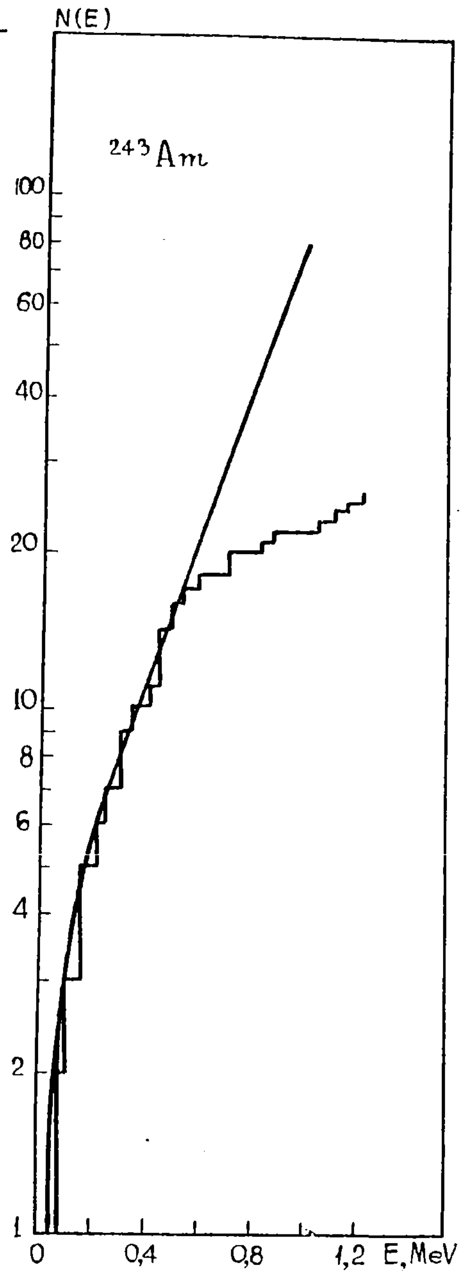

Fig. 5k

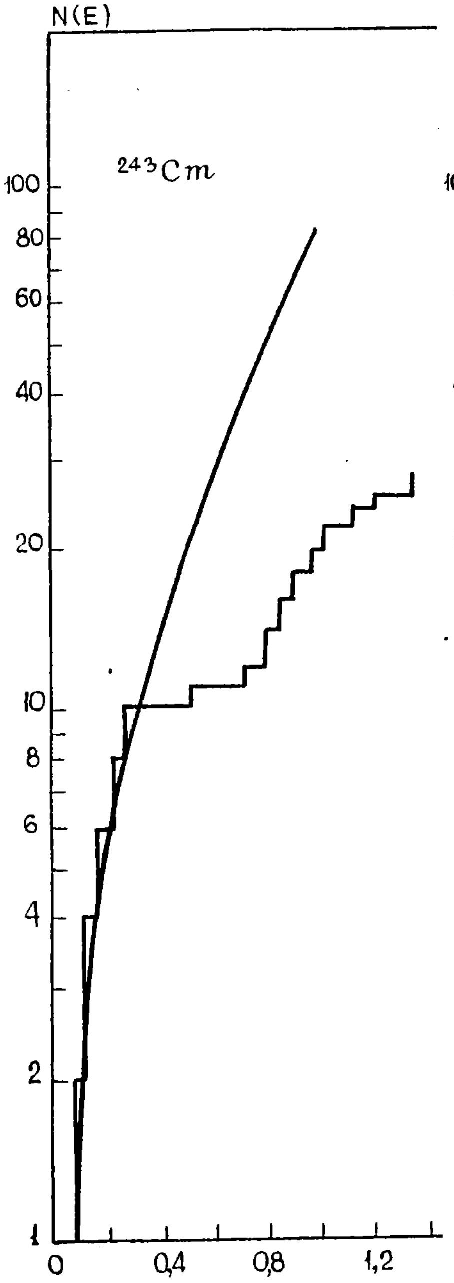

Fig. 5l

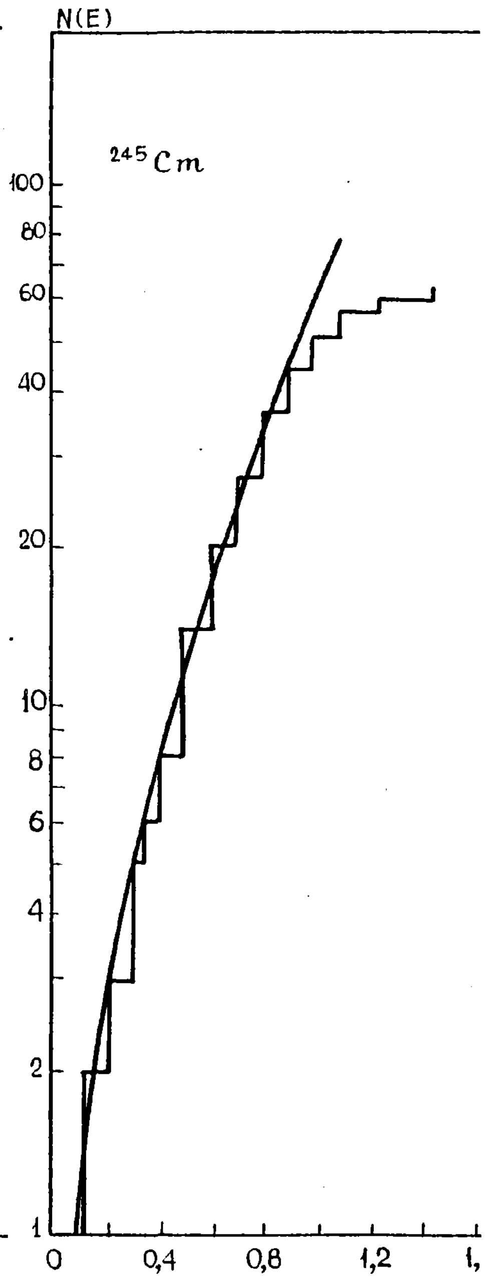

Fig. 5m

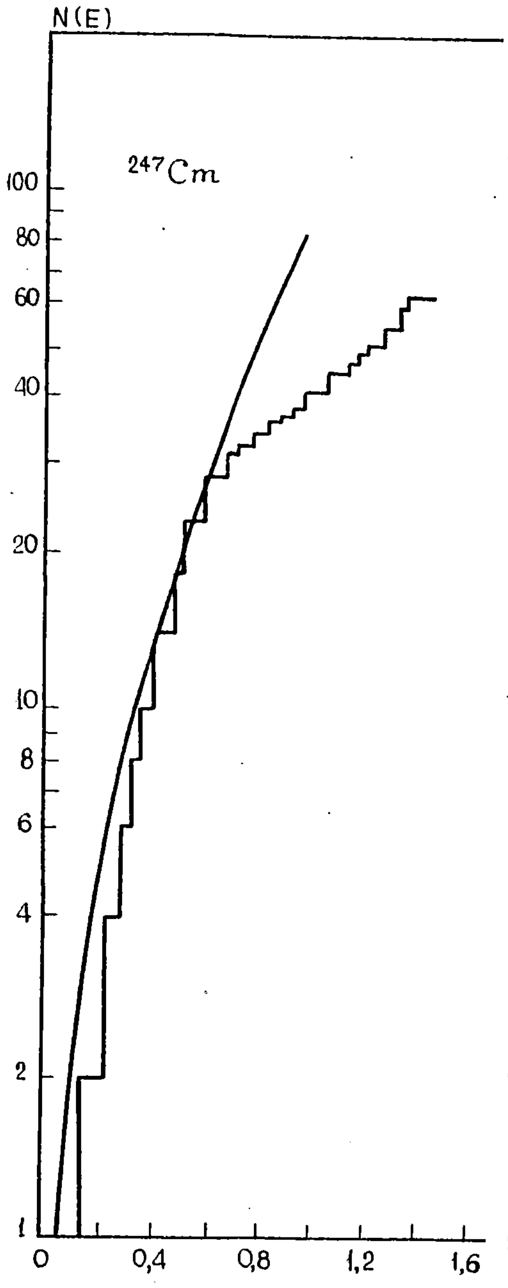

Fig. 5n

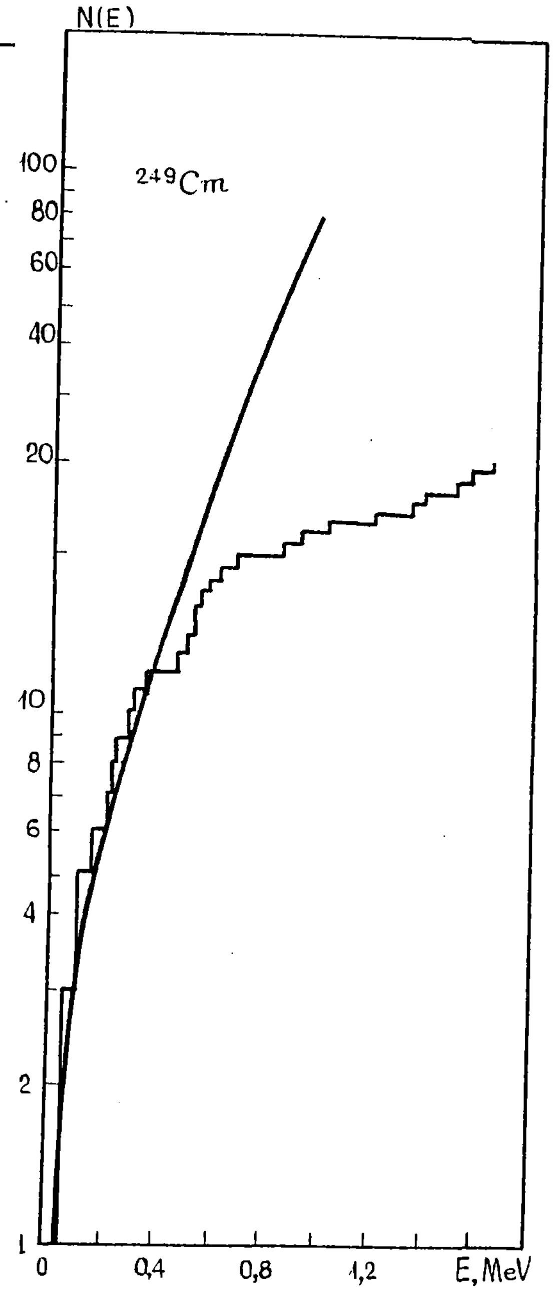

Fig. 5o

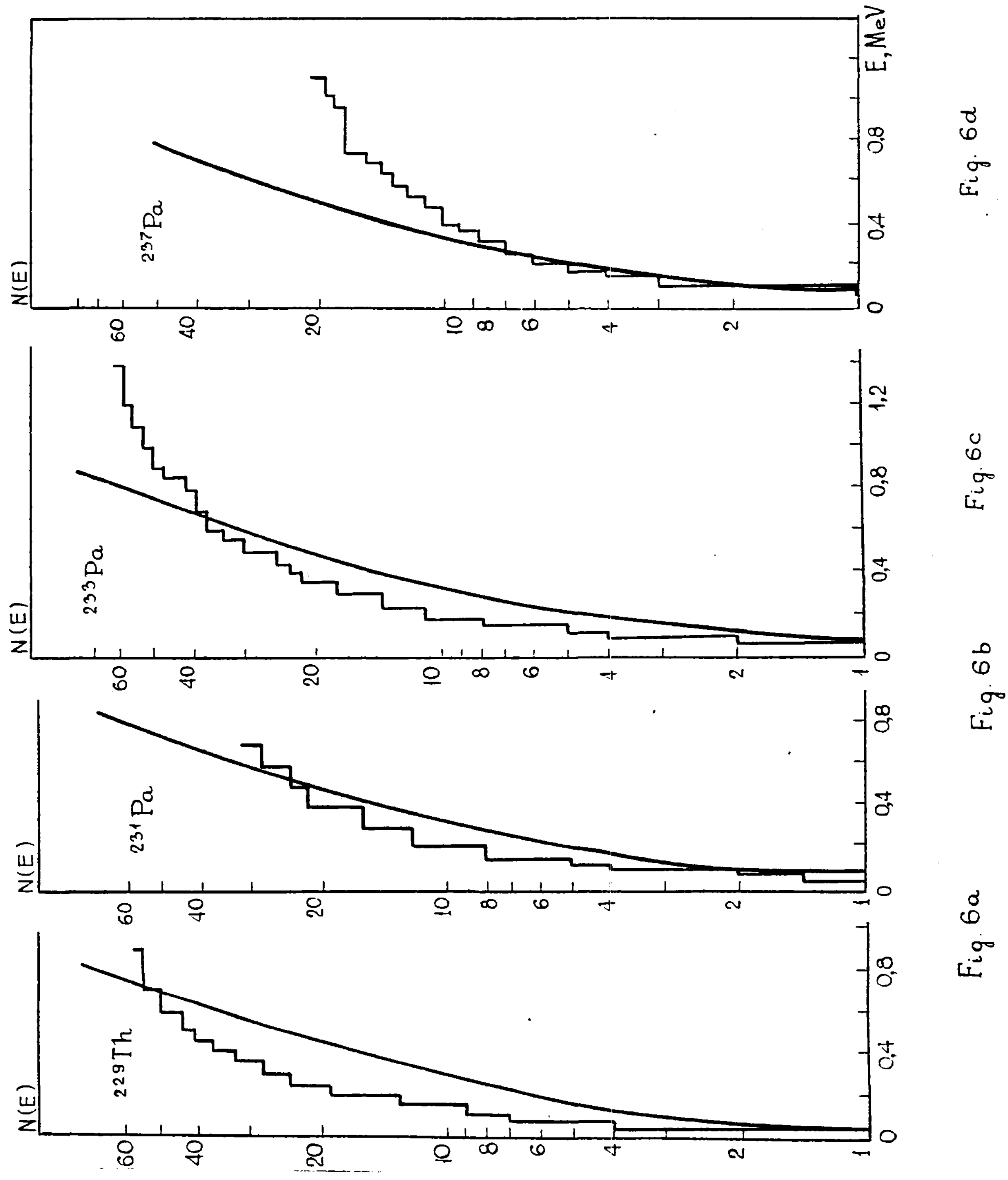

Fig. 6. The cumulative number of levels of the odd nuclei, for which no data on $\langle D \rangle_{exp}$ are available, the constant-temperature model fit. The parameters T and E_o are deduced from the systematics : a, ^{229}Th; b, ^{231}Pa, c, ^{233}Pa; d, ^{237}Pa; e, ^{235}Np; f, ^{237}Np; g, ^{239}Np; h, ^{237}Pu; i, ^{239}Am; j, ^{241}Am; k, ^{245}Am; l, ^{249}Bk; m, ^{249}Cf; n, ^{251}Cf.

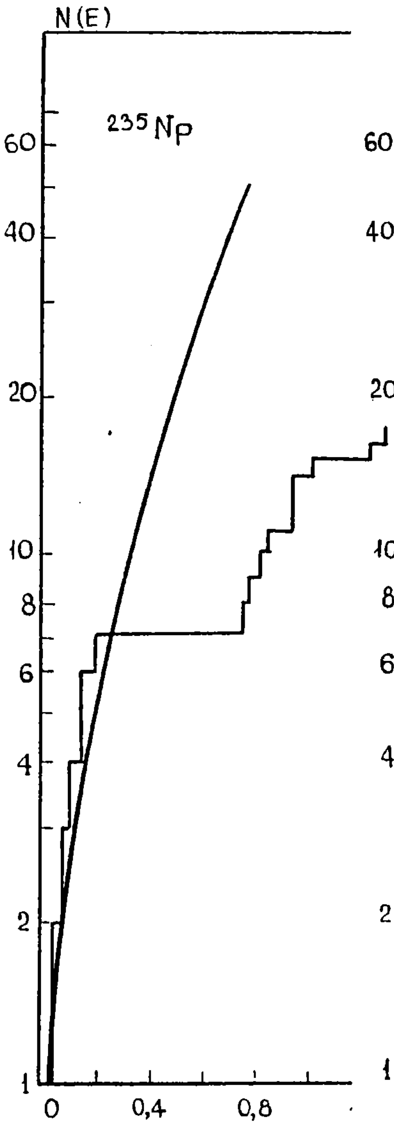

Fig. 6e

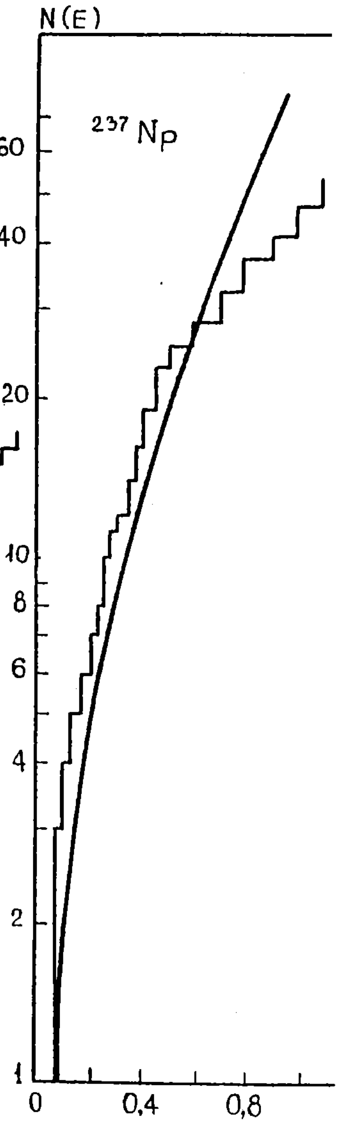

Fig. 6f

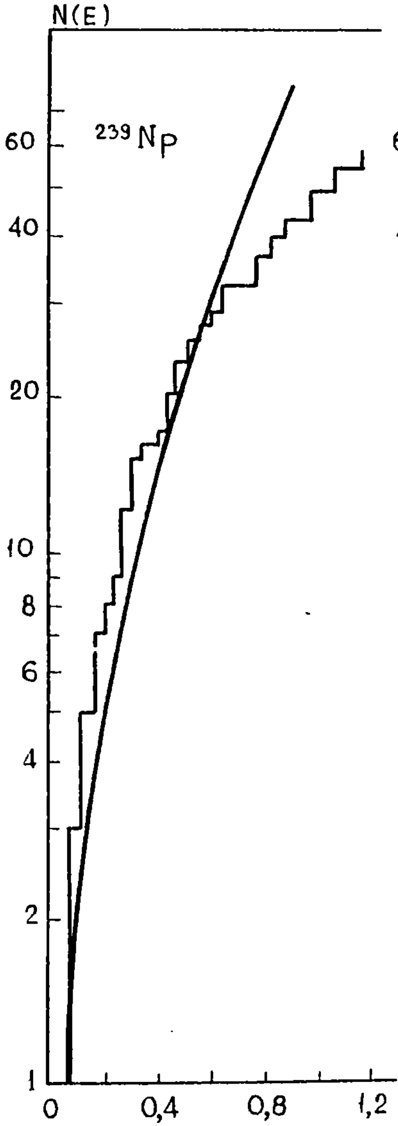

Fig. 6g

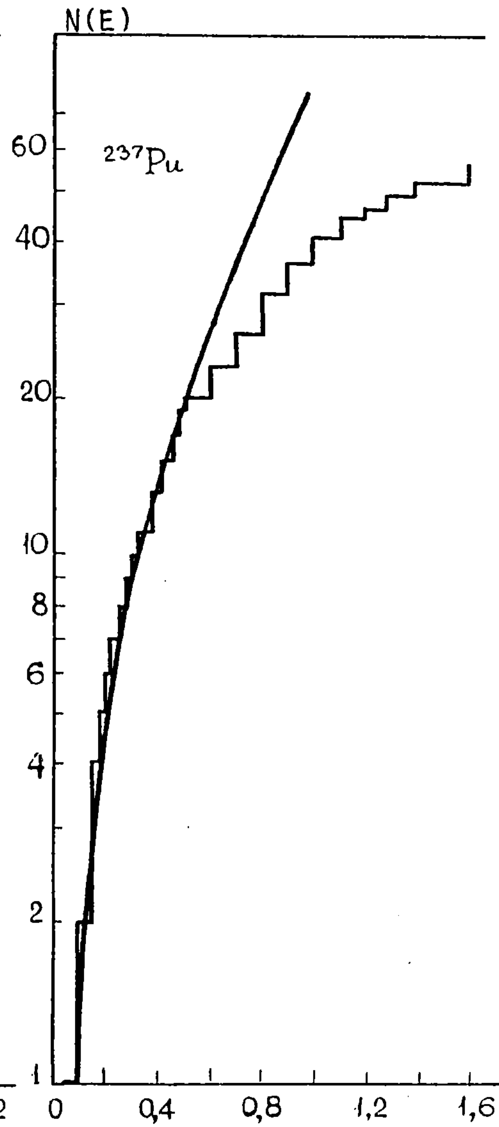

Fig. 6h

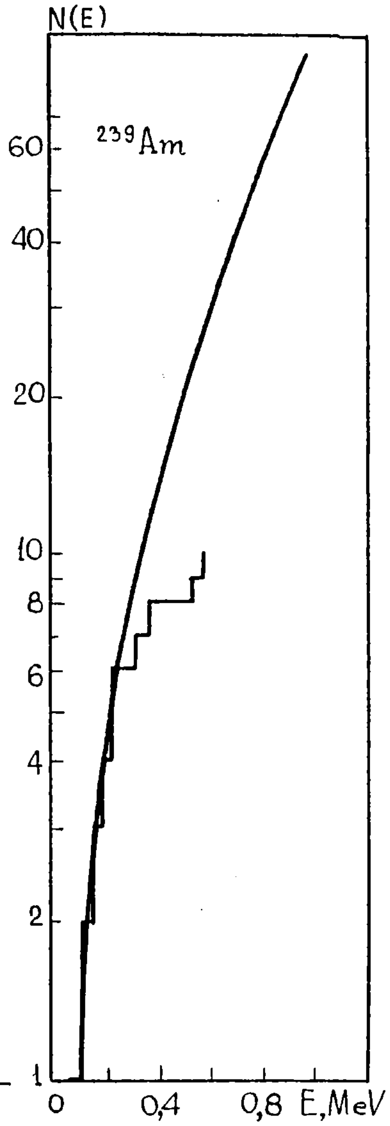

Fig. 6i

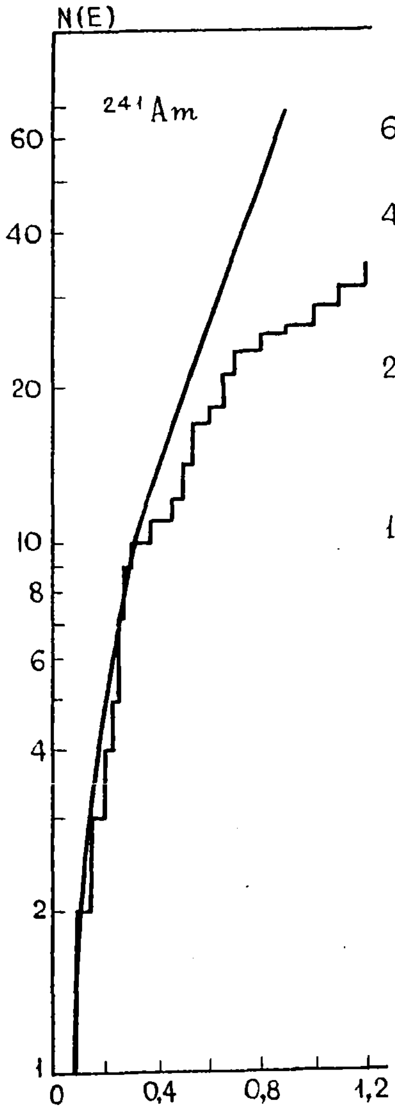

Fig. 6j

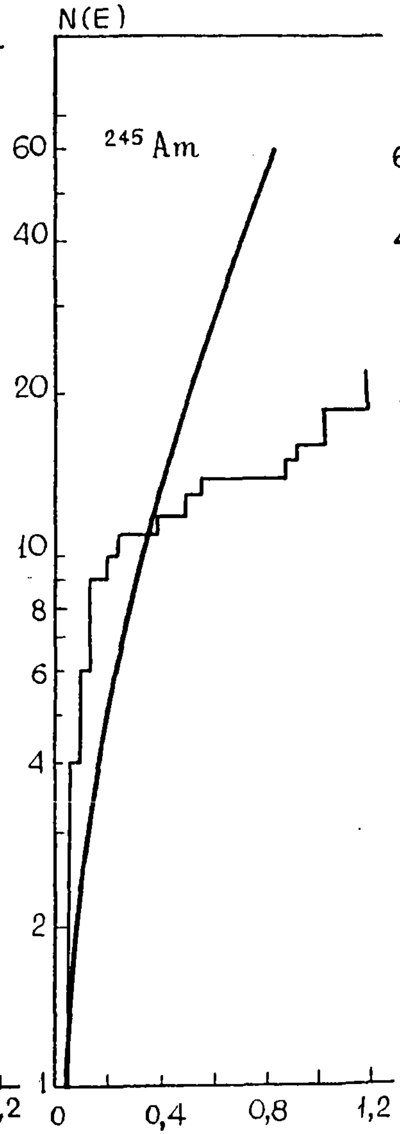

Fig. 6k

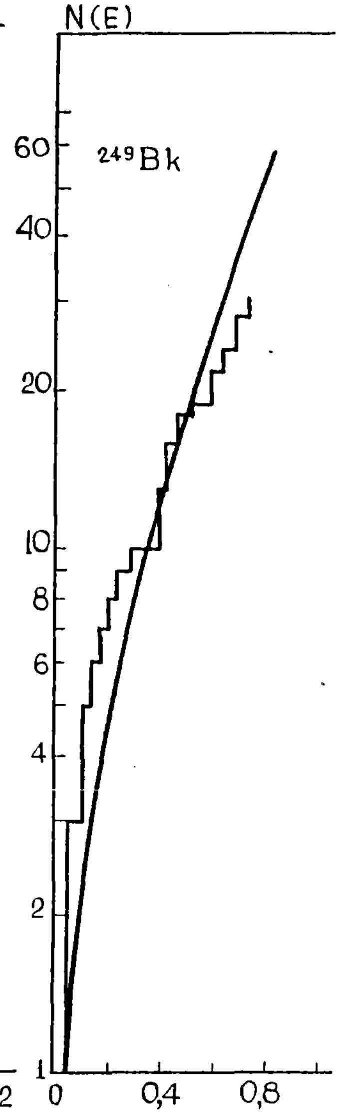

Fig. 6l

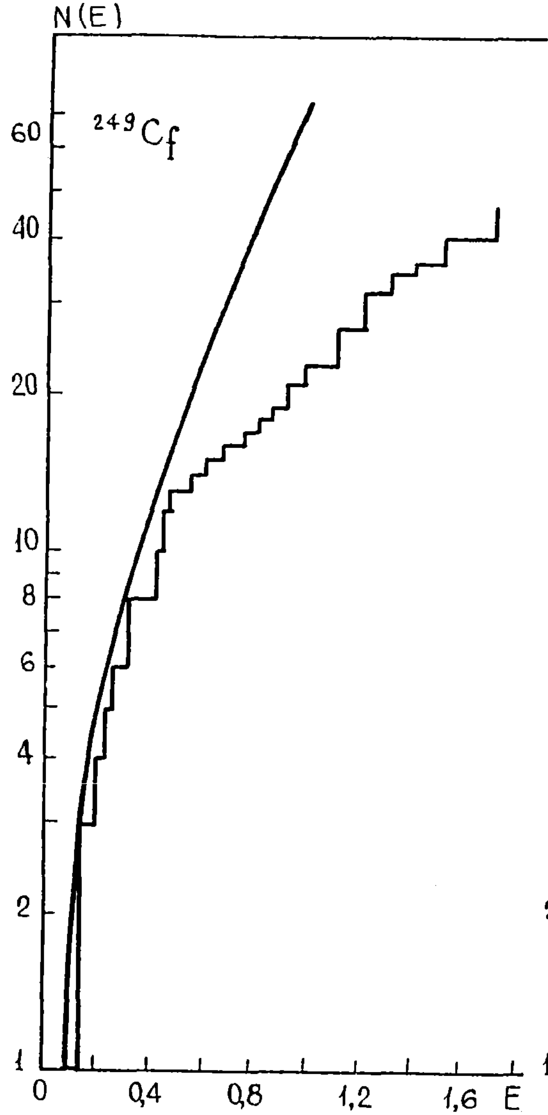

Fig. 6m

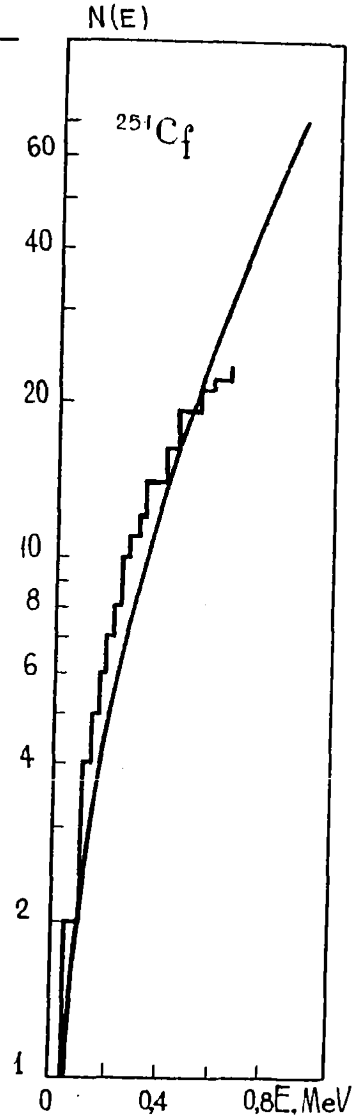

Fig. 6n

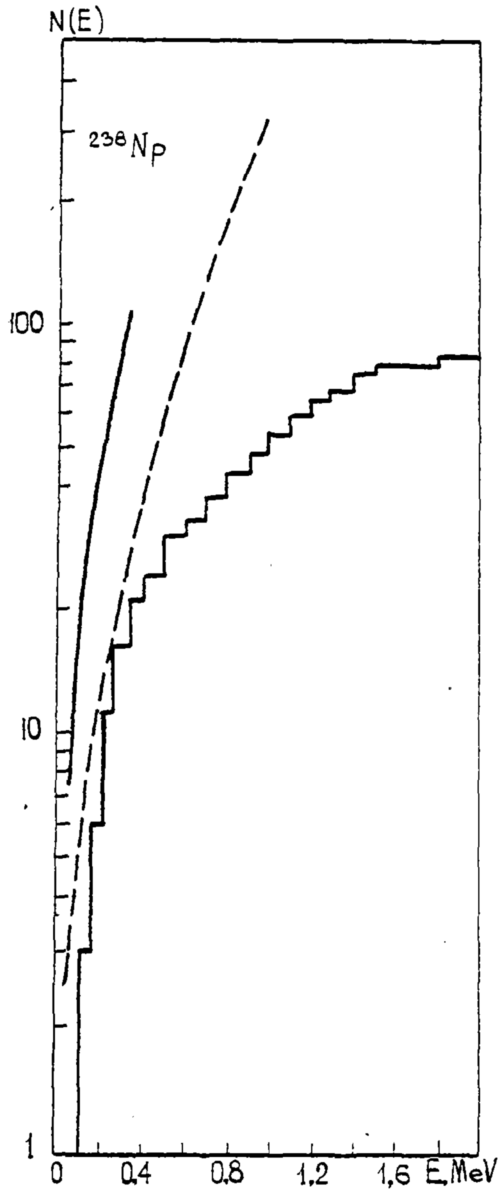

Fig. 7a

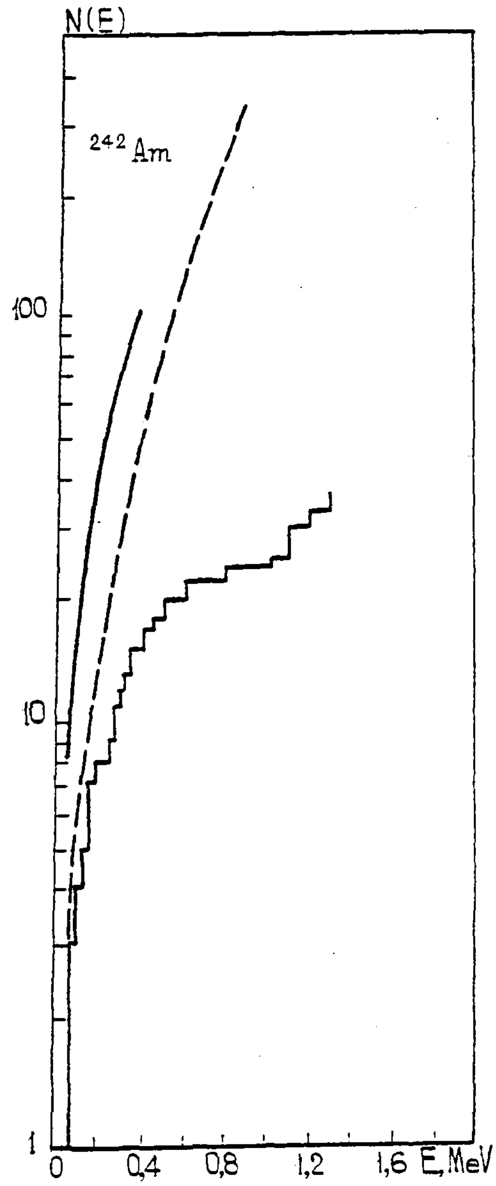

Fig. 7b

Fig. 7. The cumulative number of levels of the odd-odd nuclei calculated using the superfluid nuclear model with $\Delta_{oZ(N)_{exp}}$ (---) and the constant-temperature model (_____). The parameters T and E_o are deduced from the systematics: a, ^{238}Np; b, ^{242}Am; c, ^{244}Am; d, ^{248}Bk; e, ^{250}Bk.

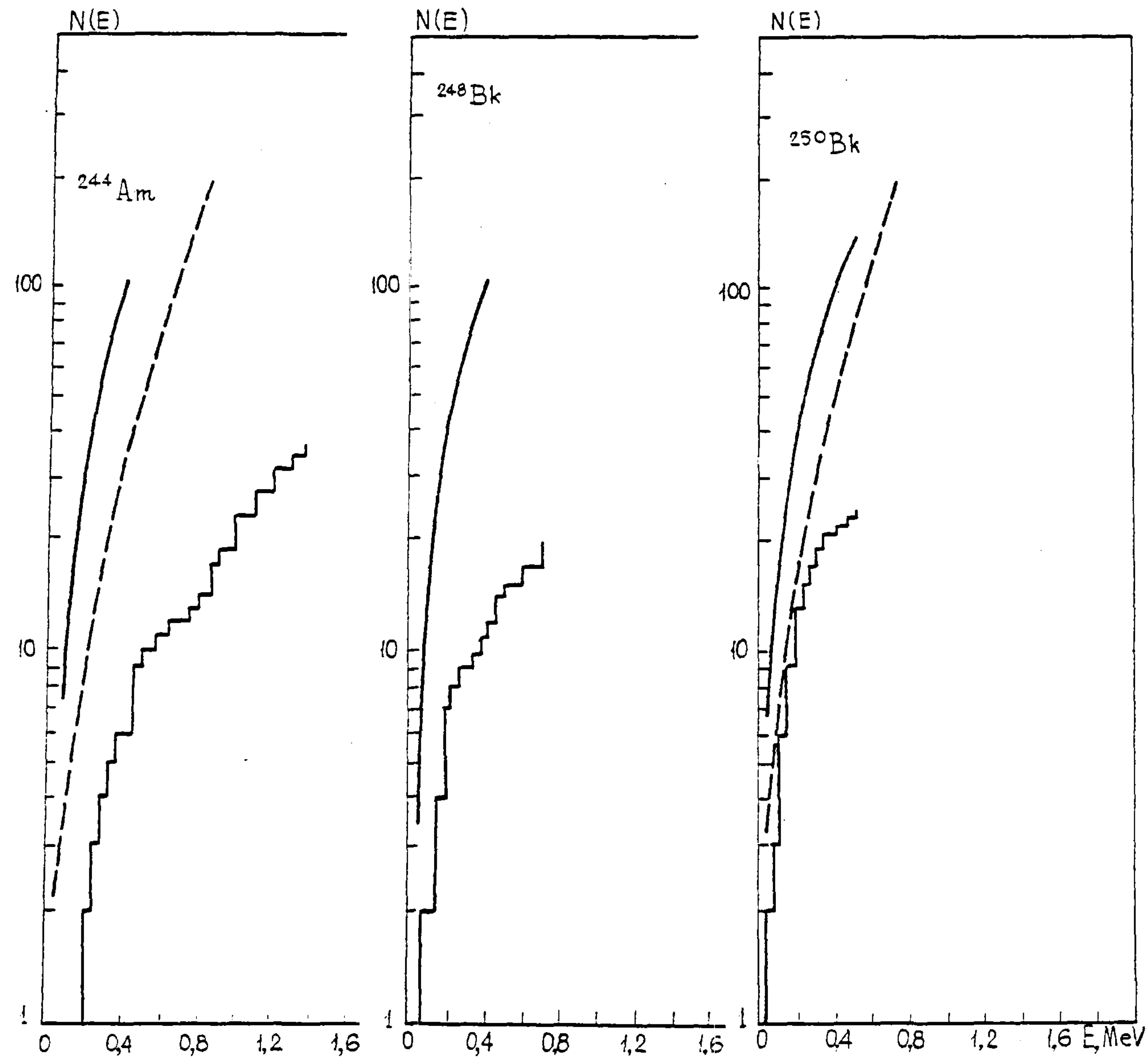

Fig. 7c

Fig. 7d

Fig. 7e

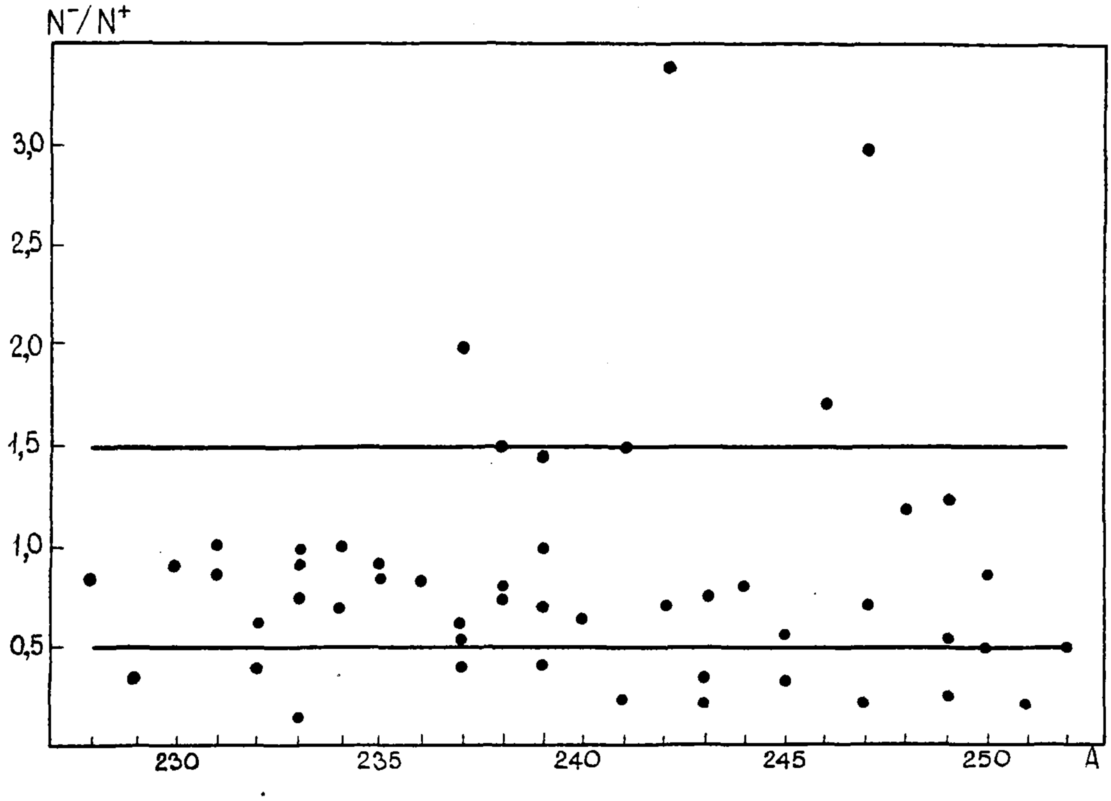

Fig 8

Fig. 8. The ratio N^-/N^+ of negative-to-positive parity level numbers vs the mass number A.

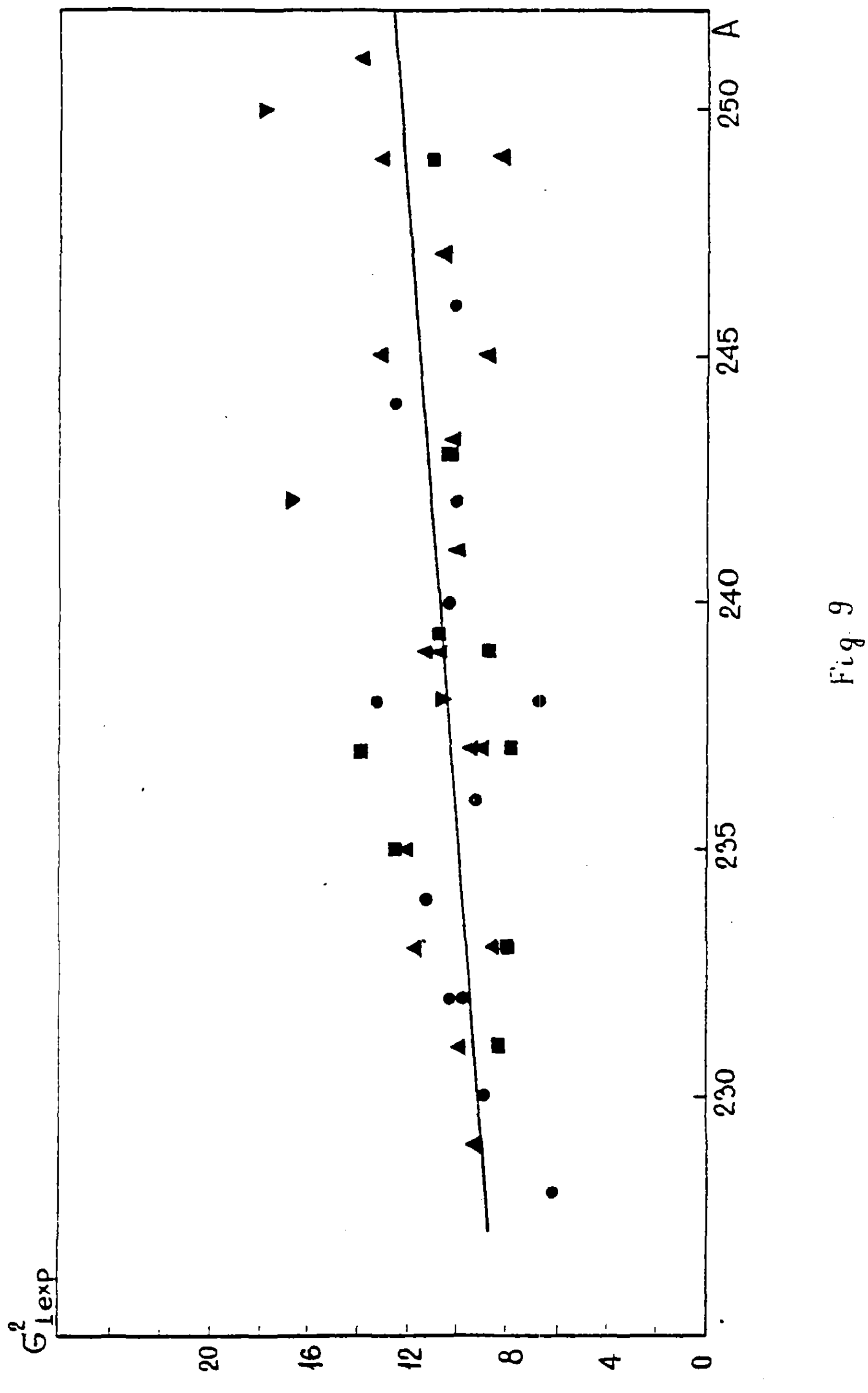

Fig. 9. Parameter $\sigma_{\perp\,\mathrm{exp}}^2$ vs the mass number A: o, even-even nuclei; ▲ , even-odd nuclei; ■ , odd-even nuclei; ◆ , odd-odd nuclei. The straight line gives $\sigma_{\perp}^2$ as suggested by (27).

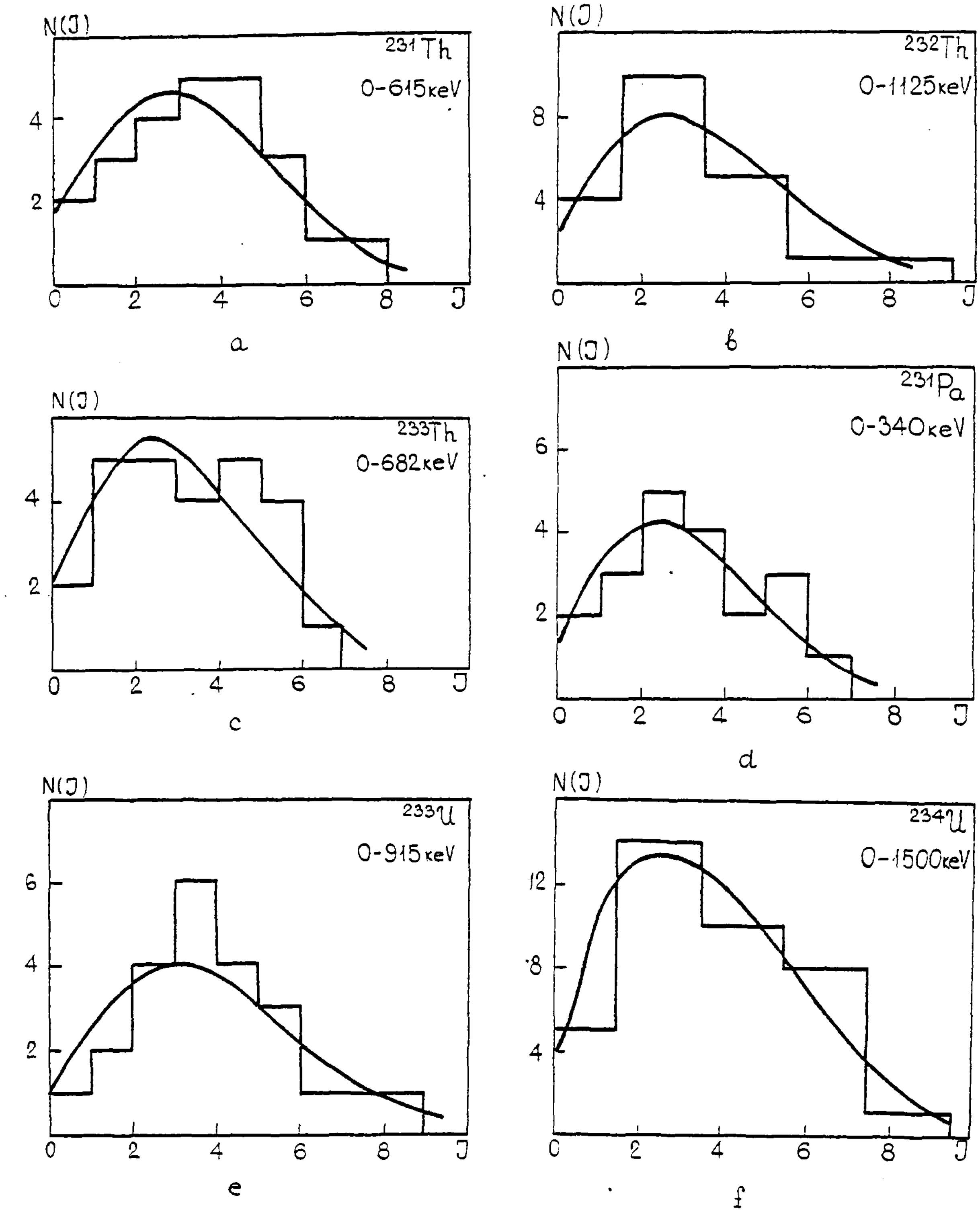

Fig. 10. Spin distributions of discrete nuclear levels and the theoretical prediction obtained using σ^2_{exp}: a, ^{231}Th; b, ^{232}Th; c, ^{233}Th; d, ^{231}Pa; e, ^{233}U; f, ^{234}U; g, ^{235}U; h, ^{236}U; i, ^{238}U; j, ^{239}Np; k, ^{239}Pu; l, ^{240}Pu; m, ^{241}Pu; n, ^{242}Pu; o, ^{242}Am; p, ^{243}Am; q, ^{245}Cm; r, ^{246}Cm; s, ^{247}Cm; t, ^{249}Cm; u, ^{250}Bk.

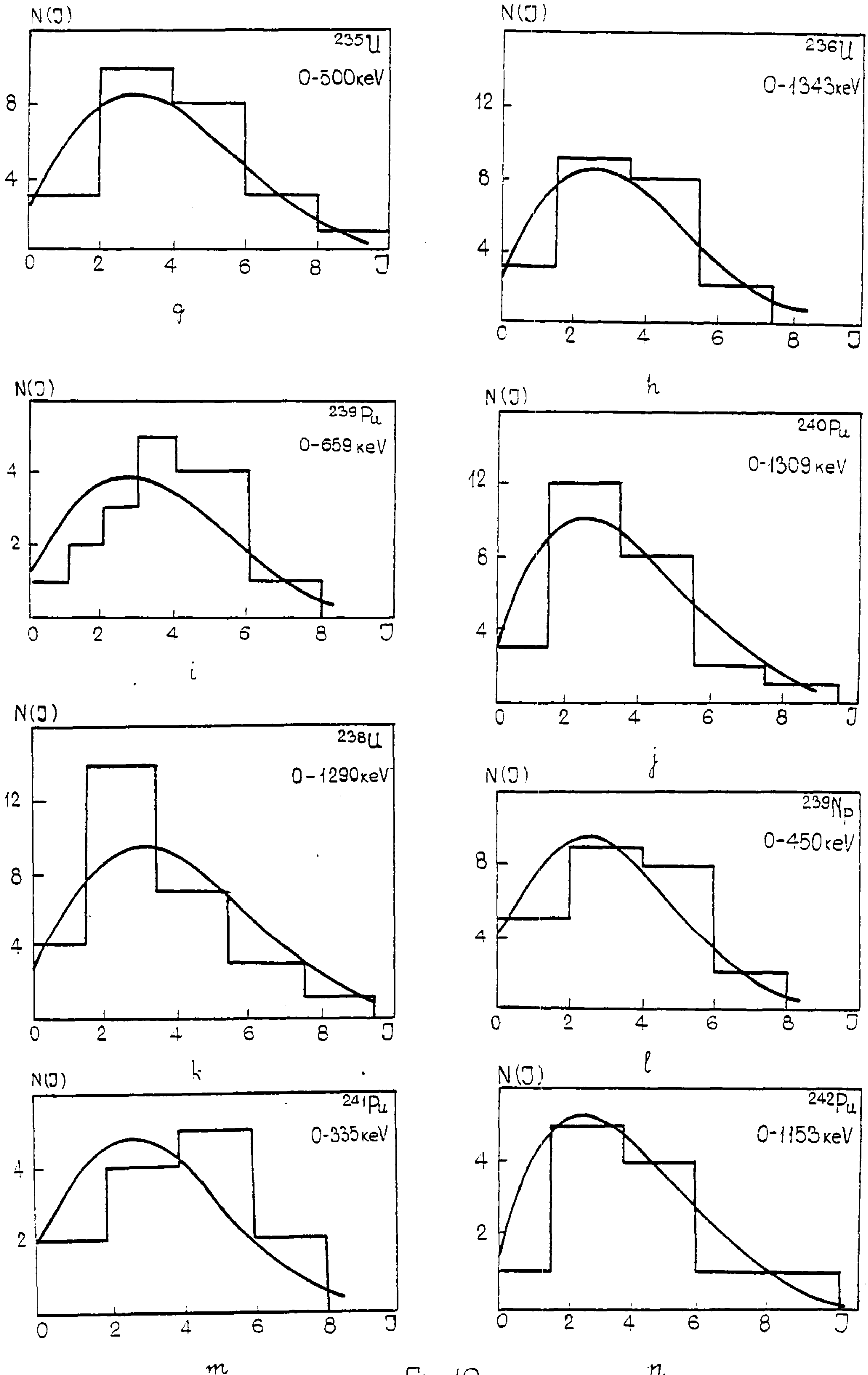
N(J)
235U
0-500keV
g
236U
0-1343keV
h
239Pu
0-659 keV
i
240Pu
0-1309 keV
j
238U
0-1290keV
k
239Np
0-450keV
l
241Pu
0-335keV
m
242Pu
0-1153keV
n
J

Fig 10

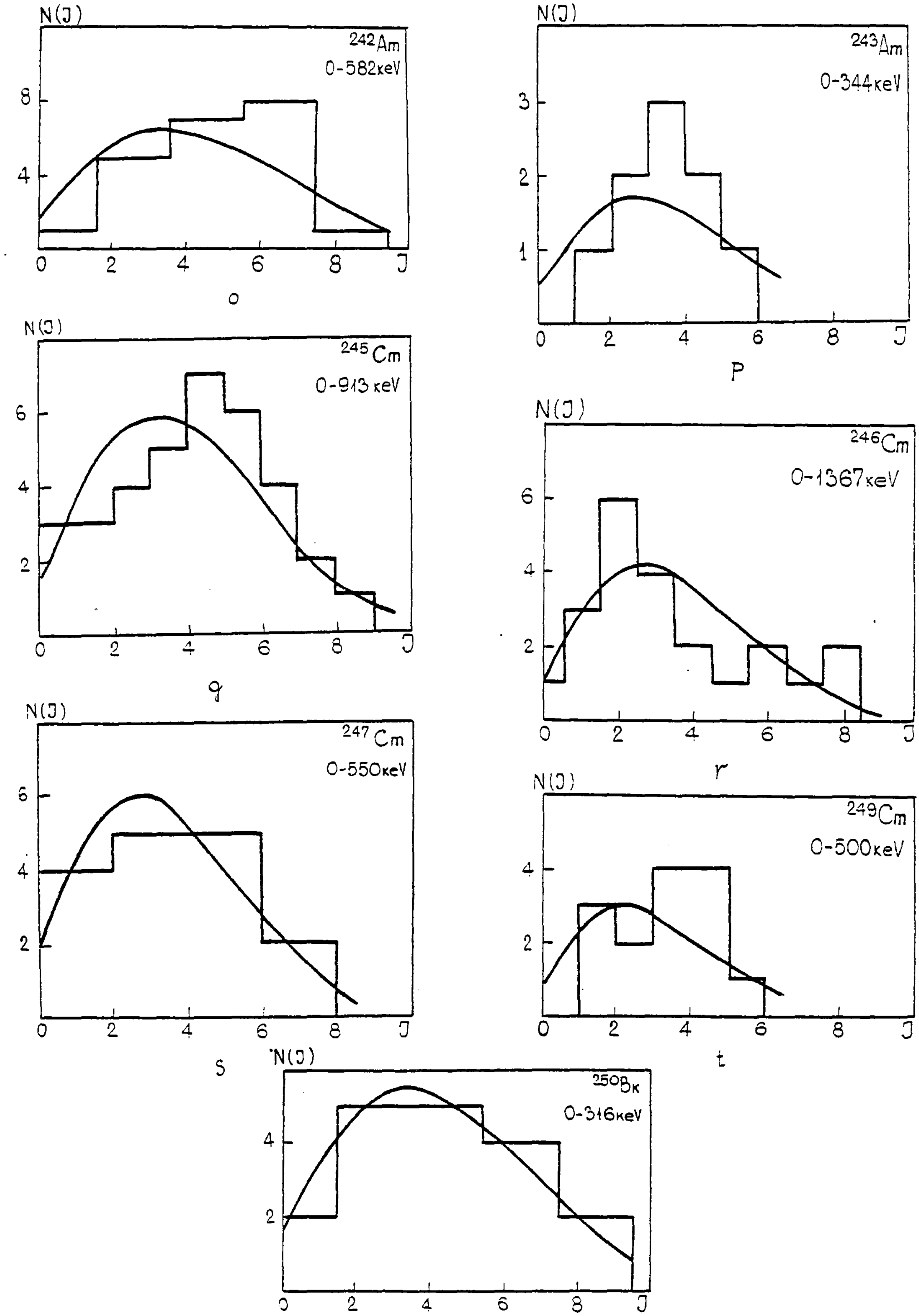
N(J)
242Am
0-582keV
o
243Am
0-344keV
P
245Cm
0-913keV
q
246Cm
0-1367keV
r
247Cm
0-550keV
s
249Cm
0-500keV
t
250Bk
0-316keV
J

Fig 10u

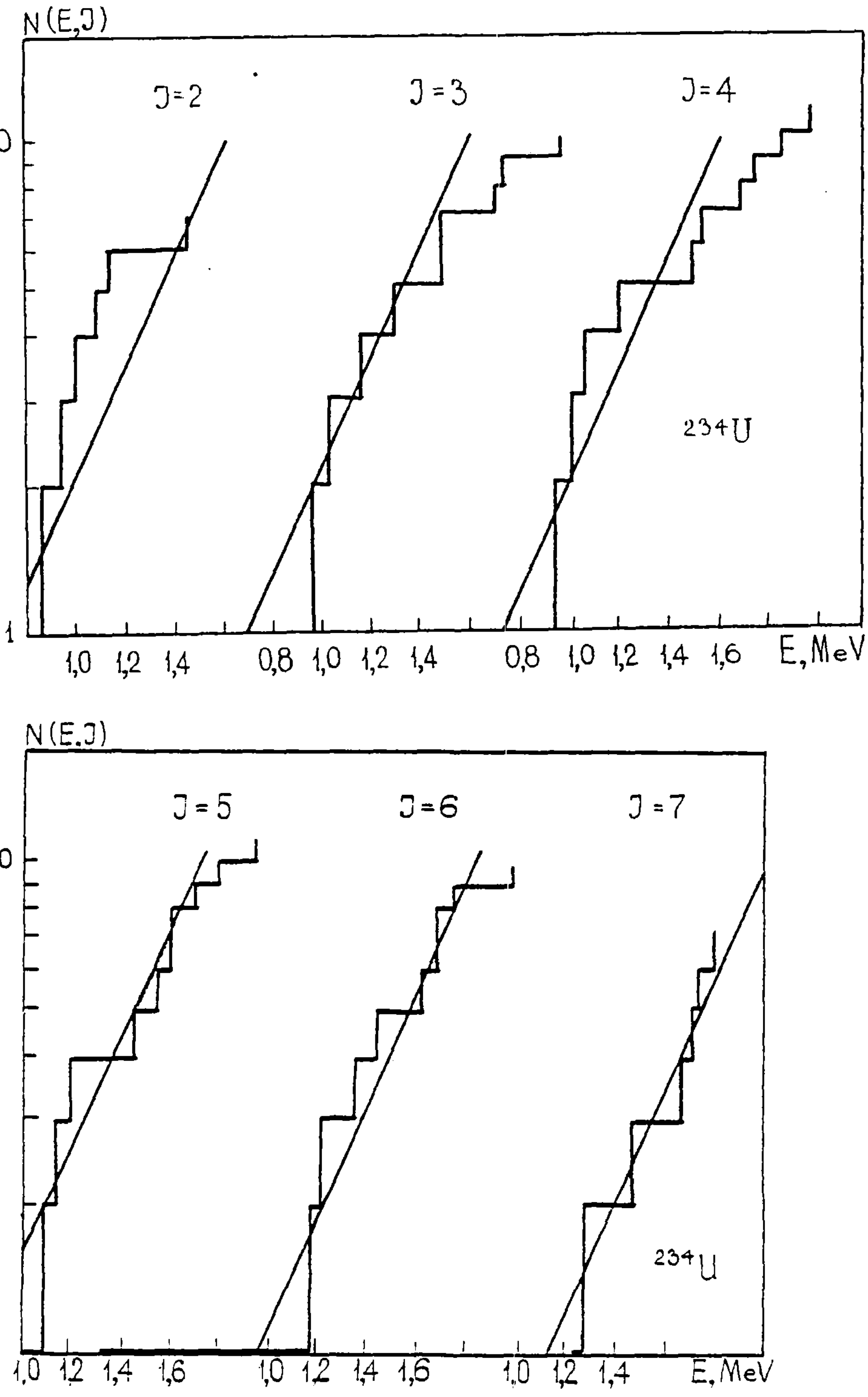

Fig. 11a

Fig. 11. The cumulative number of levels with given J. The straight solid line corresponds to the constant-temperature model and the law (25) when $\sigma^2 = \sigma^2_{exp}$: a, ^{234}U; b, ^{240}Pu; c, ^{235}U; d, ^{239}Pu; e, ^{245}Cm; f, ^{246}Cm.

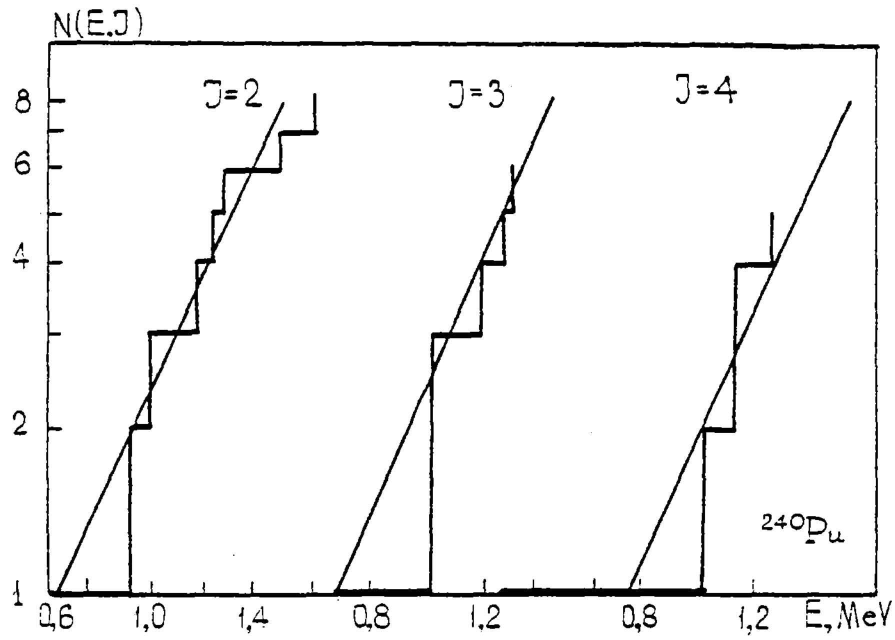

Fig. 11 b

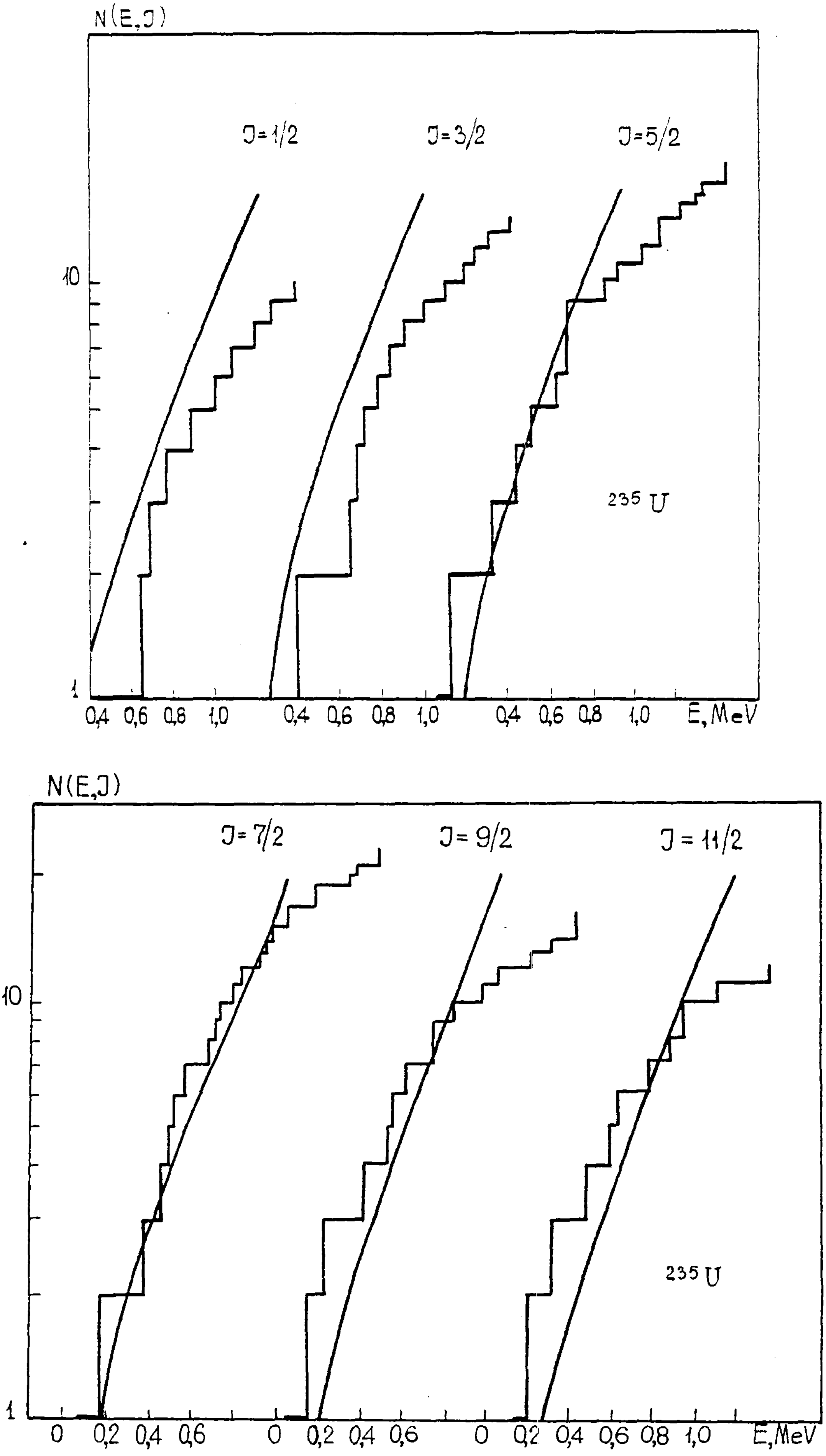
N(E,J)
J=1/2
J=3/2
J=5/2
10
1
235 U
0,4 0,6 0,8 1,0 0,4 0,6 0,8 1,0 0,4 0,6 0,8 1,0 E, MeV
N(E,J)
J=7/2
J=9/2
J=11/2
10
1
235 U
0 0,2 0,4 0,6 0 0,2 0,4 0,6 0 0,2 0,4 0,6 0,8 1,0 E,MeV

Fig. 11c

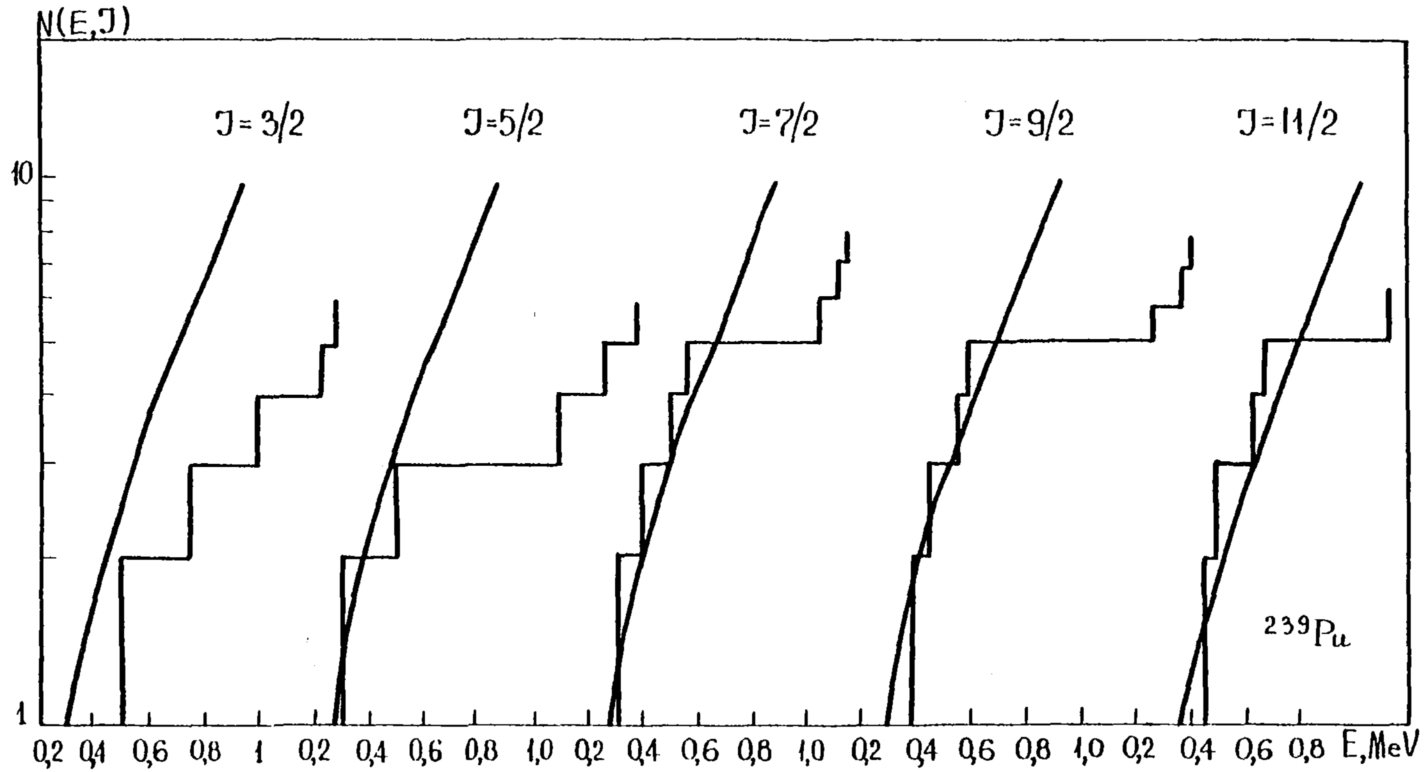
N(E,J)
J = 3/2
J=5/2
J=7/2
J=9/2
J=11/2
10
1
^{239}Pu
0,2 0,4 0,6 0,8 1 0,2 0,4 0,6 0,8 1,0 0,2 0,4 0,6 0,8 1,0 0,2 0,4 0,6 0,8 1,0 0,2 0,4 0,6 0,8 E,MeV

Fig. 11d

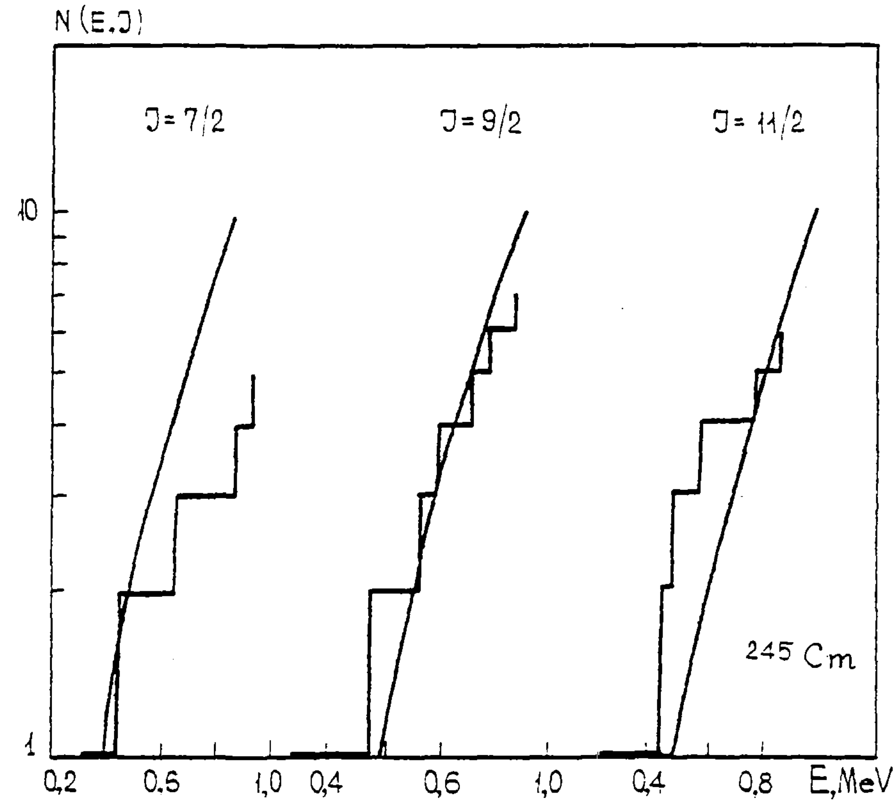

Fig. 11e

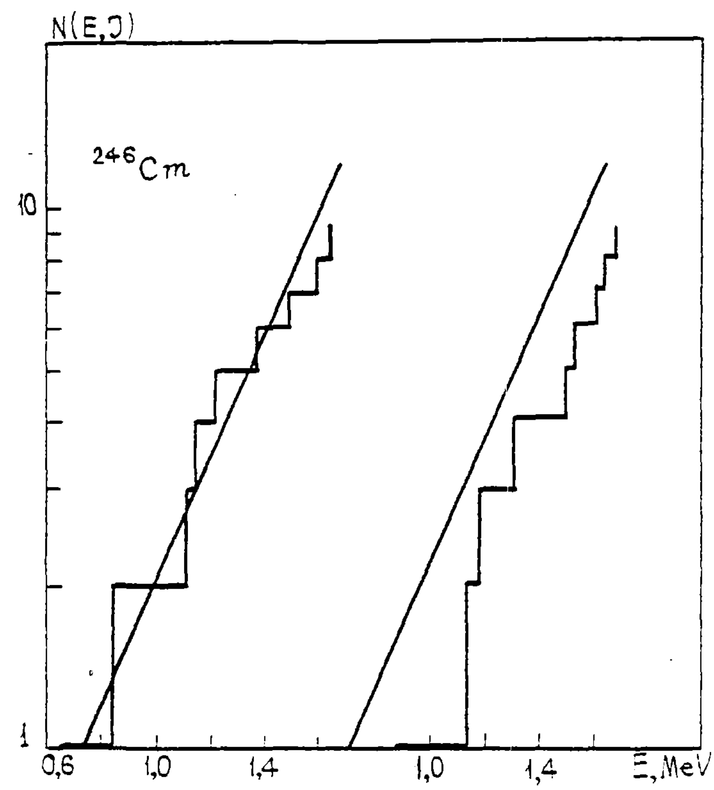

Fig. 11f

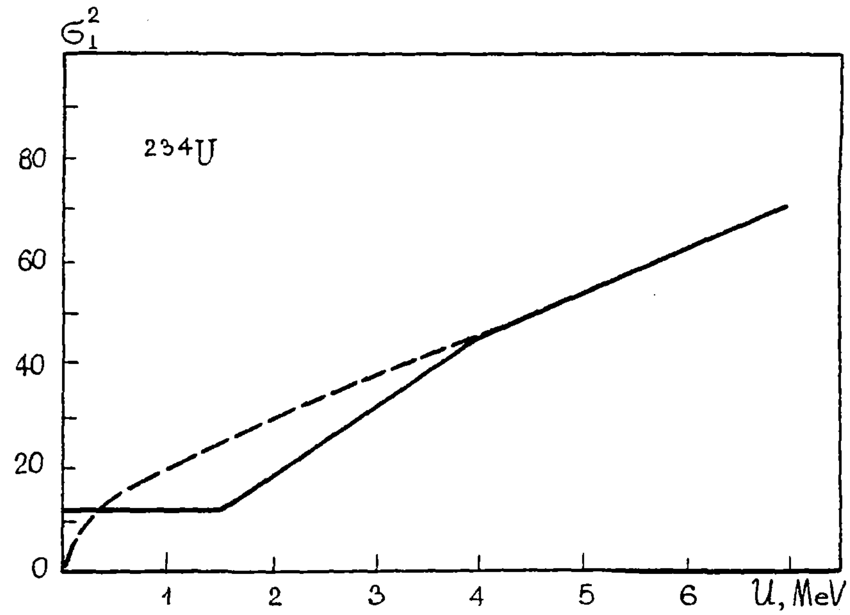

Fig. 12

Fig. 12. Energy dependence of the spin cut off parameter σ^2 (^{234}U) recommended (____) and calculated (---) using the superfluid nuclear model.

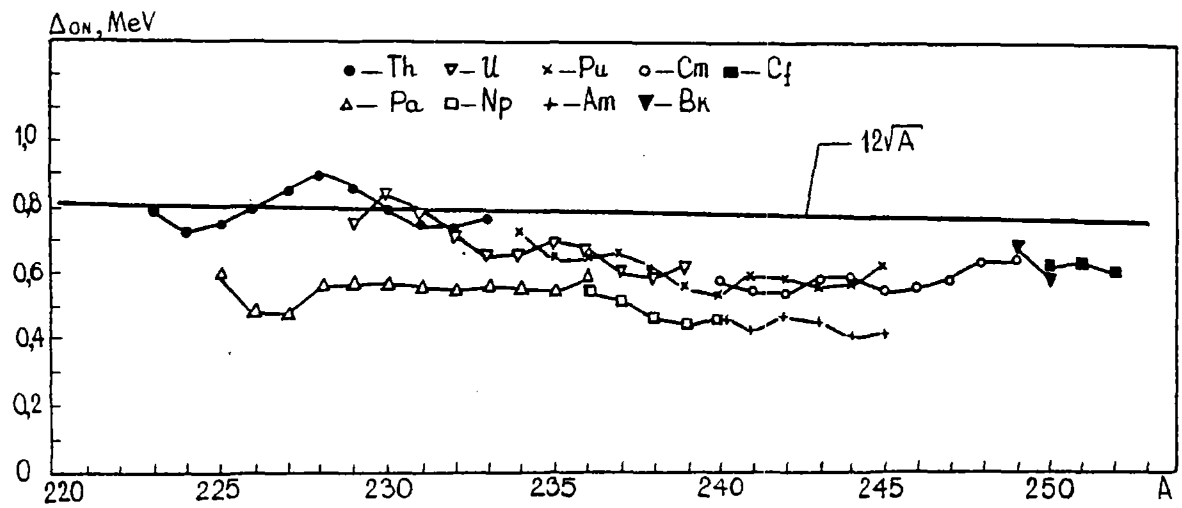

Fig. 13. Neutron pairing energies vs the mass number for transactinides: ● , Th; Δ , Pa; ∇ , U; □ , Np; X , Pu; + , Am; o, Cm; ▼ , Bk; ■, Cf.

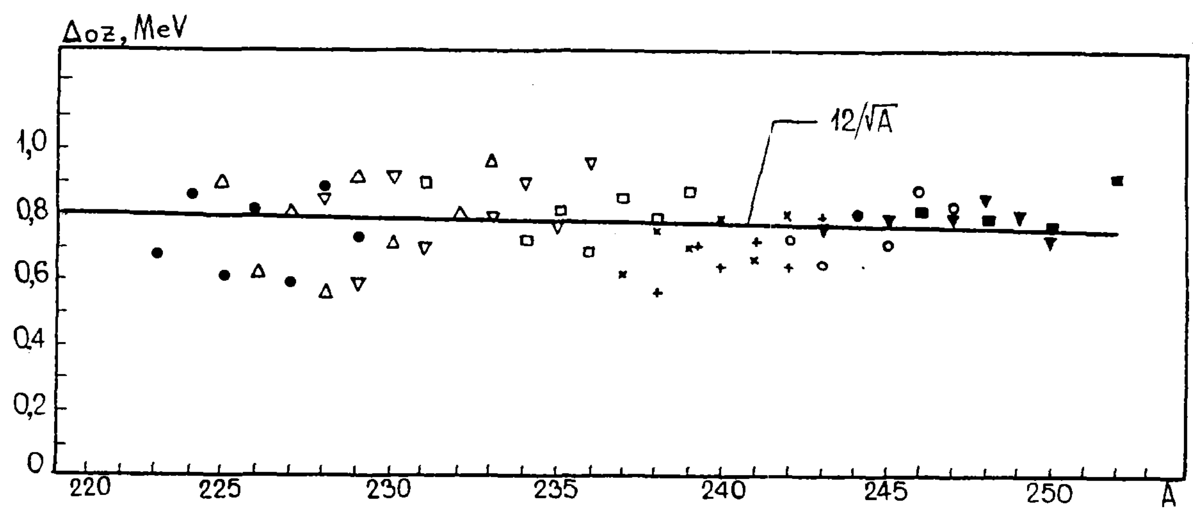

Fig. 14. Proton pairing energies vs the mass number for transactinides. For notations see Fig. 13.

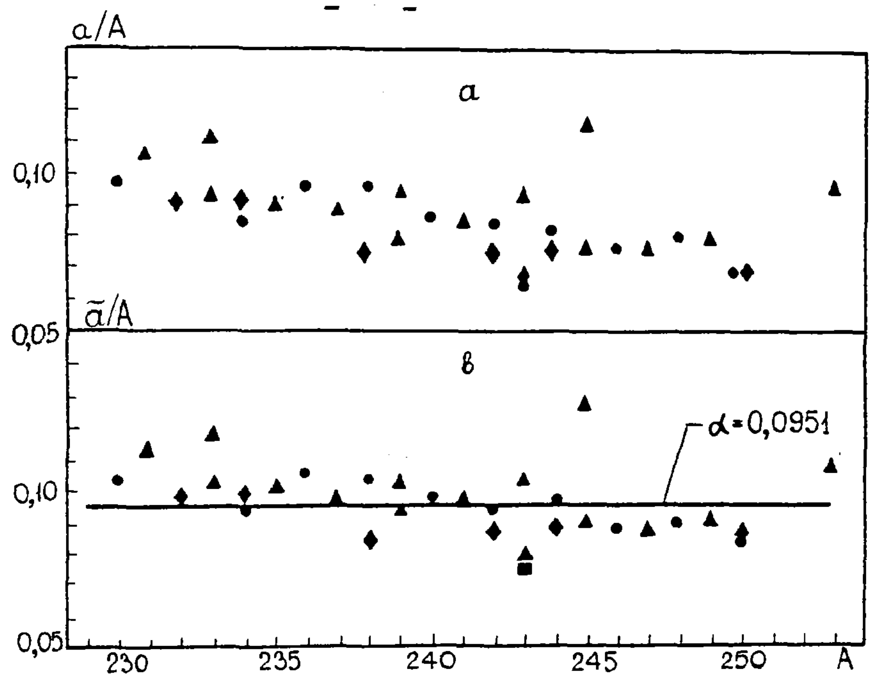

Fig. 15. Ratios a/A (a) and $\tilde{a}/A$ (b) vs the mass number for $\Delta_0 = 12/\sqrt{A}$: ●, even-even nuclei; ▲, even-odd nuclei; ■, odd-even nuclei; ◆, odd-odd nuclei.

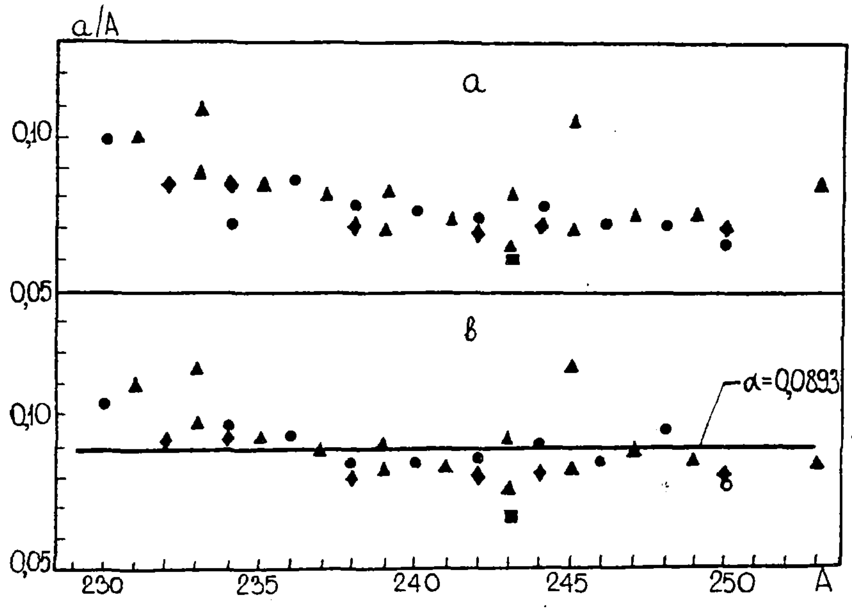

Fig. 16. Ratios a/A (a) and $\tilde{a}/A$ (b) vs the mass number for $\Delta_{0\,exp}$: ●, even-even nuclei; ▲, even-odd nuclei; ■, odd-even nuclei; ◆, odd-odd nuclei.

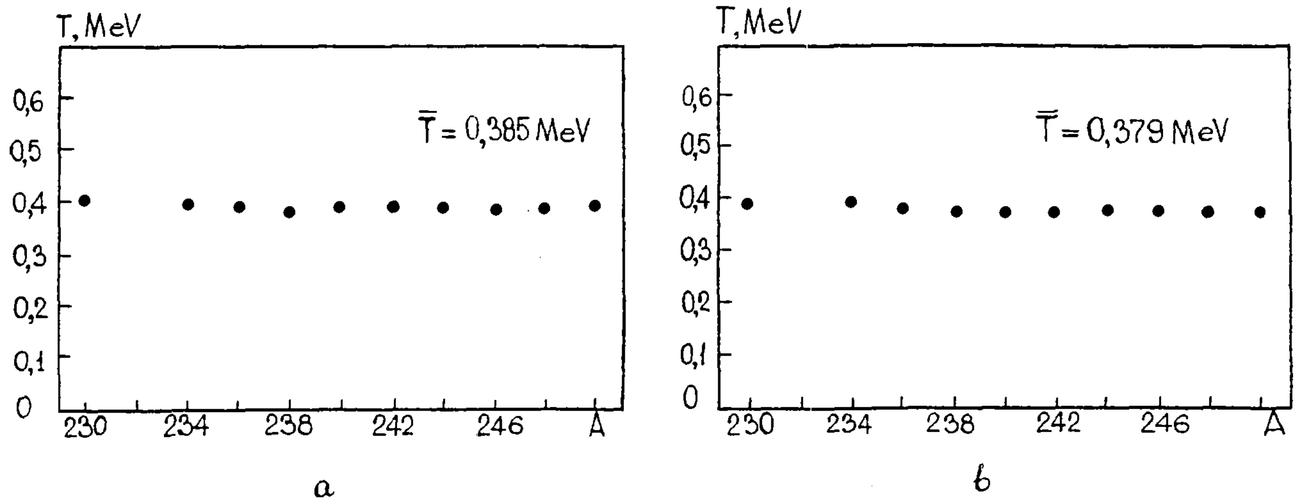

Fig. 17. The values of the parameter T for even-even nuclei obtained using the discrete spectrum fitting: a, Δ_o from $(12/\sqrt{A})$; b, $\Delta_{oZ(N)} = \Delta_{oZ(N)\ exp}$.

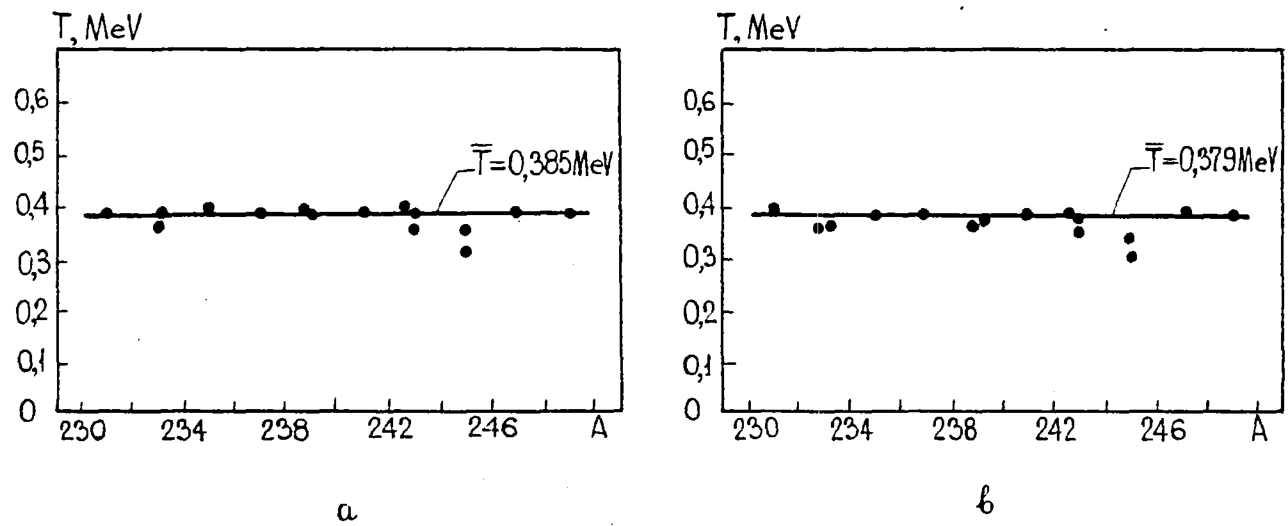

Fig. 18. The values of the parameter T for odd nuclei obtained by the cumulative number of low-lying level fitting: a, $\Delta_o = 12\sqrt{A}$
b, $\Delta_{oZ(N)} = \Delta_{oZ(N)\ exp}$.

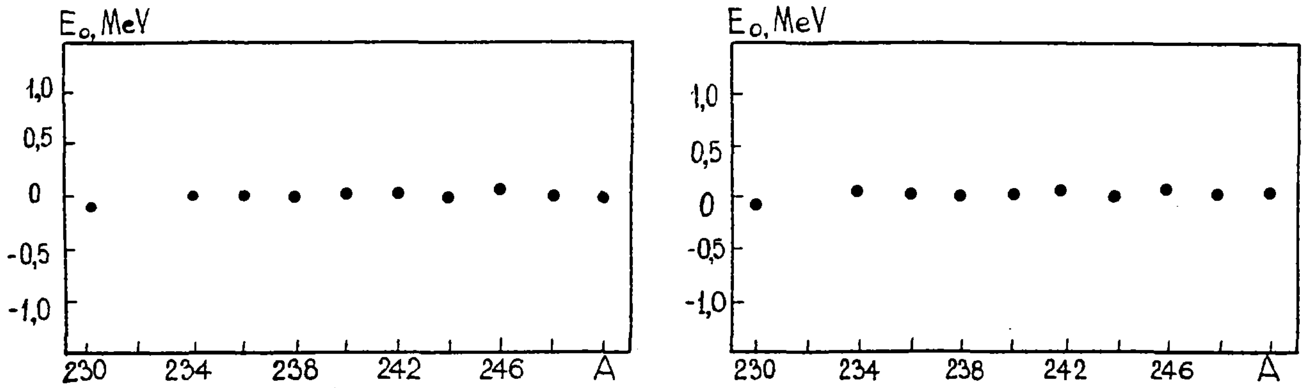

a b

Fig. 19. The values of the parameter E_o for even-even nuclei obtained by the cumulative number of low-lying level fitting: a, $\Delta_o = 12/\sqrt{A}$ b, $\Delta_{oZ(N)} = \Delta_{oZ(N)\ exp}$.

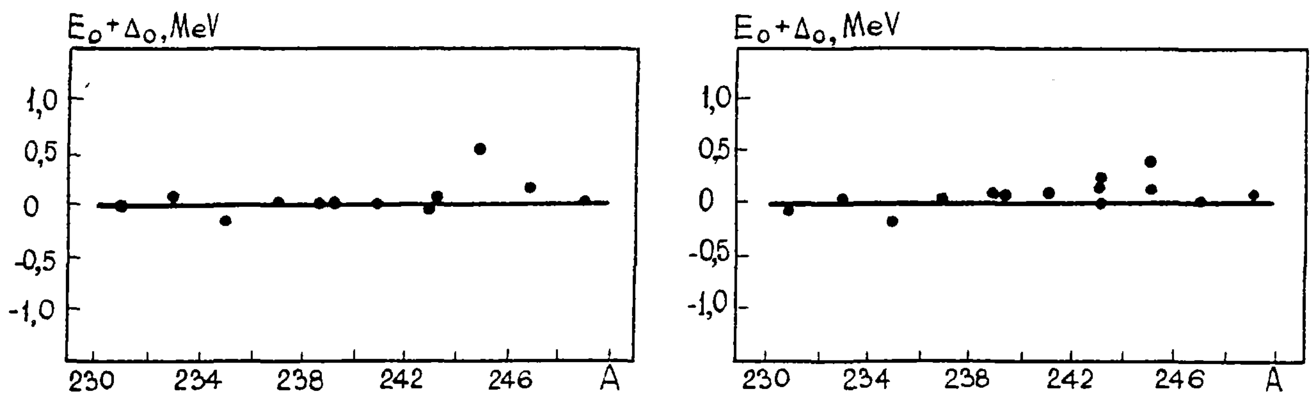

a b

Fig. 20. The values of $E_o + \Delta_o$ for odd nuclei obtained by the cumulative number of low-lying level fitting: a, $\Delta_o = 12/\sqrt{A}$; b, $\Delta_{oZ(N)} = \Delta_{oZ(N)\ exp}$.

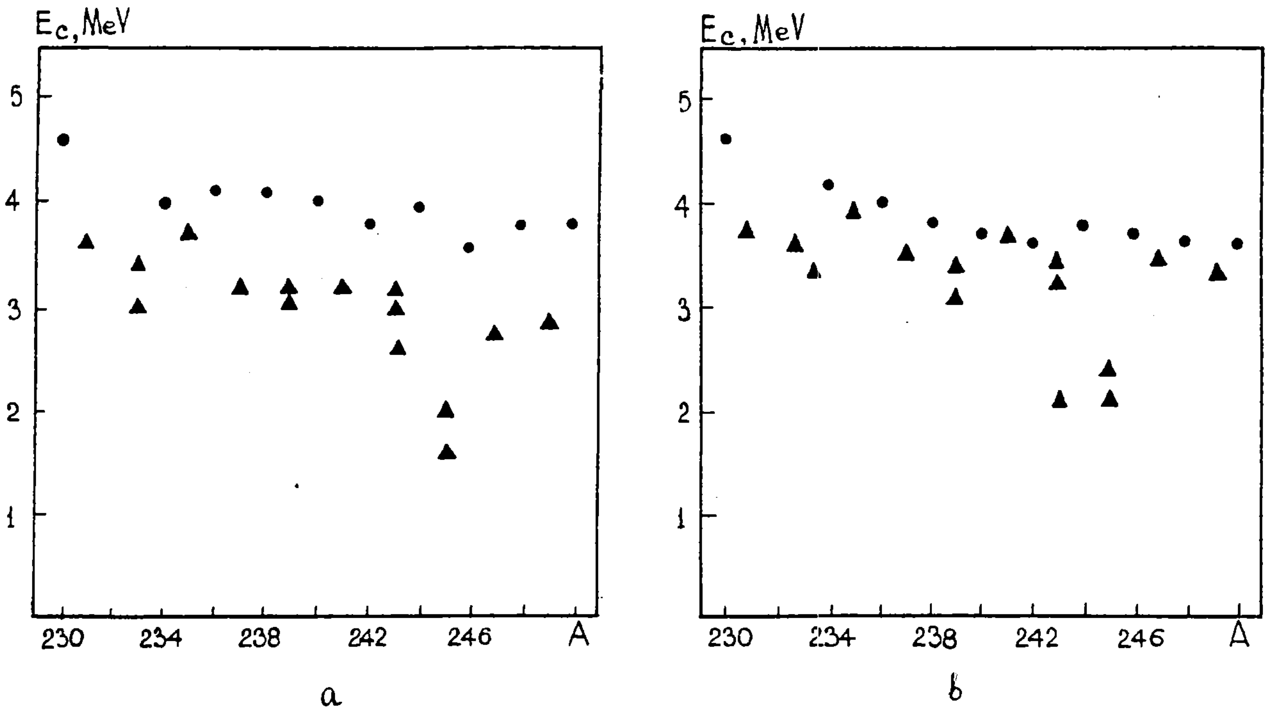

Fig. 21. The values of the parameter E_c obtained by the cumulative number of low-lying level fitting and the model curve matching: ●, even-even nuclei; ▲, odd nuclei: a, $\Delta_o = 12/\sqrt{A}$; b, $\Delta_{oZ(N)} = \Delta_{oZ(N)\ exp}$.

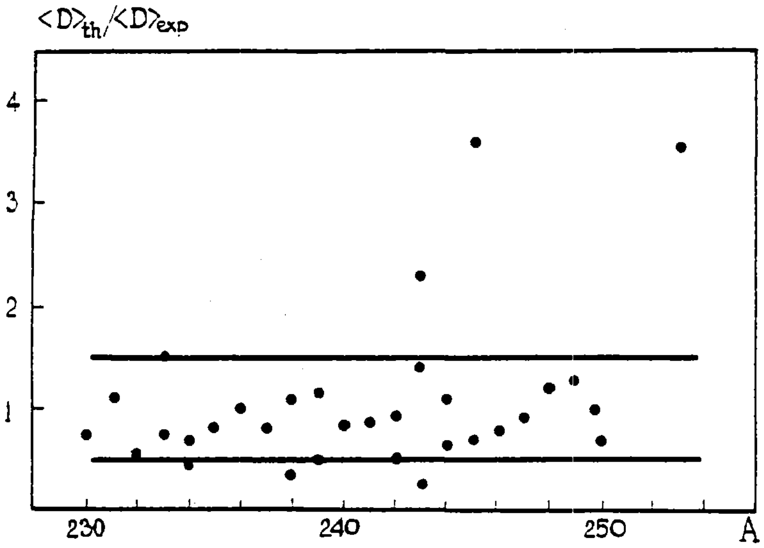

Fig. 22. The ratio $\langle D \rangle_{theor} / \langle D \rangle_{exp}$ calculated for $\Delta_o = 12/\sqrt{A}$ using the parameters derived from systematics for transactinides Th-Cf.

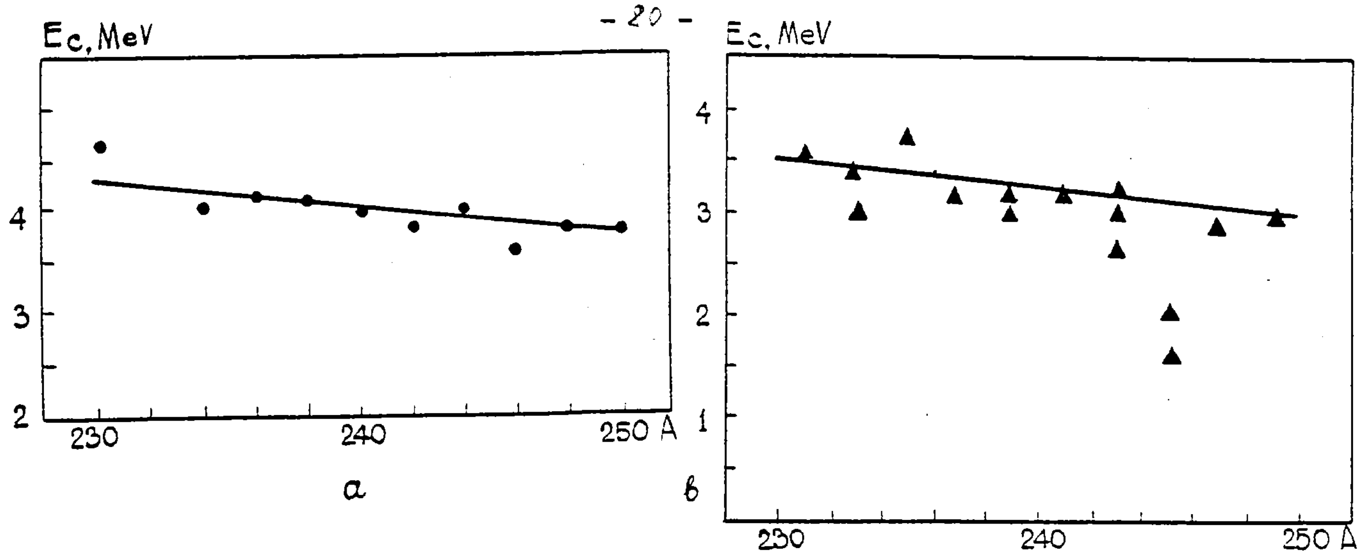

Fig. 23. Comparison of the E_c values obtained from systematics with the experimental ones: a, even-even nuclei; b, odd nuclei.

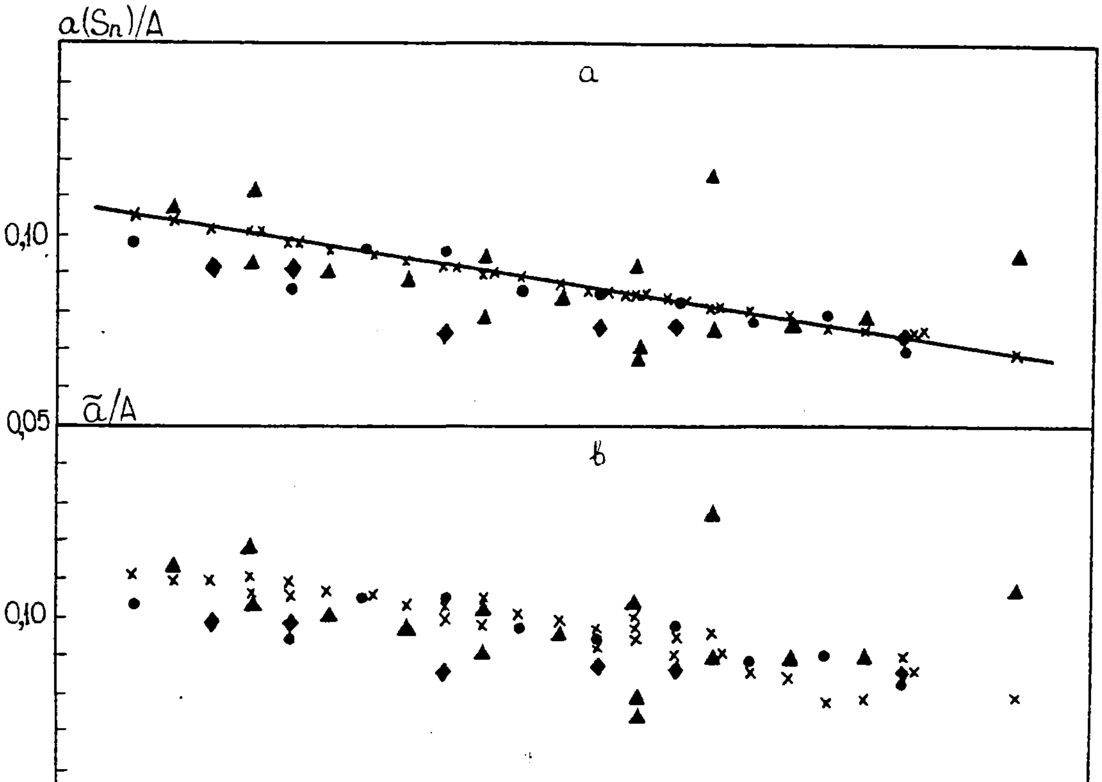

Fig. 24. Comparison of the level density parameter a/A ratios calculated from systematics (x) and its asymptotic value $\tilde{a}/A$ (b) vs the mass number with a/A and $\tilde{a}/A$ derived by the $\langle D \rangle_{exp}$ fitting: ● , even-even nuclei; ▲ , odd nuclei; ◆ , odd-odd nuclei.

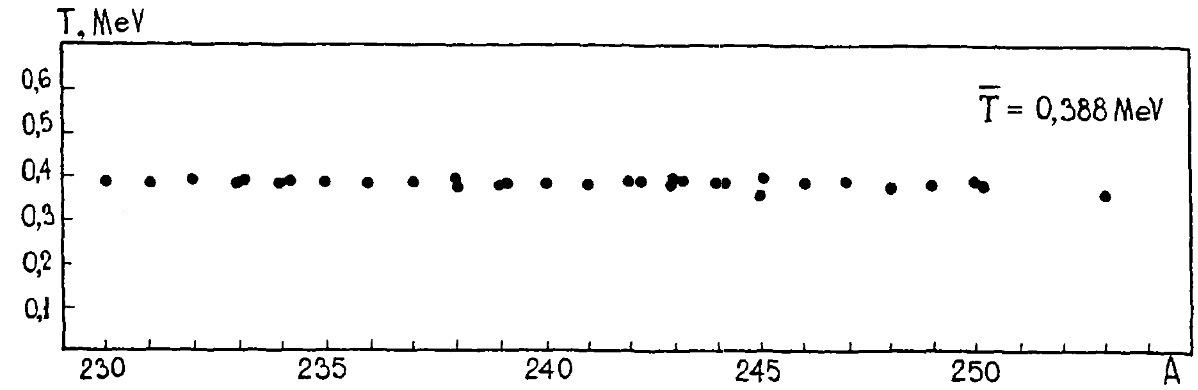

Fig. 25. The values of the parameter T obtained from $\langle D \rangle_{exp}$ when $E_0 = 0, -\Delta_0, -2\Delta_0$ for even-even, odd and odd-odd nuclei, respectively.

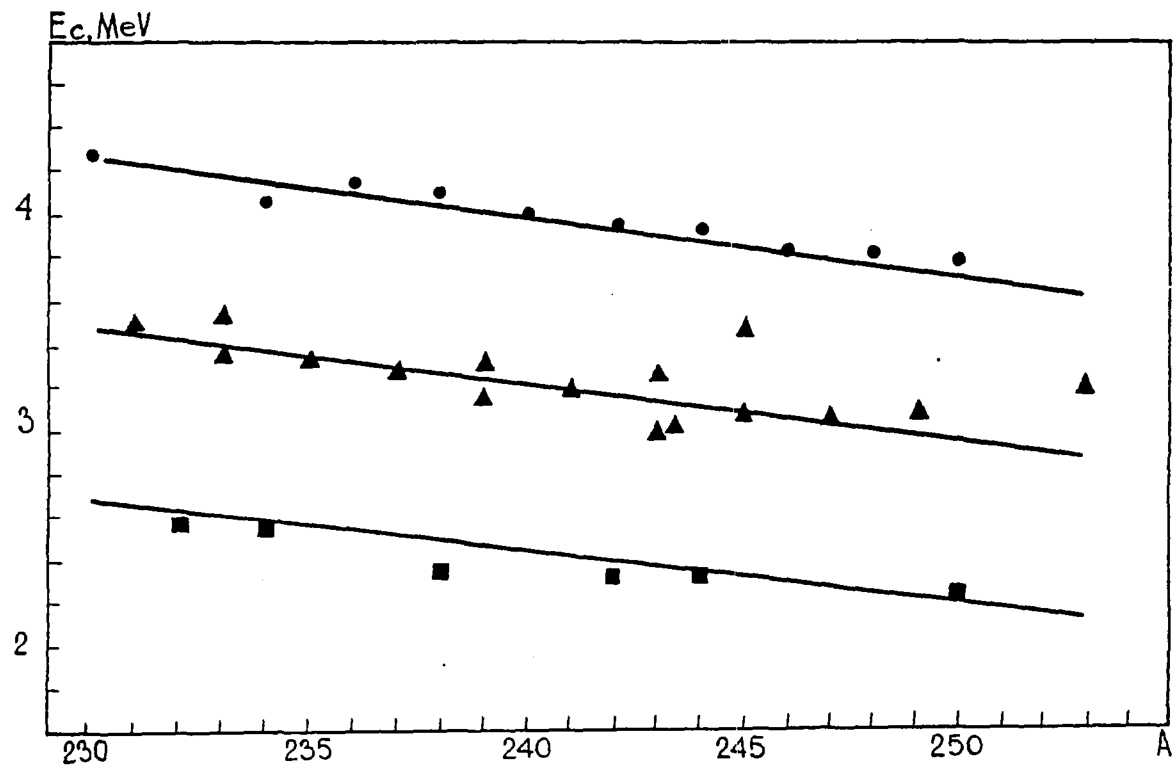

Fig. 26. Comparison of the values E_c obtained from $\langle D \rangle_{exp}$ when $E_0 = 0, -\Delta_0, -2\Delta_0$ for even-even nuclei (●), odd nuclei (▲) and odd-odd nuclei (■) and derived from systematics (______).

Distribution of this report INDC(CCP)-182:

1. INDC "G" distribution — 31 copies

2. Participants of CRP and/or CRP Meeting:

Arlt, R., German Dem. Rep.
Blinov, M.V., USSR
Condé, H., Sweden
Derrien, H., France
Fröhner, F., Germany Fed. Rep.
Goel, B., Germany Fed. Rep.
Harada, K., Japan
Igarasi, S., Japan
Konshin, V.A., USSR
Küsters, H., Germany Fed. Rep.
H. Liskien, Geel
Lynn, J.E., UK
Mattes, M., Germany Fed. Rep.
Mehta, M.K., India
Menapace, E., Italy
Patrick, B.H., UK
Petrzhak, K.A., USSR
Salvy, J., France
Shpakov, V., USSR
Tanaka, S., Japan
Usachev, L.N., USSR
Vasiliu, G., Romania
Ventura, A., Italy
Yiftah, S., Israel — 24 copies

3. IAEA

Yu.G. Bobkov
V. Bychkov
P. Cate
D.E. Cullen
N. Kocherov
H.D. Lemmel
A. Lorenz
K. Okamoto
V.G. Pronyaev
J.J. Schmidt — 10 copies